

RIVM report 550002007/2005

**The significance of climate change in the Netherlands**

An analysis of historical and future trends (1901-2020)  
in weather conditions, weather extremes and temperature-related impacts

H. Visser

contact: H.Visser  
RIVM-MNP / IMP  
Hans.Visser@rivm.nl

This investigation has been performed by order and for the account of RIVM,  
within the framework of project S/550002/01/TO, Uncertainties, Transparency and  
Communication: Tools for Uncertainty Analysis.

## ABSTRACT

### **The significance of climate change in the Netherlands**

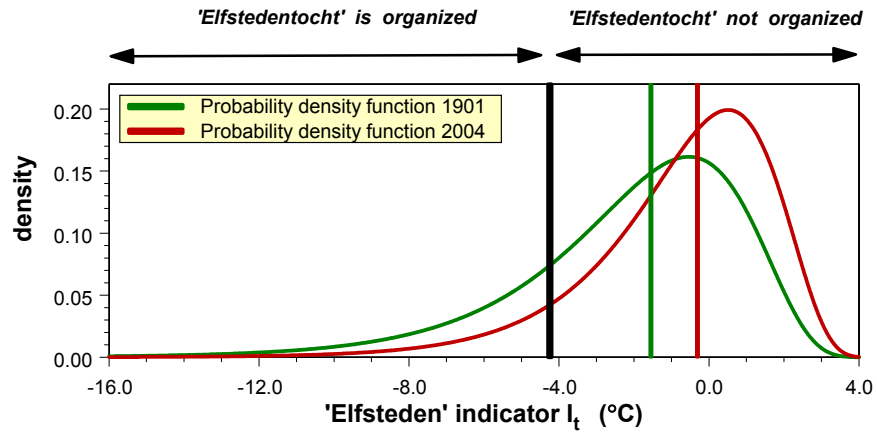
An analysis of historical and future trends (1901-2020)  
in weather conditions, weather extremes and temperature-related impacts

A rigorous statistical analysis reveals changes in Dutch climate that are statistically significant over the last century. Annually averaged temperatures have increased by  $1.5\pm 0.5$  °C; the number of summer days has roughly doubled from  $14\pm 5$  to  $27\pm 9$  days; annual precipitation has increased by  $120\pm 100$  mm; and the number of extremely wet days has increased by about 40%, from  $19\pm 3$  to  $26\pm 3$  days. Several other changes in Dutch climate, such as spring temperatures rising more rapidly than winter temperatures, the increase of the coldest temperature in each year by  $0.9$  °C and the annual maximum day sum of precipitation, turn out to be not (yet) statistically significant.

The changes in Dutch climate have already led to several statistically significant impacts. The length of the growing season has increased by nearly a month, and the number of heating-degree days, a measure for the energy needed for the heating of houses and buildings, has decreased by  $14\pm 5\%$ . Projections of future temperature continue to increase up to the year 2020, based both on statistical extrapolations and climate-model projections. It is found that temperatures increase from  $10.4\pm 0.4$  °C in 2003 to  $11.1\pm 0.6$  °C in 2010, and  $10.8\pm 1.0$  °C in 2020. Therefore, energy needed for heating of houses and buildings will decrease whereas energy for cooling will increase. The net climate effect in 2010 is expected to be a lowering of future Dutch greenhouse-gas emissions by 3.5 Mton CO<sub>2</sub> equivalents, which is relevant in the context of commitments under the Kyoto Protocol.

Finally, over the course of the 20th century the chance on an ‘Elfstedentocht’, an outdoor skating event in the Netherlands, has decreased from once every five years to once every ten years. Even though this impact change is not yet statistically significant, it resides ‘on the edge’ of significance: within a few years more evidence may become available to firmly establish the diminishing likelihood of outdoor skating in the Netherlands.

*Key words:* climate change, elfstedentocht, growing season, heating-degree days, uncertainty



*The 'Elfsteden' indicator is defined as the average temperature of the coldest period of 15 consecutive days in a specific winter.*

## RAPPORT IN HET KORT

### De significantie van klimaatverandering in Nederland

Een analyse van historische en toekomstige trends (1901-2020)  
in het weer, weersextremen en temperatuur-gerelateerde impact-variabelen

Statistische analyse van het Nederlandse weer laat veranderingen zien die reeds statistisch significant zijn, gezien over de afgelopen honderd jaar. Jaargemiddelde temperaturen zijn toegenomen met  $1.5 \pm 0.5$  °C sinds 1901. Het aantal zomerse dagen is ruwweg verdubbeld, van  $14 \pm 5$  naar  $27 \pm 9$  dagen. De jaartotale neerslag is toegenomen met  $120 \pm 100$  mm, en het aantal extreem natte dagen is met circa 40% toegenomen, van  $19 \pm 3$  naar  $26 \pm 3$  dagen. Andere onderzochte variabelen blijken niet significant te zijn veranderd, zoals de koudste dag per jaar en de maximum dagsom voor neerslag per jaar. Verder blijken de jaarlijkse temperatuur- en neerslagveranderingen homogeen over de maanden van het jaar verdeeld te zijn. Getalsmatig zijn er wel verschillen per maand of per seizoen, maar die blijken niet significant.

De veranderingen in het Nederlandse klimaat hebben reeds geleid tot significante veranderingen in weergegerelateerde impact-variabelen. Zo is de lengte van het groeiseizoen toegenomen met bijna een maand, en het aantal graaddagen per jaar, een maat gerelateerd aan ruimteverwarming, is afgenomen met  $14 \pm 5$  %.

Projecties van temperatuurveranderingen voor het jaar 2020 die gebaseerd zijn op statistische extrapolatie vanuit het verleden, zijn consistent met voorspellingen op basis van klimaatmodellen. Gevonden is dat de jaargemiddelde temperatuur in Nederland zal toenemen van  $10.4 \pm 0.4$  °C in 2003 naar  $10.7 \pm 0.6$  °C in 2010 en  $11.1 \pm 1.0$  °C in 2020. Hierdoor zal in de toekomst minder energie nodig zijn voor ruimteverwarming maar meer voor koeling. Dit klimaateffect zal zeer waarschijnlijk de projecties van CO<sub>2</sub>-emissies tot aan het jaar 2012 doen dalen met 3.5 Mton CO<sub>2</sub>-equivalenten, een resultaat dat relevant is voor de Nederlandse Kyoto-verplichtingen.

Tenslotte is onderzocht hoe de kans op een Elfstedentocht beïnvloed is door klimaatverandering. Het is gebleken dat de kans op een tocht aan het begin van de twintigste eeuw lag op 0.2, ofwel gemiddeld eens per vijf jaar. Deze kans is, na een toename tot 1950, afgenomen naar een kans van 0.10 in 2004, ofwel een gemiddelde terugkeertijd van eens per 10 jaar. De veranderingen liggen op de grens van statistische significantie. Binnen een klein aantal jaren zal blijken of de gevonden veranderingen inderdaad systematisch zijn.

*Trefwoorden:* elfstedentocht, graaddagen, groeiseizoen, klimaatverandering, onzekerheid

## **Preface**

Thanks goes to Jok Tang (TU Delft) who analysed a large number of climate indicators in the Netherlands. The analyses presented here, are a continuation of his work (Tang, 2003).

Albert Klein Tank, Adri Buishand and Theo Brandsma, all of KNMI, are thanked for their discussions on the reliability of weather data in the Netherlands, and for reviewing this report. Futhermore, Theo Brandsma kindly supplied the ice thickness data for the province of Friesland.

Arthur Petersen and Anton van der Giessen (both MNP/RIVM) are thanked for their thorough comments on earlier versions of this report.

# Contents

<b>SUMMARY</b> .....	<b>9</b>
<b>1. INTRODUCTION</b> .....	<b>11</b>
1.1 GOALS .....	11
1.2 HISTORICAL DATA.....	13
1.3 FUTURE PROJECTIONS .....	13
1.4 STATISTICAL APPROACH .....	15
1.5 THIS REPORT .....	15
<b>2. DATA AND META DATA</b> .....	<b>17</b>
2.1 TEMPERATURE .....	17
2.1.1 <i>Main observatory at De Bilt</i> .....	17
2.1.2 <i>Spatially averaged temperature record</i> .....	20
2.1.3 <i>Global temperatures</i> .....	22
2.2 PRECIPITATION .....	24
<b>3. ESTIMATION AND DETECTION OF TRENDS</b> .....	<b>29</b>
3.1 FLEXIBLE TRENDS .....	32
3.2 EXAMPLE .....	33
3.3 STRUCTURAL TIME-SERIES MODELS .....	35
3.3.1 <i>Model structure</i> .....	35
3.3.2 <i>How to choose the flexibility of the trend?</i> .....	38
3.3.3 <i>Predicting future data</i> .....	38
3.4 SOFTWARE .....	40
<b>4. ANNUAL MEANS AND ANNUAL CYCLES</b> .....	<b>41</b>
4.1 TEMPERATURE .....	41
4.1.1 <i>Annual means</i> .....	41
4.1.2 <i>Annual cycle</i> .....	43
4.1.3 <i>Are the results consistent with seasonal estimates?</i> .....	45
4.2 PRECIPITATION .....	47
4.2.1 <i>Annual totals</i> .....	47
4.2.2 <i>Annual cycle</i> .....	49
4.2.3 <i>Are the results consistent with seasonal estimates?</i> .....	51
<b>5. EXTREME WEATHER CONDITIONS</b> .....	<b>53</b>
5.1 TEMPERATURE .....	53
5.1.1 <i>Absolute minimum temperatures</i> .....	53
5.1.2 <i>Absolute maximum temperatures</i> .....	56
5.1.3 <i>Number of summer days</i> .....	58
5.2 PRECIPITATION .....	61
5.2.1 <i>Maximum daily precipitation</i> .....	61
5.2.2 <i>Number of extremely wet days</i> .....	64
5.2.3 <i>Maximum number of consecutive dry days</i> .....	67

<b>6.</b>	<b>TEMPERATURE-RELATED IMPACTS .....</b>	<b>71</b>
6.1	PREMATURE DEATHS DURING HEAT WAVES .....	71
6.1.1	<i>Low estimates</i> .....	73
6.1.2	<i>High estimates</i> .....	73
6.1.3	<i>Combination of estimates</i> .....	76
6.1.4	<i>Fewer premature deaths in winter</i> .....	76
6.2	CHANGES IN THE START OF THE GROWING SEASON .....	77
6.3	HEATING- AND COOLING-DEGREE DAYS .....	81
6.3.1	<i>Heating-degree days</i> .....	81
6.3.2	<i>Cooling-degree days</i> .....	83
6.4	OUTDOOR SKATING AND THE ‘ELFSTEDENTOCHT’ .....	85
6.4.1	<i>History</i> .....	85
6.4.2	<i>Indicator for maximum ice thickness</i> .....	87
6.4.3	<i>Trend estimate ‘Elfstedentocht’ indicator</i> .....	89
6.4.4	<i>Chance for an ‘Elfstedentocht’</i> .....	91
<b>7.</b>	<b>FUTURE WEATHER CONDITIONS: A TWO-WAY APPROACH .....</b>	<b>95</b>
7.1	PREDICTING GLOBAL WARMING UP TO 2020 .....	98
7.2	PREDICTING LOCAL WARMING UP TO 2020 .....	100
7.3	CONSEQUENCES FOR WEATHER-RELATED INDICATORS .....	105
7.3.1	<i>Heating-degree days</i> .....	106
7.3.2	<i>Premature deaths</i> .....	110
<b>8.</b>	<b>SUMMARY AND CONCLUSIONS .....</b>	<b>111</b>
	<b>REFERENCES .....</b>	<b>119</b>
	<b>Appendix A Comparison of historical station data .....</b>	<b>125</b>
	<b>Appendix B Wind .....</b>	<b>133</b>
	<b>Appendix C Global and local climates are connected .....</b>	<b>141</b>
	<b>Appendix D Cooling- and heating-degree days in 2040 .....</b>	<b>150</b>



## SUMMARY

Recently, the Dutch Parliament raised the Commission Climate Change. This commission poses the following questions, among others: (i) what are actual insights and dimensions of climate change for the Netherlands, (ii) how should uncertainties be judged, (iii) what can we expect for the near future, and (iv) what policy measures should be taken to mitigate adverse societal and economical consequences of climate change? This report is directed to the first three questions.

The method applied here is that of a rigorous time-series analysis, applied to a set of homogenized weather data in the Netherlands (non-homogenized data are characterized by changes in instrumentation, changes in the height of an instrument, changes in location of the instrument and/or changes in the environment of the instrument). The time-series approach is based on Structural time series analysis and the Kalman filter. This approach yields, apart from flexible trend estimates, *uncertainties* for changes in the trend estimates.

Results reveal that a number of daily temperature and precipitation series can be regarded as homogeneous over the period 1901-2003. However, series for wind speed and wind direction were not reliable enough for trend analyses. Subsequently, the latter data have not been analysed.

Statistical trend analyses reveal changes in Dutch climate that are statistical significant over the last century: annual temperatures have increased by  $1.5 \pm 0.5$  °C, annual precipitation sums by  $120 \pm 100$  mm. The length of the growing season has increased by nearly a month, and the number of heating-degree days, a measure for the energy needed for the heating of houses and buildings, has decreased by  $14 \pm 5\%$ . Over the course of the 20<sup>th</sup> century the chance on an 'Elfstedentocht', an outdoor skating event in the Netherlands, has decreased from once every five years to once every ten years. Even though this impact change is not yet statistically significant, it resides 'on the edge' of significance.

Statistical extrapolation of future temperatures shows to be consistent with projections based on GCM calculations. Temperatures will continue to increase from  $10.4 \pm 0.4$  °C in 2003 to  $10.7 \pm 0.6$  °C in 2010 and  $11.1 \pm 1.0$  °C in 2020. As a consequence, emissions of CO<sub>2</sub> equivalents for the year 2010 are likely to be 3.5 Mton lower than is to be expected on economic grounds and a stable climate for the near future.

The trends identified clearly show the need for policy measures to mitigate the consequences of climate change. The projected warming and subsequent increase in extreme weather conditions will have significant societal impacts, even on the short term.



# 1. Introduction

## 1.1 Goals

What are the actual insights and dimensions of climate change for the Netherlands, and to what extent are these caused by the greenhouse effect? How should uncertainties be judged? What policy measures should be taken in the near future, and what will be the societal, economic and environmental implications of these measures? These represent the main questions recently posed by the Dutch Parliament to the *Commission Climate Change*.

The report before you will focus on the first three questions raised above, concerning actual insights and dimensions of climate change for the Netherlands and ways to judge uncertainties. More specifically, the following questions are dealt with.

- What are the trends in weather conditions in the Netherlands over the past century? What is the uncertainty in these trends?
- Have there been shifts in the frequency of extreme events such as heat waves or droughts? To what extent are these shifts certain/uncertain?
- What are societal impacts of weather conditions or weather extremes? How have these impacts evolved over the past century?
- Is it permissible to extrapolate trends in weather conditions over the past century to the near future, i.e. the years up to 2020?
- If so, what should we expect in the 16 years ahead? And what are the uncertainties in these projections?

As for changes in weather conditions, trends are often presented for annual averaged temperatures or annual totals of precipitation. These series have been published in numerous publications, such as IPCC (2001) and the references contained. Annual series in the Netherlands can be found in KNMI (2003) and MNP (2003, 2004).

Of equal importance are *extreme* weather conditions. In fact, societal implications of weather extremes are much more severe than changes in annual averages. Because of the importance of extremes, the European Climate Support Network (ECSN) took the initiative in 1998 for a European Climate Assessment (ECA) project. Key questions were ‘*how did the past warming affect the occurrence of temperature extremes*’ and ‘*was the past warming accompanied by a detectable change in precipitation extremes*’? The Royal Netherlands Meteorological Institute (KNMI), coordinator of the project (Klein Tank *et al.*, 2002a; Klein Tank, 2004), has pointed out that small shifts in annual averages may lead to disproportionate shifts in the chance of extreme events, making the study of extremes even more important. This aspect is illustrated in **Figure 1.1**.

On the one hand, this report answers the same questions as posed by the KMNI project, although only for the Netherlands, but on the other, questions on ‘how weather-related impacts evolved’ and ‘what future developments are expected up to 2020’ are also answered.

As for weather-related impacts, only a limited number of situations are dealt with here: (i) the influence of warm periods on premature deaths, (ii) shifts in the onset of the growing season, (iii) the influence of climate change on the number of heating-degree days and (iv) the effect of global warming on the chance of maintaining outdoor skating, a sport very popular in the Netherlands.

A number of impacts are not dealt with here, such as: forest fires, extension of the hay fever season, storm damage, bad harvests due to drought or due to large amounts of rain in a few days time, and flooding of the Meuse and Rhine. Positive impacts could be: increasing harvests due to prolonged growing season, winegrowing and tourism. An even larger set of impacts has been defined in EEA (2004) and impacts are described in a more popular form in a special issue of National Geographic (2004a,b).

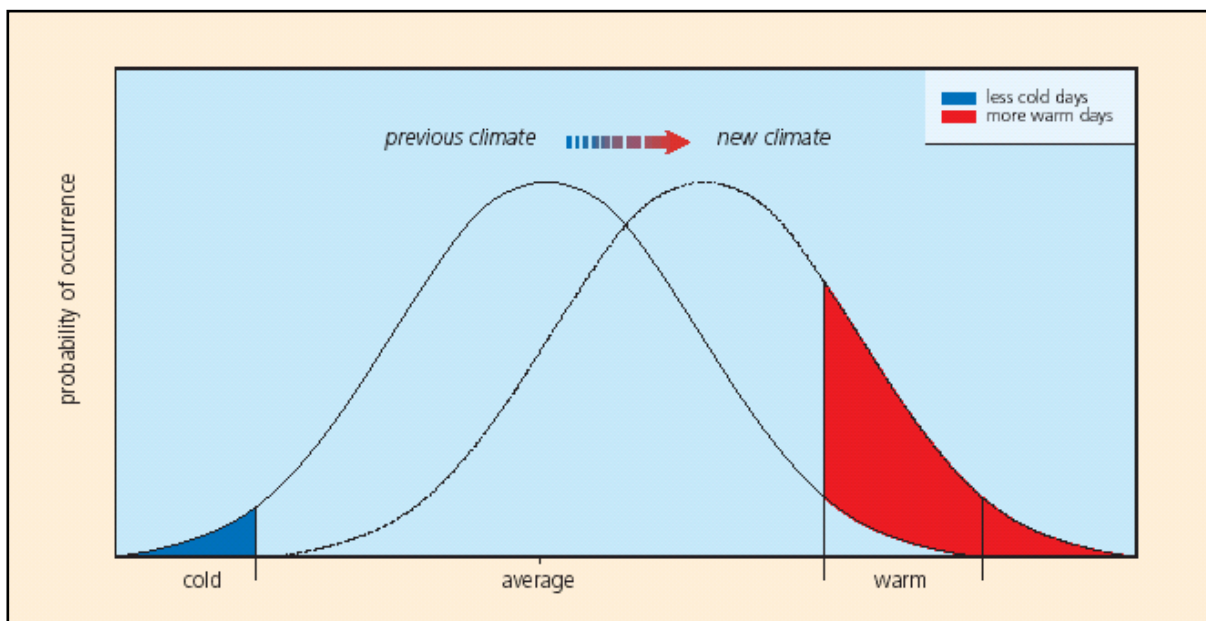


Figure 1.1 Schematic effect on the number of cold and warm days for a ‘symmetric’ increase in the mean temperature. Source: Klein Tank et al. (2002a).

## 1.2 Historical data

We are very fortunate in the Netherlands to have a large number of historical time series available. Recently the KNMI published a number of series extending back to the 18th and 19<sup>th</sup> centuries, all data measured before the start of the KNMI in the year 1854 (this year is the 150<sup>th</sup> anniversary of the institute!). However, the use of these historical data is limited for use in *long-term trends*, as is explained below. For the analyses reported here, 1901 was chosen as the initiation year, although many data prior to this date are available. Here, 1901 is the starting year of the main observatory at location De Bilt.

The reason for limiting the use of these data is our uncertainty on the homogeneity of these series influenced by:

- changes in instrumentation
- changes in the height of an instrument
- changes in locations of instruments and
- changes in the surroundings of the stations, such as the growth of trees.

The main source of data was the main observatory of KNMI in De Bilt, as shown in **Figure 1.2**. The photo shows an open pagoda type of screen, a pluviograph hut just in front of the pagoda and, more to the right, the open precipitation instrument, which has been manually recorded every day at 8.00 hours since 1901.

## 1.3 Future projections

As for future data, a robust approach has been chosen, in which weather conditions are predicted in two-ways: one method is based on GCM predictions for both natural and anthropogenic warming, the other method is purely based on historical data.

The simple idea behind this two-way approach is that one can be more confident in future developments if two independent approaches yield similar and consistent results. Furthermore, it is generally felt amongst climatologists that future trends are best predicted by GCMs, while the year-to-year variability is best captured by analysing historical data. The latter variability is not captured good enough by GCMs with their inherent uncertainties and large grid sizes.

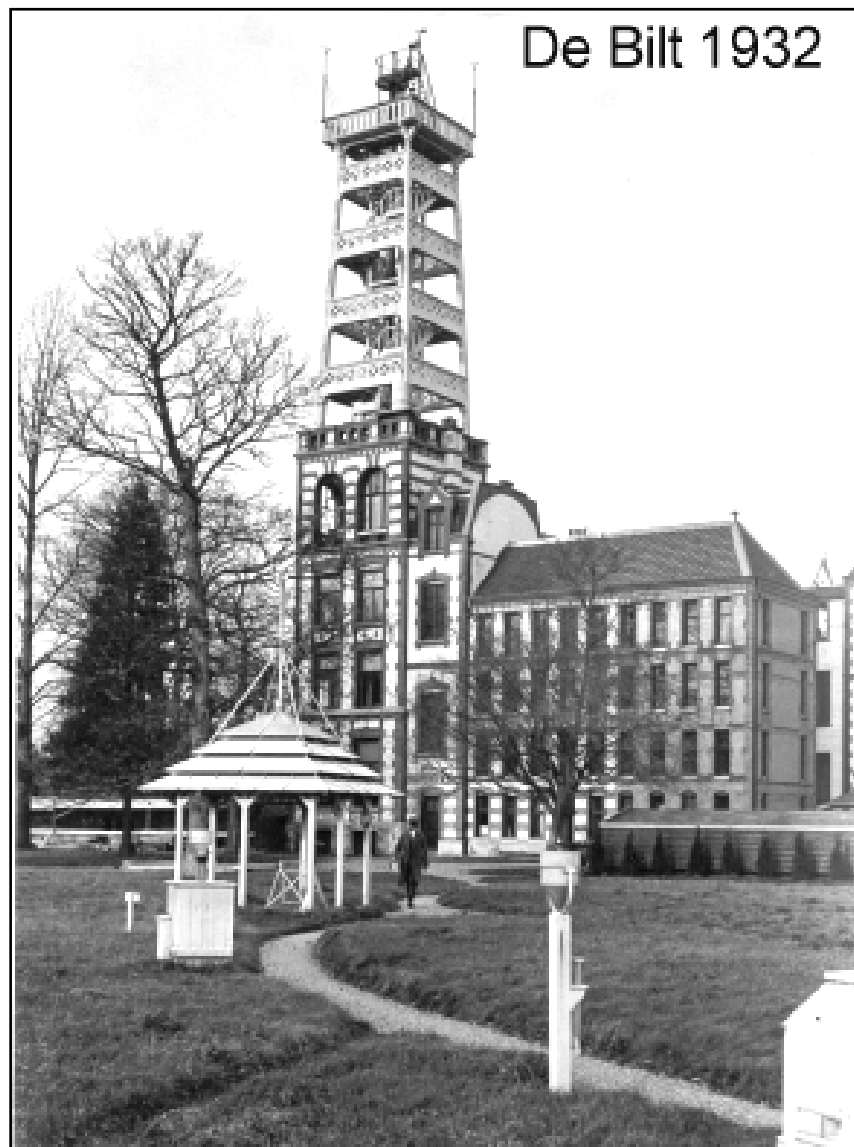


*Figure 1.2* Main KNMI observatory in De Bilt in a photo taken around 1932. Shown are the pagoda type of measurement screen (to the left, in front of the tower) and the rain gauge (to the far right up front). Photo: KNMI.

## 1.4 Statistical approach

An important aspect of the approach followed here concerns the *statistical treatment of trends*. There are many methods available for estimating (flexible) trends in data. However, the number of suitable methods are limited if one is interested in estimates for *uncertainty*.

Why is uncertainty important within this context? Suppose some weather-related variable  $x_t$  has a value of 9.0 in 1901 and 10.0 in 2003. It is tempting to conclude in this case that this variable has increased over a century. However, if the year-to-year variability follows a normal distribution with a standard deviation of 0.5, the 95% confidence limits are  $\pm 1.0$ . In other words,  $x_{1901} = 9.0 [8.0, 10.0]$  and  $x_{2003} = 10.0 [9.0, 11.0]$ . Clearly, uncertainties are too large for drawing inferences on significant increases. At best, one could conclude that there is a *tendency* to increase. More data are needed to prove the significance of this tendency (in most cases confidence limits become narrower as more data become available).

Visser (2003; 2004) has presented an approach in which three trend-derived uncertainties are estimated, the most notable of which is the uncertainty in the trend estimate in the final year relative to trend estimates in all preceding years. This approach is followed throughout this report.

## 1.5 This report

The report will continue in Chapter 2 to describe the data and meta data, i.e. the history of stations and instrumentation. The statistical approach is given in Chapter 3, while Chapter 4 analyses trends of annually averaged temperatures and annual sums of precipitation. The yearly cycle for precipitation is given as well. Chapter 5 is devoted to a select number of extreme weather indicators, such as the coldest and hottest moments in a year, or the maximum number of consecutive dry days. Chapter 6 deals with four temperature-related impact variables, such as the number of premature deaths during warm summers.

Subsequently, there is a switch to *future* climate change in Chapter 7. Here it is verified if trends estimated over the 1901-2003 period can be extrapolated to the 2004-2020 period. Chapter 8 brings the report to a close with the conclusions.

The report ends with three Appendices giving details not mentioned in the main text. For policy purposes a special Appendix has been inserted giving predictions for heating- and cooling-degree days over the period 2004 - 2040.



## 2. Data and meta data

The origin of the weather record used throughout this report is described here, along with the history of the series, i.e. the meta data. Because the goal here is to detect changes over more than a century's time, we have to be very careful for inhomogeneities, inducing false trends.

For example, if a temperature record shows a warming trend over the 1901-2003 period, it is easy to make inferences on climate warming, possibly due to the enhanced greenhouse effect. However, such warming could be (partially) caused by urbanization in the surroundings of the station. Thus, the effect of urbanization should be dealt with in temperature records. Other sources of inhomogeneity are relocations of the station, changes in the height of the instrument, changes in the type of instrument, and changes in the station surroundings, such as tree growth.

Temperature records will be covered in section 2.1, precipitation sums in section 2.2. Conclusions are drawn in section 2.3. Records of windspeed and wind direction are treated in Appendix A. Because of a lack of homogeneity these records fall short. For applications on relative short time series (1961 onwards) the reader is referred to KNMI (2003, p. 14) and Smits, Klein Tank and Können (2004).

### 2.1 Temperature

#### 2.1.1 Main observatory at De Bilt

The station called De Bilt (52.10 °N, 5.18 °E, 2.0 m) is representative of the mean climate conditions in the Netherlands (see **Figure 1.2**). Its temperature series is considered to be the most homogeneous long-term record of the Netherlands. The daily mean temperature series for De Bilt, from 1901 to date is available from the KNMI website and the European Climate Assessment data set (Klein Tank *et al.*, 2002, [www.knmi/samenw/ECA](http://www.knmi/samenw/ECA)). Series can also be downloaded from the KNMI website ([www.knmi.nl/product](http://www.knmi.nl/product)). Click on [English] and choose data in the upper panel on the page). The meta data can be found on this website as well.

The monthly means of this series have recently been homogenized by Brandsma (Brandsma *et al.*, 2003) for the effects of a relocation and change of the thermometer screen in 1950, another relocation in 1951, the lowering of the screen from 2.20 m to 1.50 m in 1961 and urbanization effects. For the 1951-1970 period the monthly mean temperature is now derived from hourly 'climatological measurements'. The 'synoptic measurements'— which, for

practical reasons, have been used up to now for that period – are inferior in quality. The size of these corrections is about 0.2 K; a few months in the 1950-1960 period have corrections of more than 0.4 K. Changes in the measurement screen in 1980 (wood to plastic) and 1993 (Stevenson to unventilated saucer) have not yet been corrected for, but these corrections are estimated to be much smaller. The need for an urbanization correction is illustrated in **Figure 2.1**.

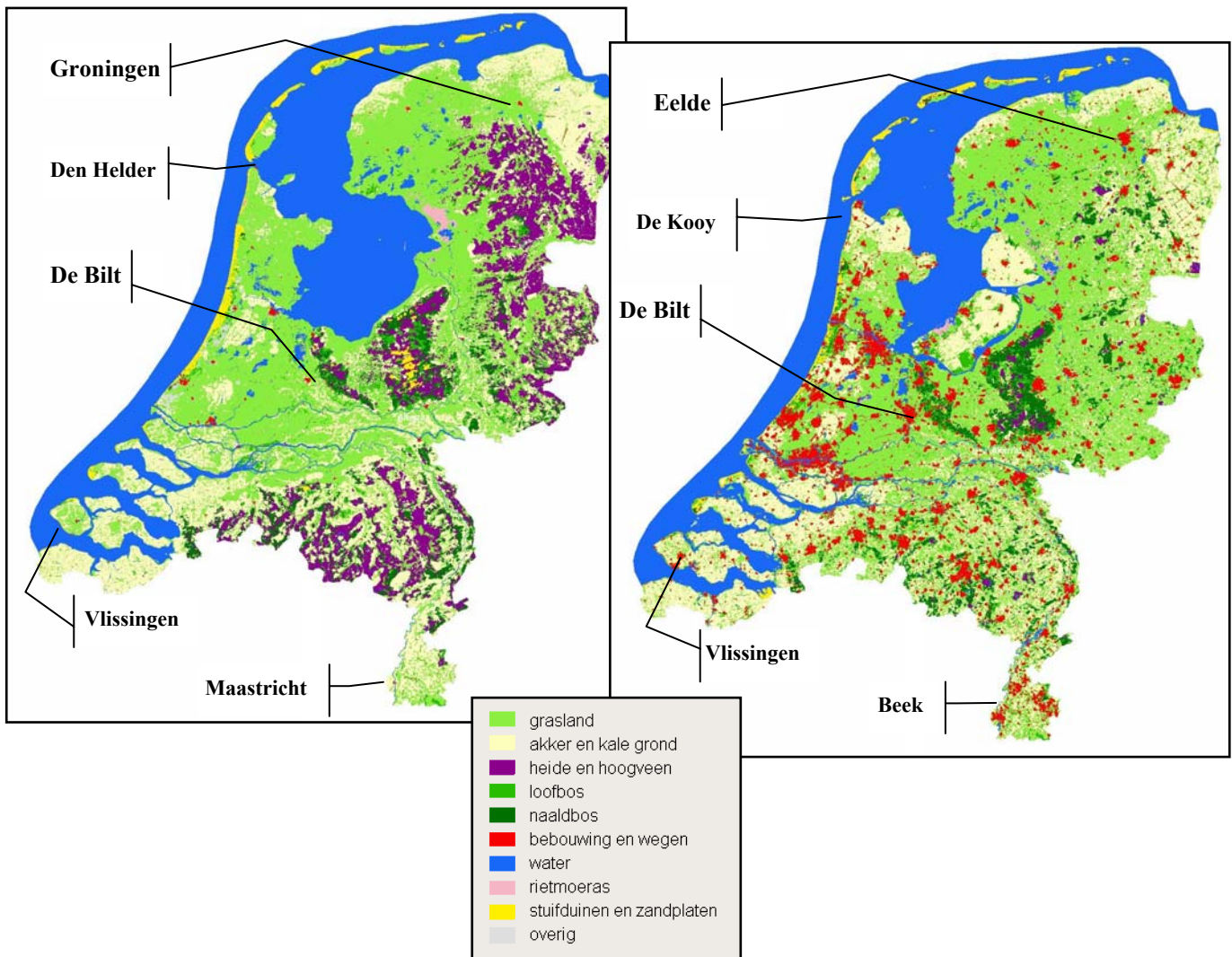


*Figure 2.1 Land-use changes from the year 1900 (left panel) to the year 2000 (right panel).*

The five main observatories are also shown in the maps. Three observatories were moved to an airport nearby. Legend is (from top to bottom): grassland, crops and bare ground, heathland and high moorland, deciduous forest, coniferous forest, built-up areas and roads, water, reedy swamps, shifting dunes and sandbars, other uses. Source: HGN database, Alterra ([www.hgnnederland.nl](http://www.hgnnederland.nl)).

The degree of urbanization (the red areas in the figure) has strongly increased since 1900 (left panel). De Bilt is located just east of the city of Utrecht, which grew immensely in the last century. Brandsma derived a correction factor for annual averaged temperatures of  $0.10 \pm 0.06$  K, which is in fact relatively small.

A number of analyses in this report are based on *daily* data rather than monthly averages. To use the improvements found by Brandsma, each daily temperature (daily average, daily maximum and daily minimum temperature) was adjusted using the correction factors found by Brandsma for the *monthly* averages. In this way we three semi-homogeneous daily records could be constructed. However, it should be noted that daily minimum and maximum temperatures are more sensitive to changes in the height of thermometers (Brandsma found for the lowering of an instrument from 220 cm to 150 cm, that the daily cycle will increase by 0.33 K).

There is only one situation where we have to be careful, i.e. the warmest moment of a year (section 5.1.2). This indicator is very sensitive to type of screen. The open pagoda type of screen, used from 1901 to 1950, will tend to give temperatures that are somewhat too high on sunny days with low wind speeds (see **Figure 2.2**). Under these circumstance the air under

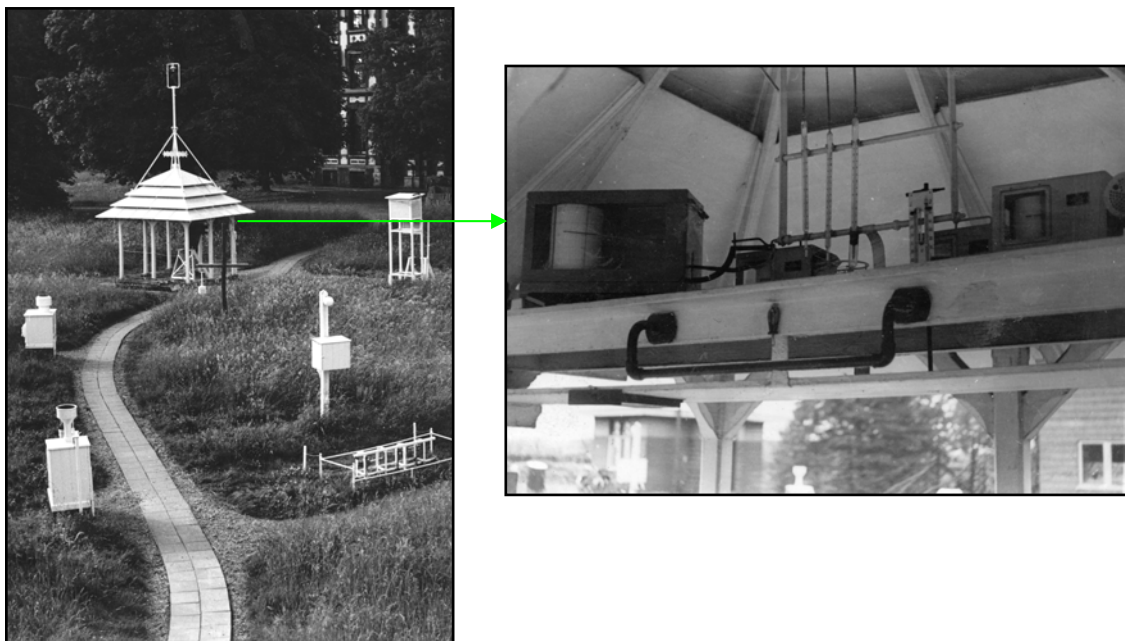


*Figure 2.2* Pagoda type of measurement screen at De Bilt.

The photo left shows an interesting detail: a Stevenson cabin to the right of the pagoda screen. Temperature recordings from this screen would be useful for homogenization purposes. However, according to the station manager these recordings were lost, probably due to reductions in archive space... The photo on the right shows the thermograph along with min-max thermometers.

the roof of the ‘pagoda’ will be heated by sunlight reflected by the ground around the screen, creating, in fact, a ‘micro greenhouse effect’.

### 2.1.2 Spatially averaged temperature record

At the start of the 20<sup>th</sup> century five major observatories were erected. These were Den Helder, Groningen, De Bilt, Vlissingen and Maastricht. Their locations are given in **Figure 2.1**. The stations were chosen the ‘corners of a rectangle’, with De Bilt situated around the crossing of the diagonals of this rectangle. The stations are shown in **Figure 2.3**. Daily data can be downloaded from [www.knmi.nl/samenw/ECA](http://www.knmi.nl/samenw/ECA).

The stations Den Helder, Groningen and Maastricht have been moved to airports nearby: De Kooy, Eelde and Beek, respectively. The influence of these movements on homogeneity is shown for annual averaged temperatures in the scatter-plot matrix in **Figure 2.4**. The scatter plots show two parallel lines for Maastricht station. It has been verified that one line corresponds to the 1901- 1972 period (Maastricht) and the other line to 1973-2003 (Beek). Therefore, Maastricht/Beek has been omitted for a check on homogeneity at the De Bilt station.

A comparison between the De Bilt record and the four-station mean records is given in **Figure 2.5**. The upper panel shows the scatterplot between each series. The graph shows a good correspondence between both series ( $R = 0.99$ ), with results indicating, from a different angle, that the homogenized De Bilt series is reliable for use in trend analyses.

Graphs analogous to Figure 2.5, are shown in **Appendix A** for the indicators treated in Chapter 5. These indicators are: absolute minimum and maximum temperatures, number of summer days, maximum daily precipitation, number of extreme wet days and the maximum number of consecutive dry days.

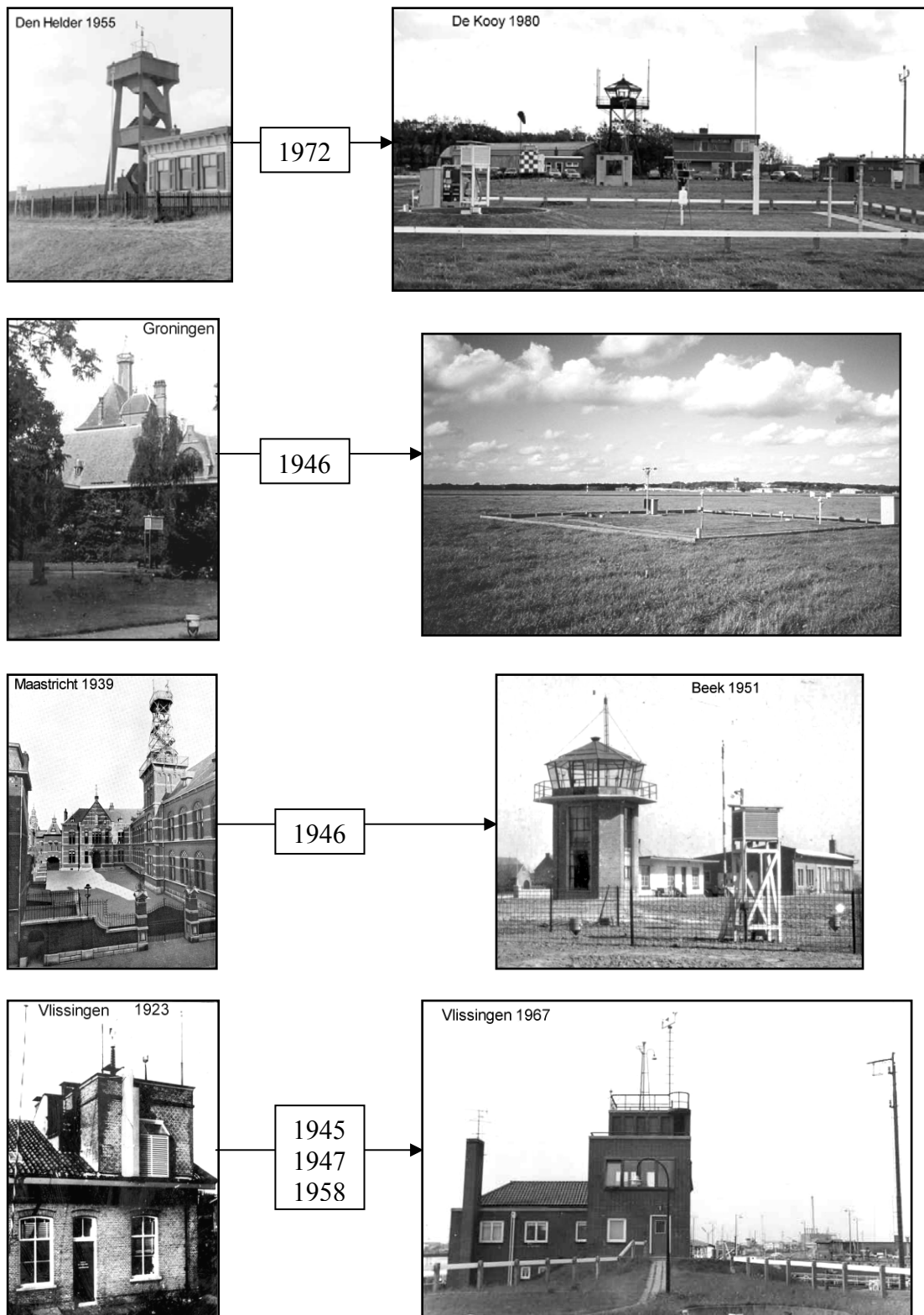


Figure 2.3 From top to bottom: the stations of Den Helder - De Kooy (moved in 1972), Groningen - Eelde (moved in 1946), Maastricht - Beek (moved in 1946) and Vlissingen (moved in 1945, 1947 and 1958 in the Vlissingen area).

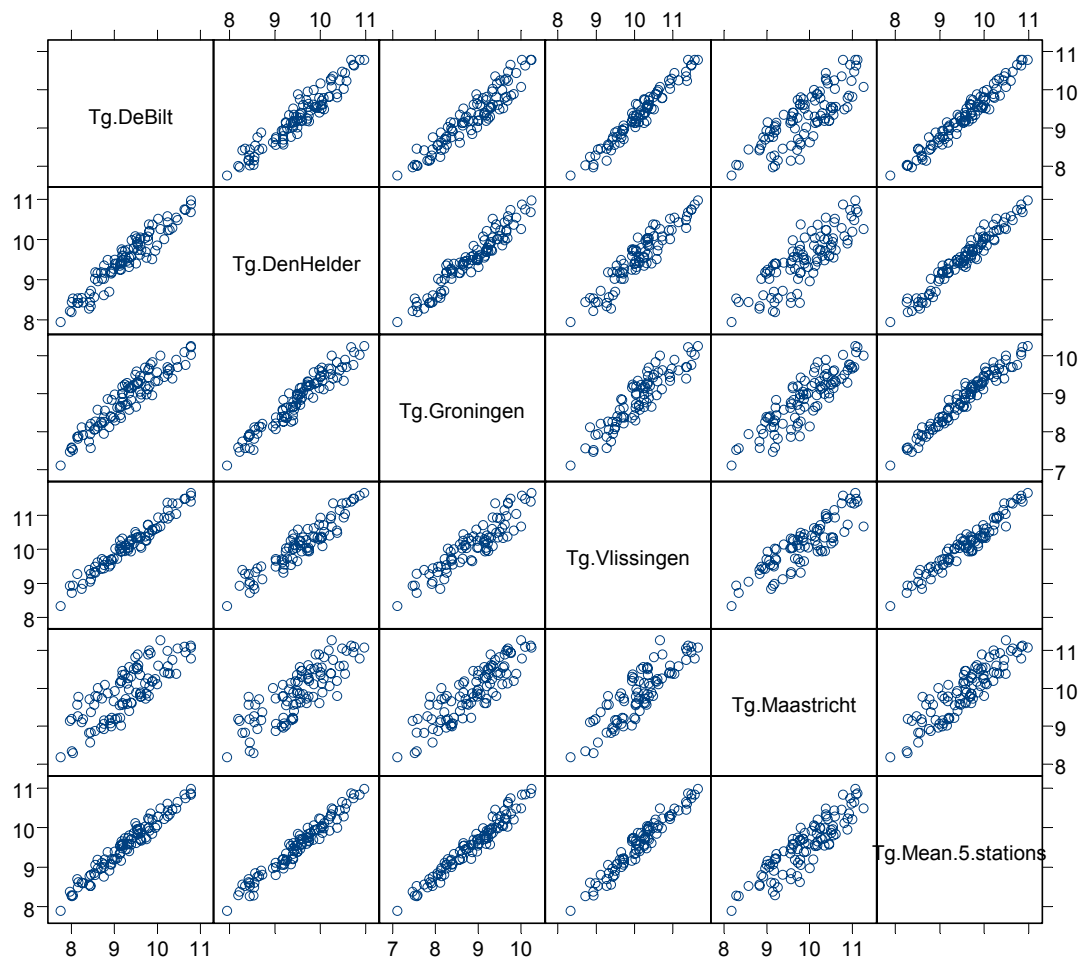


Figure 2.4 Scatterplot matrix for annual averaged temperatures at De Bilt, Den Helder, Groningen, Vlissingen and Maastricht. Scatterplots for the average of these five stations are also shown.

### 2.1.3 Global temperatures

The global temperatures used in this report are taken from Jones *et al.* (2001). Data can be downloaded from [www.cru.uea.ac.uk/cru/data/temperature](http://www.cru.uea.ac.uk/cru/data/temperature). For discussions on the construction and homogeneity of this series please refer to Jones (2001) and references contained. The series was extensively used in IPCC (2001).

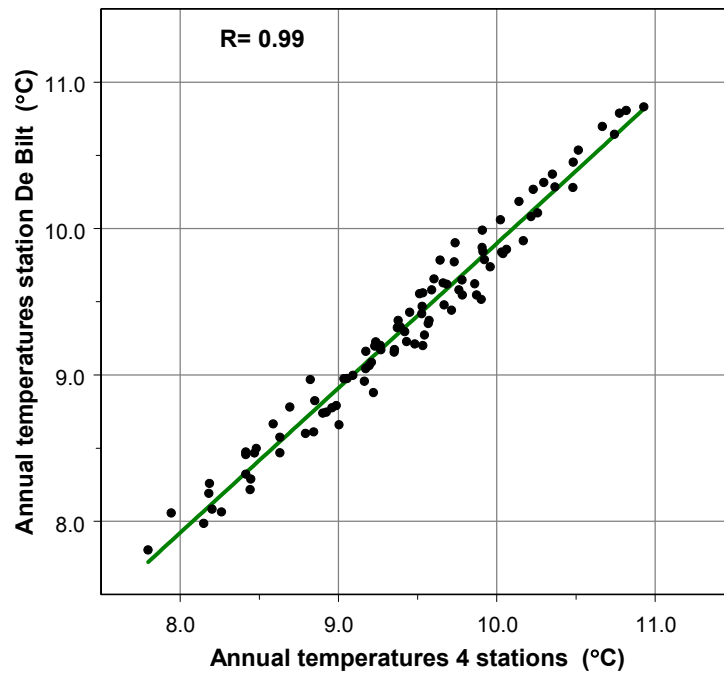
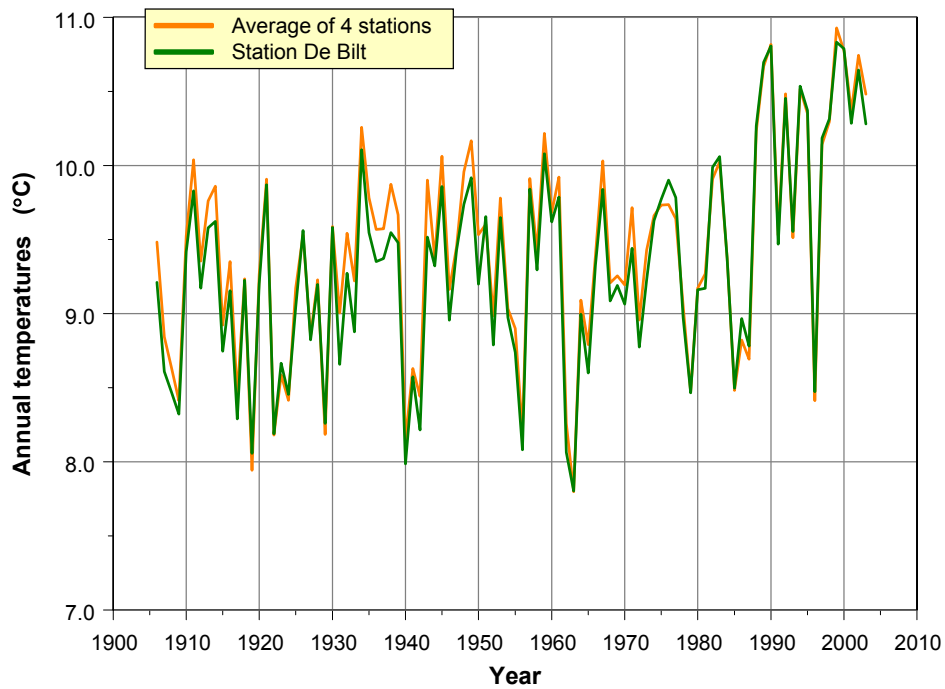


Figure 2.5 Time series of annual temperatures for the De Bilt station (green line) and annual averages of four stations (Den Helder, Groningen, De Bilt and Vlissingen; orange line). The lower panel shows the scatter plot between both series.

The correlation coefficient is 0.99. Period is 1906 – 2003.

## 2.2 Precipitation

Within the ECA project 13 stations in the Netherlands were homogenized over the 1901-2003 period (Klein Tank *et al.*, 2002b). Station names are, from north to south: West Terschelling, Groningen, Den Helder, Ter Apel, Hoorn, Heerde, Hoofddorp, De Bilt, Winterswijk, Kerkwerpe, Oudenbosch, Axel and Roermond. All these stations were corrected for a lowering of the instrument from 2.0 m to 0.50 m (Bruin, 2002). As homogeneity tests can be found on the ECA website, they are not repeated here. See **Figure 2.6**.

The daily time series are all taken from the manual network. Within this network precipitation is recorded by an observer every day at 8.00 hours (**Figure 2.7**). An important advantage of measurements taken manually over automated stations using pluviographs is that long-term trends in the latter series may be biased due to calibration errors, changes in types of pluviographs, and incidental influences of leaf fall, hail and snow.

Errors in *manual* measurements on the other hand will be *random* rather than *systematic* (bias). Readings from the observer may be incidentally too high or too low, or sometimes somewhat before or after 8h.00 or even forgotten for one day. However, by taking precipitation sums over months or years these errors will average out. For more detailed information the reader is referred to Buishand and Velds (1986) and Bruin (2002).

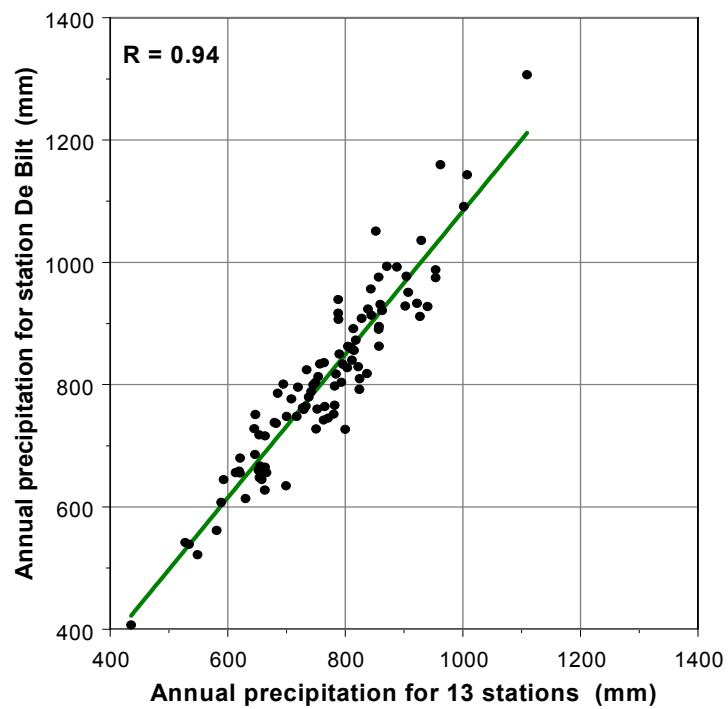
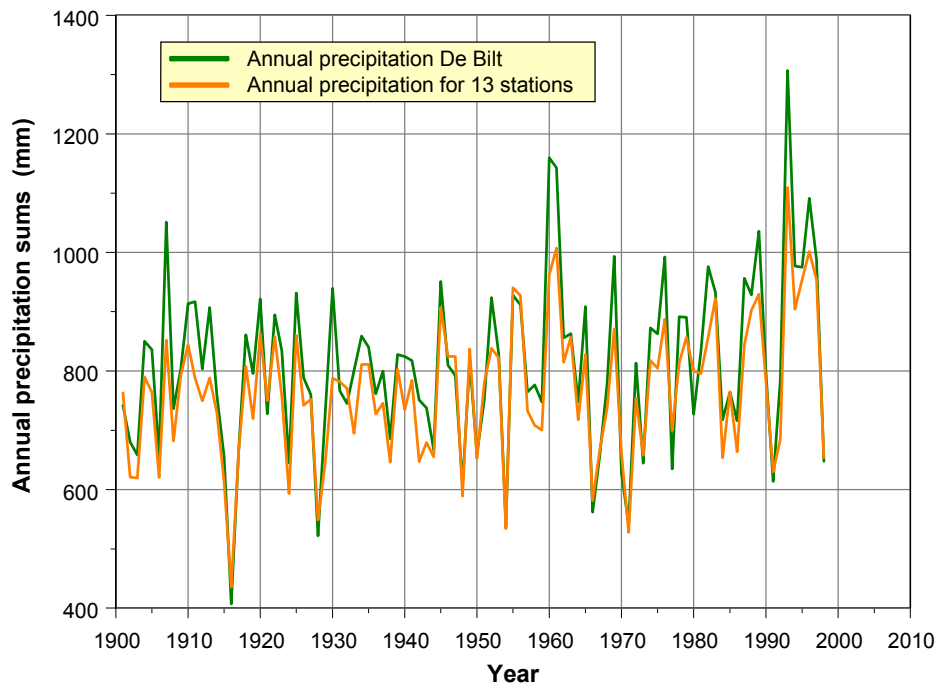
The annual totals of precipitation for De Bilt and the 13-station records are compared in **Figure 2.8**. Both series appear to be very similar. The correlation coefficient is  $R = 0.94$ , a relatively high value, signifying the fact that though precipitation is a phenomenon which occurs on more local scales than temperature, this locality is largely smoothed out on a yearly basis.



Figure 2.6 Map of the Netherlands showing 283 precipitation stations, divided over 15 precipitation districts. All stations have been in operation since 1970. The stars refer to the 13 stations used in this report.



*Figure 2.7 Observer at Hoofddorp station. Photo: H. Visser.*



*Figure 2.8* Time series of annual precipitation sums for De Bilt (green line) and the annual sums of 13 stations (location given in **Figure 2.6**; see orange line). The lower panel shows the scatter plot between each series. The correlation coefficient is 0.94 and the period covers 1906 – 2003.



### 3. Estimation and detection of trends

In this chapter a trend estimation approach is introduced which allows the estimation of flexible trends with corresponding uncertainty information on the trend itself and trend increments. The latter information is important for the question: is the final trend estimate larger or smaller than some trend estimate in the past, given the uncertainty ('noise') in the data? The importance of such information is illustrated in the inset ( $9 > 10$  ???!).

The methodological aspects of estimating flexible trends (versus linear trends) will be given in section 3.1, and clarified by an example in section 3.2. Section 3.3 gives a concise summary of the mathematical formulation of the trend models used throughout this report, and section 3.4 describes the corresponding TrendSpotter software.



*Systematic treatment of uncertainties in trend estimates is essential for drawing robust inferences on climate change.*

*A general framework for dealing with uncertainties is given in Petersen et al. (2003).*

*Photo: H. Visser.*

### 9 > 10 ???!

The trend models throughout this report are taken from the class of *structural time series models*. The rationale is not that these trend models are necessarily *better* than other trend models, such as moving averages or splines, but that uncertainty information is easily gained. Why is such uncertainty information important? We will illustrate this by a hypothetical example showing that two measurements or estimates X and Y do not necessarily follow the standard calculation rules. Of course,  $9 < 10$ , but is it possible that  $10 < 9$ ? The answer is ‘yes’ if both variables have measurement or modelling errors.

Suppose the errors in X and Y follow normal distributions with expectations 9.0 and 10.0, respectively. As variances we choose  $0.4^2$  for X and  $0.5^2$  for Y. In statistical notation:  $X \approx N(9.0, 0.16)$  and  $Y \approx N(10.0, 0.25)$ . Both probability density functions are shown in **Figure 3.1A**. The figure shows that there is a (small) chance that  $X > 10.0$ :  $P(X > 10.0) = 0.6\%$ , and a chance that  $Y < 9.0$ :  $P(Y < 9.0) = 2.3\%$ . Thus, there is a chance that  $X > Y$ , although their expected values are 9.0 and 10.0, respectively.

The chance that  $X > Y$  follows from the distribution of Z:  $Z = Y - X$ . If X and Y are mutually independent, it follows  $Z \approx N(1.0, \text{var}(X) + \text{var}(Y))$ , or  $Z \approx N(1.0, 0.41)$ . The

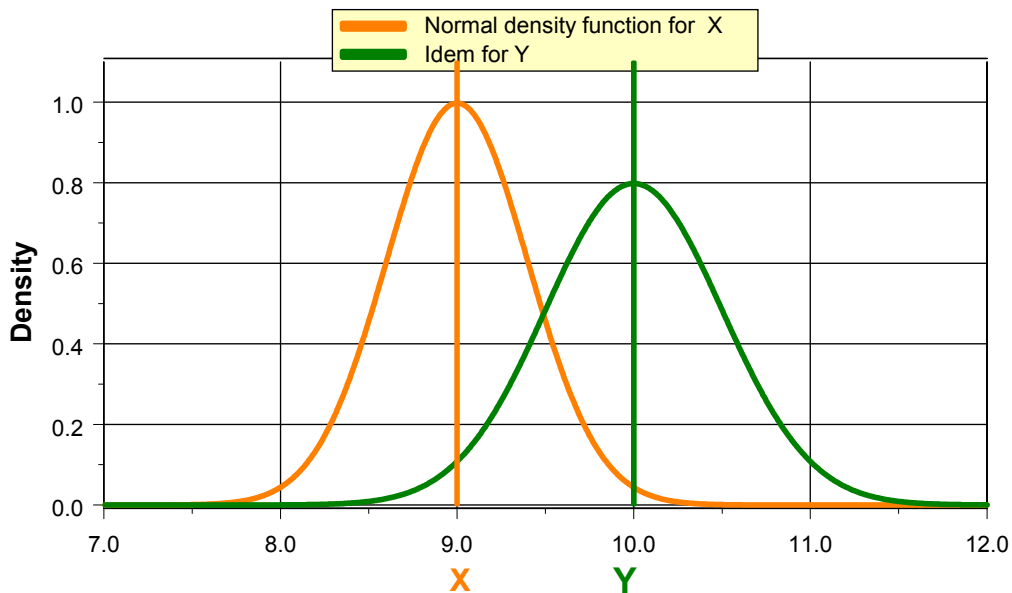


Figure 3.1A Normal probability density functions of X and Y.

probability function of  $Z$  is shown in **Figure 3.1B** (black line). It is found that  $P(Z < 0.0) = 5.9\%$ .

However, the variables may be correlated, for example with a correlation coefficient of  $R = 0.70$ . Now, the variance of  $Z$  will be **smaller**:

$$Z \approx N(1.0, \text{var}(X) + \text{var}(Y) - 2.0 \cdot \text{cov}(X, Y)), \text{ or } Z \approx N(1.0, 0.21)$$

The probability function of  $Z$  is also shown in Figure 3.1B (blue line). Now, it is found that  $P(Z < 0.0) = 1.5\%$ .

This hypothetical example shows that measurements or model outputs do not always follow traditional calculation rules. Although the expectation of  $Y$  is larger than that of  $X$ , it can be found that  $X > Y$ , in the examples above with a chance of 5.9% and 1.5%.

In this report the variable  $X$  can be seen as a trend estimate for some historic year  $t$  ( $\mu_t$ ), with  $1900 < t < 2003$ , and  $Y$  as the trend estimate for the year 2003 ( $\mu_{2003}$ ). If we want to draw inferences on trends, we have to know the probability distribution of the difference  $Z = \mu_{2003} - \mu_t$ . Here, the variables  $\mu_{2003}$  and  $\mu_t$  are typically correlated. The distribution of  $Z$  follows from Kalman filter theory (Visser, 2004). The importance of having significance limits for the trend differences  $\mu_{2003} - \mu_t$  has been demonstrated.

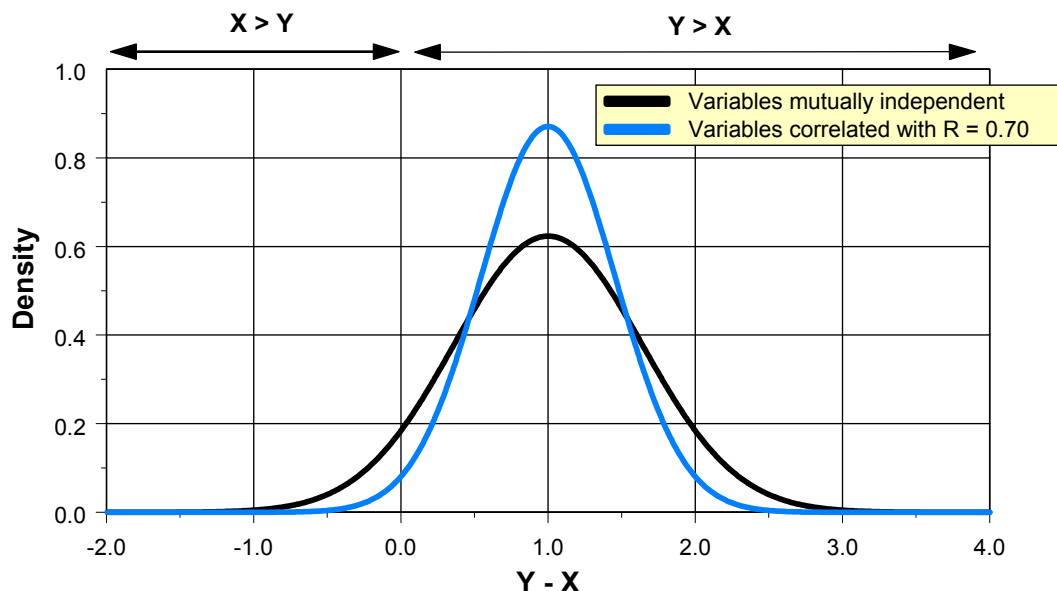


Figure 3.1B Probability density functions for the difference  $Z = Y - X$ .

### 3.1 Flexible trends

Many studies on trend estimation deal with linear or monotonously increasing/decreasing trends. For example, Hess *et al.* (2001) presented an overview of six statistical methods for this type of trend. However, not all trends in environmental applications behave in a more-or-less linear manner. If one analyses historical climate data such as temperatures or precipitation sums over a period of centuries, alternating periods of increase or decrease are seen, as well as periods where the variable is more-or-less constant. Linear trends do not give sufficient information for these kinds of situations and could even be misleading. Another situation where linear trends may lead to incorrect inferences, is that of data with strong serially correlated errors (Woodward and Gray, 1993 and 1995, and references in Visser, 2004, Appendix B).

If we are interested in the *significance* of a trend, there are also important differences between linear and flexible trend estimation. A test for a linear or monotonous trend will have only one answer – ‘yes’ or ‘no’. Or more formally, we either fail to reject the null hypothesis ( $H_0$ ) of no trend, or reject it, given some choice for  $\alpha$ . Here  $\alpha$  stands for the chance of rejecting  $H_0$  while it is true in reality.

For example, one could choose the ordinary least squares (OLS) regression trend line (section 3.3 in Hess *et al.*, 2001). The model is formulated as follows:  $y_t = a + b \cdot t + \varepsilon_t$ , where  $\varepsilon_t$  is a white noise process. Here, the trend,  $\mu_t$ , is defined as  $a + bt$ , with  $t = 1, \dots, N$ . The significance of the trend follows directly from the variance  $\sigma_b^2$  of the slope  $b$ . If  $-2 \cdot \sigma_b < b < 2 \cdot \sigma_b$ , the decision fails to reject the  $H_0$  hypothesis, and there is no significant trend.

In the case of a flexible trend, the slope  $b$  becomes *time-dependent* and a single test on slope will no longer suffice. Now the variances of all possible trend differences,  $\mu_t - \mu_s$  could be of interest. Since the presentation of all these differences is not practical, the following two functions of time will be useful:

- $\mu_t$  with corresponding  $2 \cdot \sigma_t$  confidence limits,  $t = 1, \dots, N$ . These limits are also calculated in the case of the OLS regression trend.
- the lagged differences,  $\mu_N - \mu_t$ , with corresponding  $2 \cdot \sigma_t$  confidence limits,  $t = 1, \dots, N$ .

The first function allows us to test significant differences at certain levels. The second function, with the form  $\mu_N - \mu_t$ , was chosen since, in practice, we are interested in how the present ( $\mu_N$ ) deviates from the past ( $\mu_t$ ). Are present levels of temperature or precipitation significantly lower than those in the preceding years? Policymakers typically want to know

whether *recent* values are extraordinary or not. This wish is reflected in the choice of the function,  $\mu_N - \mu_t$ .  $N$  will be the year 2003 throughout this report.

The approach will be illustrated in the following by an example in section 3.2, and a short description of the mathematical background given in section 3.3. Software is described in section 3.3. For a more detailed description the reader is referred to Visser (2003; 2004).

## 3.2 Example

**Figure 3.2** shows a series of annually averaged global temperatures over the 1901-2003 period (black line). The series is extensively used in publications such as IPCC (2001); compare this to section 2.1.3.<sup>1)</sup> It should be noted that the average global temperature over the 1960-1990 period has been subtracted from all annual data, leading to a ‘relative’ zero point.

From the upper panel it is clear that a linear OLS trend fit is not what the data reveals. There is a period showing increase (1901-1940), a period showing stabilization (1941-1970), and again, a period with increasing temperatures from 1971 onwards. A flexible trend  $\mu_t$  with  $2\text{-}\sigma_t$  confidence limits was therefore estimated. Limits may be interpreted as 95% confidence limits (residuals of the model are normally distributed). The trend difference of  $\mu_{2003} - \mu_t$  is given in the lower panel of Figure 3.2.

Trend statistics are:

- $\mu_{1901} = -0.39$  [-0.47, -0.31] °C
- $\mu_{2003} = 0.45$  [0.36, 0.54] °C
- $\mu_{2003} - \mu_{1901} = 0.86$  [0.74, 0.98] K
- $\mu_{2003} - \mu_{2002} = 0.020$  [0.004, 0.036] K

The estimation results clearly show the gradually increasing temperatures over the 1901-1949 period, the stabilization from 1940 to 1970 and the acceleration of global warming afterwards. The trend value in 2003 is statistically larger than all trend values in the period of 1901-2002 (using  $\alpha = 0.05$ , which corresponds to a two-sided test of significance, using the 95% confidence limits in the lower panel).

---

<sup>1)</sup> For this particular series it is known that early global temperatures are less reliable than values at the end of the series. The TrendSpotter software is not able to give weights to individual measurements in its present form. The software will be extended with such a weighing option early 2005.

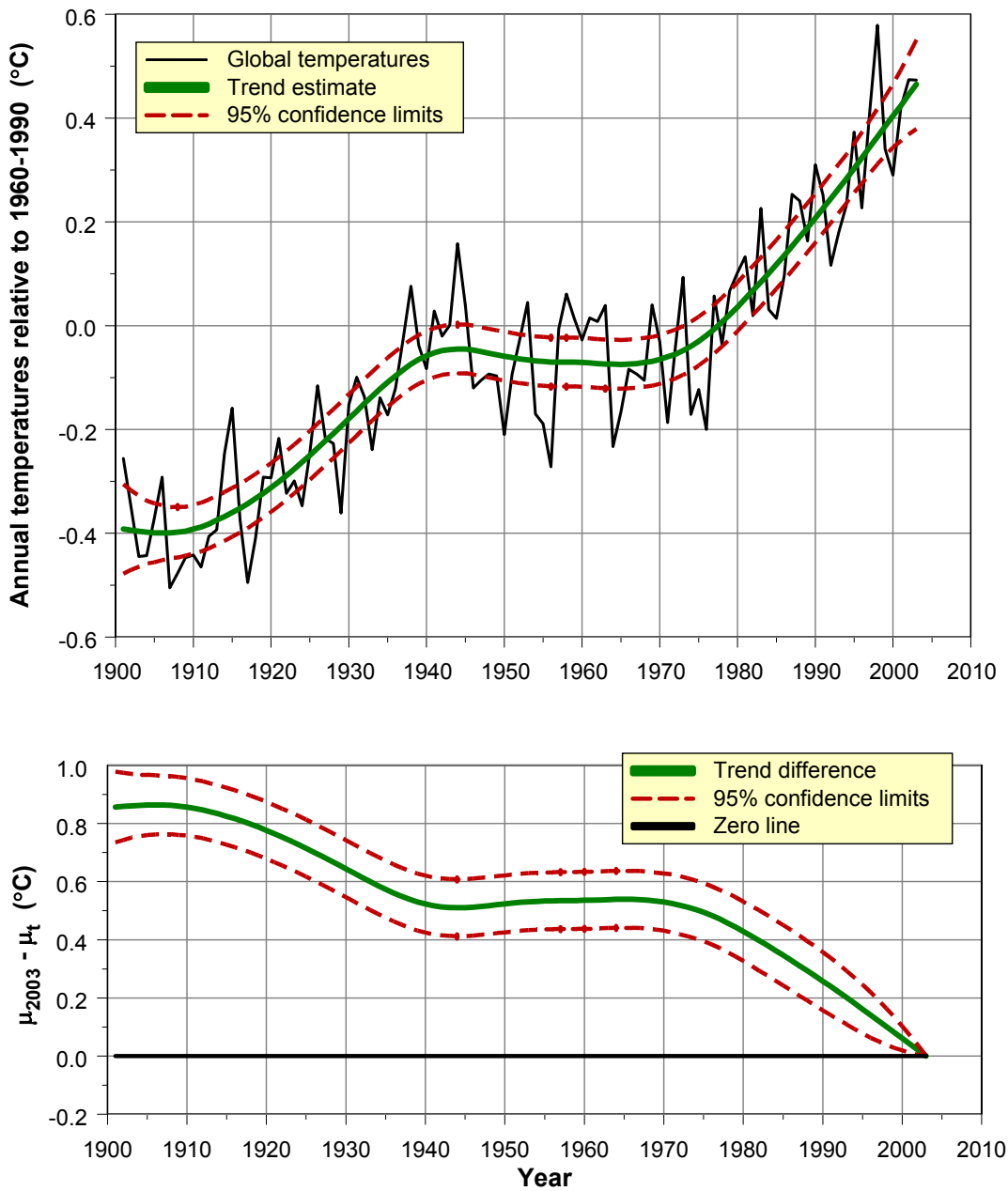


Figure 3.2 Analysis of the combined land, air and sea surface temperatures for the 1901-2003 period, relative to the 1960-1990 period.

Data are from Jones *et al.* (2001), University of East Anglia (CRU). The upper panel shows the data and the trend with 95% confidence limits. The lower panel shows the difference function of  $\mu_{2003} - \mu_t$  with 95% confidence limits. All differences are above the zero line. In other words, the trend value in the final year, 2003, is significantly higher than all preceding trend values (given the choice of  $\alpha = 0.05$  and a two-sided test).

### 3.3 Structural time-series models

#### 3.3.1 Model structure

Only a few methods give some sort of confidence limits for trend estimates for the detection of flexible trends, here, the LOESS estimators, as described by Cleveland and Grosse (1991), polynomial regression fits (models of the form,  $y_t = a + b*t + c*t^2 + d*t^3 + \dots + \varepsilon_t$ ), and trends from the class of structural time-series models. Confidence limits for the *individual trends estimates*  $\mu_t$  for the first two models are known from the literature. But, as far as we know, no formulae have been derived for the first and lagged differences. However, such formulae *have* been derived for trends from the class of structural time-series models in combination with the Kalman filter (De Jong, 1988 and Visser, 1994).

There is a vast amount of literature on structural time-series models. The most important references, mainly from the field of econometrics, are Harvey (1984; 1989), and Durbin and Koopman (2001). Structural time-series models have a modular structure, with measurement,  $y_t$ , at time,  $t$ , seen as an additive sum of four components:

$$y_t = \text{trend}_t + \text{cycle}_t + \text{influence of explanatory variables } x_t + \text{noise}_t \quad (1a)$$

or, more formally,

$$y_t = \mu_t + \gamma_t + \alpha_{1,t} * x_{1,t} + \alpha_{2,t} * x_{2,t} + \dots + \varepsilon_t \quad (1b)$$

If the relationship between  $y_t$  and its components is multiplicative rather than additive, a logarithmic transformation of  $y_t$  may be taken, i.e.  $y_t' = \ln(y_t + c)$  for a suitable constant  $c$ , and 'ln', the notation for the natural logarithm. From equation (1) the model appears conceptually simple. Other transformations, such as the Box-Cox transformation, will not be taken up in the following chapters.

The trend model used for the examples in this report is called the *integrated random walk (IRW)*, suggested by Kitagawa (1981) and Young *et al.* (1991). This model was used with environmental applications by Visser and Molenaar (1990; 1995), van den Brakel and Visser (1996), and Visser (2003). The trend model reads:

$$\mu_t - 2\mu_{t-1} + \mu_{t-2} = \eta_t \quad \text{and} \quad y_t = \mu_t + \varepsilon_t \quad (2a)$$

where  $\eta_t$  and  $\varepsilon_t$  are independent white noise processes with a zero mean, with respective variances of  $\sigma_\eta^2$  and  $\sigma_\varepsilon^2$ .

Model (2a) can be written in the so-called state-space form:

$$\begin{pmatrix} \mu_{t+1} \\ \lambda_{t+1} \end{pmatrix} = \begin{bmatrix} 2 & -1 \\ 1 & 0 \end{bmatrix} \begin{pmatrix} \mu_t \\ \lambda_t \end{pmatrix} + \begin{pmatrix} \eta_t \\ 0 \end{pmatrix} \quad \text{and} \quad y_t = (1 \ 0) \begin{pmatrix} \mu_t \\ \lambda_t \end{pmatrix} + \varepsilon_t \quad (2b)$$

$$\text{with } \eta_t \approx N(0, \sigma_\eta^2) \quad \text{and} \quad \varepsilon_t \approx N(0, \sigma_\varepsilon^2)$$

Other trend models from the class of structural time-series models are given in Visser (2004, Appendix B). The question on what model to choose, given a data set, is also dealt with.

The cycle model  $\gamma_t$  in model (1b) is defined by

$$\sum_{i=0}^{S-1} \gamma_{t-i} = \omega_t \quad \text{with } \omega_t \approx N(0, \sigma_\omega^2) \quad \text{and } S \text{ the period length} \quad (3)$$

As a consequence of model (2a) we have the complete distribution of the trend  $\mu_t$  and a prediction of an observation  $\hat{y}_t$ . As an illustration we have plotted the normal density functions for the estimates  $\mu_{1901}$ ,  $\hat{y}_{1901}$ ,  $\mu_{2003}$  and  $\hat{y}_{2003}$  in **Figure 3.3**. The figure shows that  $\mu_{1901} \ll \mu_{2003}$ , being consistent with the findings in the lower panel of Figure 3.2.

The notation in state-space form is a necessary condition for estimating models (1) and (2) through use of the Kalman filter. This filter, designed by Kalman in 1960, has been used since in numerous applications. Where the noise processes,  $\eta_t$  and  $\varepsilon_t$ , in (2) are normally distributed, the Kalman filter yields optimal estimates for the trend  $\mu_t$ . In jargon, the filter yields the Minimum Mean Square Estimator (MMSE) for the vector  $(\mu_t, \lambda_t)'$  from (2b), based on observations up to and including time  $t$ . If the noise processes have a distribution *other than normal*, the filter is still optimal, albeit somewhat less powerful. In the latter case the filter generates the Minimum Mean Square Linear Estimator (MMSLE) for  $(\mu_t, \lambda_t)'$ . These optimal estimator properties have made the Kalman filter very popular.

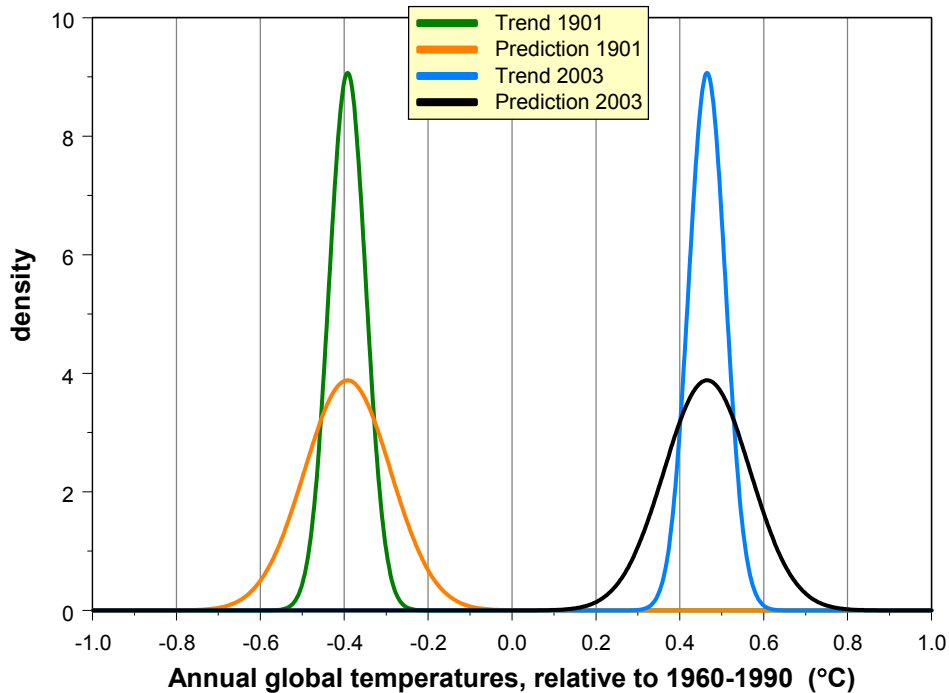


Figure 3.3 Normal density functions for the estimates  $\mu_{1901}$ ,  $\hat{y}_{1901}$ ,  $\mu_{2003}$ , and  $\hat{y}_{2003}$ . Data are based on model estimates shown in Figure 3.2.

For more details on the Kalman filter, please refer to Harvey (1984; 1989, Chapter 3), and Durbin and Koopman (2001). A number of tests given by Harvey (1989, Chapter 5) have been applied here for diagnostic checks. For understanding the trend models presented in the following chapters, it will be essential to highlight one aspect of the estimation process in the next section, i.e. the flexibility of the trend.

### 3.3.2 How to choose the flexibility of the trend?

By varying the variances of the noise process,  $\eta_t$ , the flexibility of the trend can be set. If  $\sigma_\eta^2 = 0.0$  is set, model (2) equals an OLS linear trend fit: a straight line. If  $\sigma_\eta^2$  is set to a very large number, the trend will be passed on to all the measurements. Thus,  $\sigma_\eta^2$  will serve as a ‘smoothing parameter’ in the model. But, what is the right choice for  $\sigma_\eta^2$ ?

To obtain an objective measure,  $\sigma_\eta^2$  is estimated by means of a maximum likelihood optimization. In essence, this estimator tries to minimize the errors in the one-step-ahead predictions generated by the Kalman filter. The filter iteratively generates a trend prediction,  $\mu_{t+1}$ , based on all measurements  $y_1, \dots, y_t$ . This prediction  $\mu_{t+1}$  is then compared to the actual measurement,  $y_{t+1}$ , yielding the one-step-ahead prediction error or *innovation*  $v_{t+1} = y_{t+1} - \mu_{t+1}$ . We now choose  $\sigma_\eta^2$  so that the sum of squared innovations  $v_s^2 + \dots + v_N^2$  is minimal (note that the summation starts at time step  $s$ , and not at time step 1, since the filter needs some iteration steps to converge; in practice, the filter has a start-up phase of between 10 and 20 time steps).

This is, in short, the rationale behind the maximum likelihood estimator. For details, please see Harvey (1989, section 3.4). The maximum likelihood estimation process has been applied throughout this report.

### 3.3.3 Predicting future data

The prediction of future data is part of the mathematical framework of structural time-series models and the Kalman filter (Harvey, 1989; Visser, 2003). This characteristic will be applied in Chapter 7 of this report. Here, we will give an example for the global temperature series of Jones *et al.* (2001), as presented in Figure 3.2.

We have estimated a trend model for the 1901–2020 period. The estimation results are shown in **Figure 3.4** and the trend statistics below:

- $\mu_{1901} = -0.39$  [-0.47, -0.31] °C
- $\mu_{2003} = 0.47$  [0.39, 0.55] °C
- $\mu_{2010} = 0.61$  [0.42, 0.80] °C
- $\mu_{2020} = 0.81$  [0.39, 1.23] °C
- $\mu_{2020} - \mu_{1901} = 1.20$  [0.76, 1.63] K
- $\mu_{2020} - \mu_{2019} = 0.02$  [-0.01, 0.05] K

Clearly, the trend is extrapolated linearly over the 2004-2020 period. Furthermore, the confidence limits in the upper panel show that the further we predict into the future, the wider the confidence limits become. The lower panel shows  $\mu_{2020}$  to be significantly higher than all trend values before the year 2000.

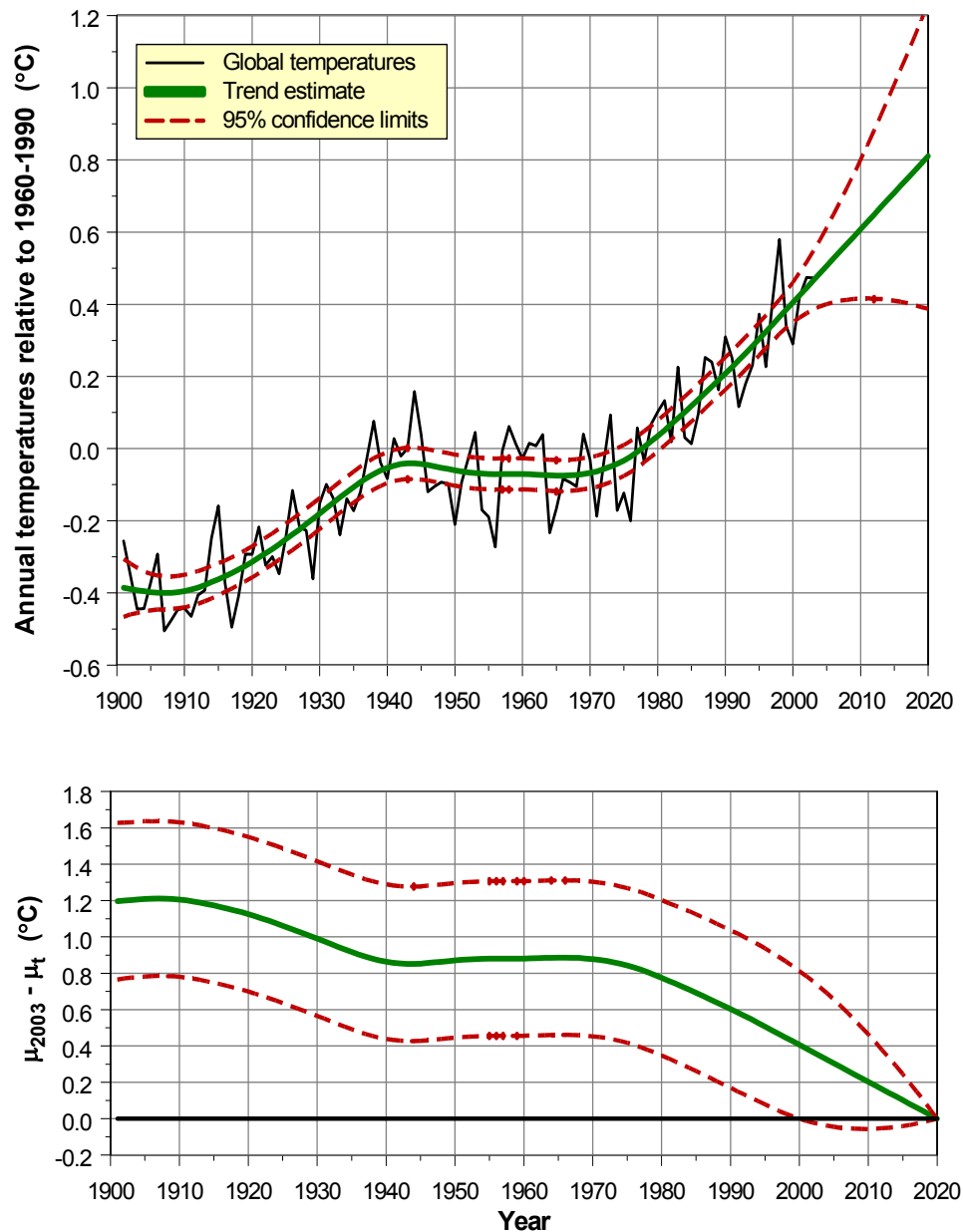


Figure 3.4 Analysis of the combined land air and sea surface temperatures for the 1901-2003 period, relative to the 1960-1990 period.

Estimates are extrapolated over the 2004-2020 period. Data are from Jones *et al.* (2001). The upper panel shows the data and the trend with 95% confidence limits. The lower panel shows the difference in function  $\mu_{2020} - \mu_t$ , with 95% confidence limits.

### 3.4 Software

There is not much software on structural time-series models. And this may explain why this class of models is not as widely applied as the ARIMA models, for example. The main software implementation is the Structural Time-series Analyser, Modeller and Predictor (STAMP, in short), distributed by Timberlake Consultants LTD. Information can be found on the websites: <http://stamp-software.com> and <http://www.timberlake.co.uk>

The TrendSpotter software was initially developed at KEMA, but since 2001 at the RIVM. All examples in this report have been calculated using this software package, written in Fortran and running on a standard PC. Computation results are given as ASCII data files. Statistical tests and graphical presentations are created through scripts written in S-PLUS (Dekkers, 2001; Millard and Neerschlag, 2001). The software can be obtained free of charge from the author. See Visser (2003;2004a,b).

Two main differences between STAMP and TrendSpotter:

- STAMP incorporates more types of time-series models than TrendSpotter. An example is the wide range of multivariate models, in which the measurements  $y_t$  are not scalar, as in model (1), but presented by vector processes.
- STAMP provides confidence limits for the trend level,  $\mu_t$ , but not for the function,  $\mu_N - \mu_t$ .
- STAMP does not contain the IRW trend model used throughout this report.



*The TrendSpotter software is unique in estimating various confidence limits for trend estimates.*

## 4. Annual means and annual cycles

### 4.1 Temperature

#### 4.1.1 Annual means

How did annual mean temperatures evolve in the Netherlands? The structural time-series model for De Bilt is shown in **Figure 4.1**, with the estimation results presented in the same style as Figure 3.2. The period in question is 1901-2003.

The minimum temperature in the annual data falls in 1963 (7.75 °C). The maximum falls in 1990 (10.77 °C), 10.79 °C and 2000 (10.78 °C).

Trend statistics are:

- $\mu_{1901} = 8.8 [8.4, 9.2] \text{ }^\circ\text{C}$
- $\mu_{2003} = 10.3 [9.9, 10.7] \text{ }^\circ\text{C}$
- $\mu_{2003} - \mu_{1901} = 1.5 [0.9, 2.1] \text{ K}$
- $\mu_{2003} - \mu_{2002} = 0.042 [0.006, 0.078] \text{ K}$

The results show a gradually increasing temperature series with an acceleration of this increase since 1970. The trend value in 2003 is statistically larger than any of trend values in the 1901-2002 period!

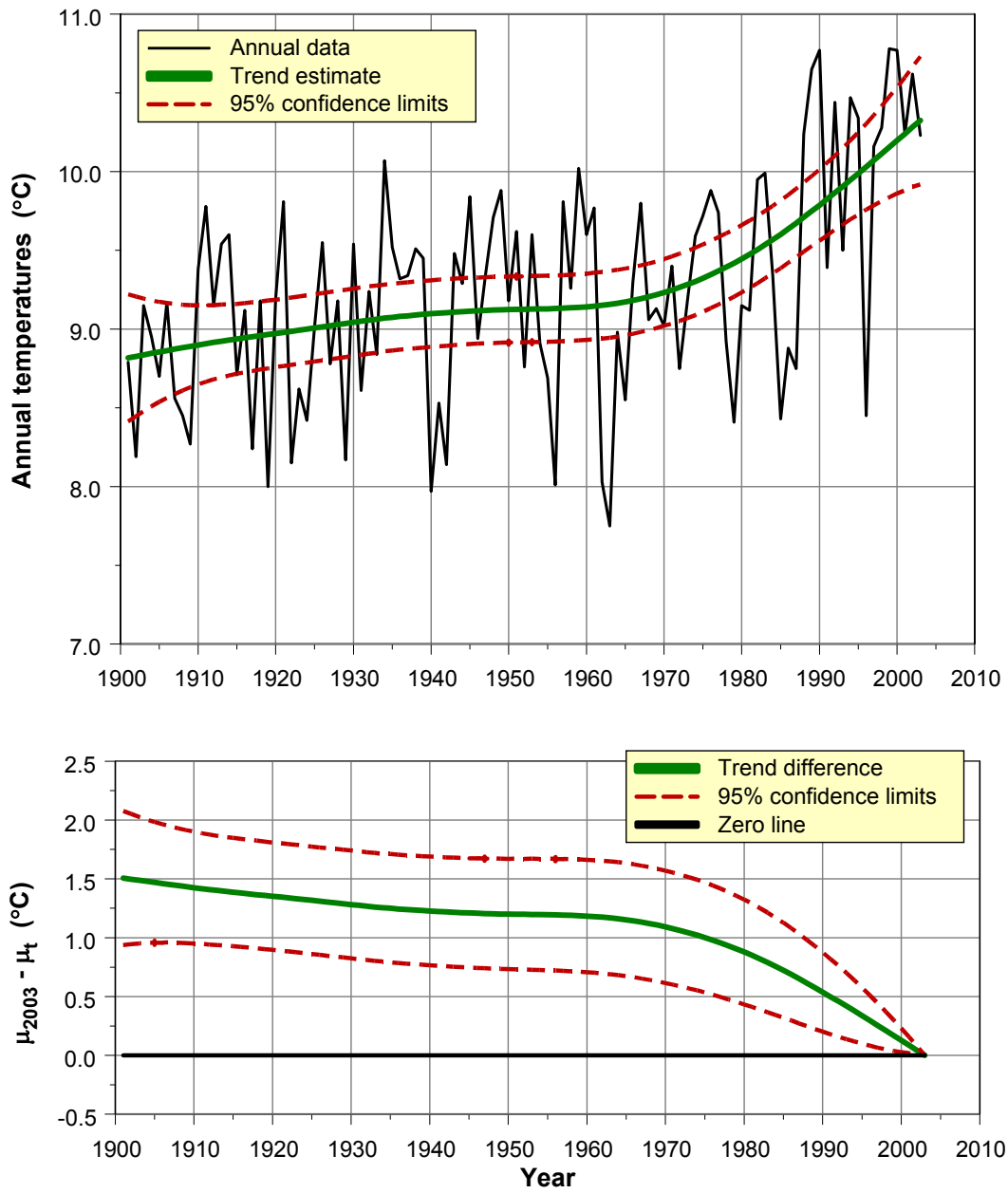


Figure 4.1 Annual temperatures for De Bilt station (black line), the estimated trend (green line) and the corresponding 95% confidence limits (dashed red lines). Period is 1901-2003. The lower panel shows the trend differences,  $\mu_{2003} - \mu_t$  (K).

### 4.1.2 Annual cycle

We have also estimated the annual cycle along with the long-term trend. This annual cycle has been based on monthly averaged data. Again, the estimation period is 1901-2003. The estimation results are given in **Figure 4.2**.

The coldest month in the record is that of February 1956, with a value of -6.8 °C. The warmest month is that of July 1994 with a value of 21.3 °C.

The trend is identical to the trend shown in Figure 4.1:

- $\mu_{\text{Jan 1901}} = 8.8 [8.4, 9.2] \text{ } ^\circ\text{C}$
- $\mu_{\text{July 1950}} = 9.2 [9.0, 9.3] \text{ } ^\circ\text{C}$
- $\mu_{\text{Dec 2003}} = 10.4 [10.1, 10.7] \text{ } ^\circ\text{C}$ .

The structural time-series model allows the annual cycle to change over time. However, evaluation of the maximum likelihood function showed that the best model for the data is the one with a *constant* annual cycle. The annual cycle is given in **Table 4.1**.

We note that the residuals of the estimated model, shown in Figure 4.2 are slightly skewed and we estimated a comparative model using the transformation  $y_t' = \ln(30 - y_t)$ . However estimation results do not differ much. Therefore, we have chosen to present the simplest model, the one *without* transformation.

To show the impact of annual warming more clearly, we have redrawn the estimates from Figure 4.2. **Figure 4.3** shows the annual cycles for five different years. We have also drawn a horizontal line at 5 °C. This line corresponds to the definition of ECA for the beginning and the end of the growing season.

The graph shows considerable growth in the length of the growing season over the 1950-2003 period. It starts ~16 days earlier in spring and ends ~14 days later in autumn. The graph also shows that an extra 1 or 2 degrees warming in the near future will have dramatic effects: the growing season will disappear completely (seen in the red), found completely above the 5 °C threshold. One of the implications is that the winter hardening period for plants will disappear. A further discussion on the ecological impact of these shifts will be given in section 6.2.



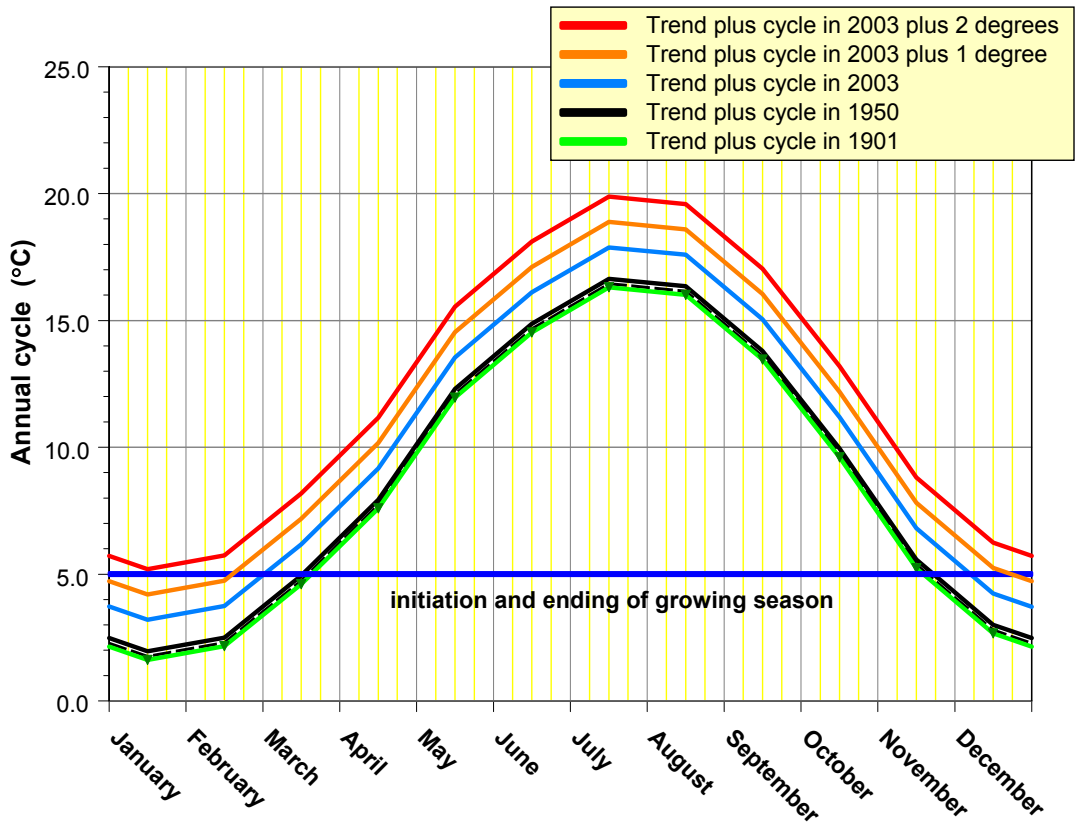


Figure 4.3 Annual temperature cycles for five different years.

The cycles are achieved by taking the estimated trend,  $\mu_t$ , and adding the cycle,  $\gamma_t$ , from Table 4.1. The blue horizontal line marks the threshold for initiating and ending the growing season. The orange and red cycles are added to the graph to show the impact of an extra 1 and 2 degrees warming in the near future. According to the inference made in section 8.1, these respective warming curves may become real around the years 2010 and 2020.

### 4.1.3 Are the results consistent with seasonal estimates?

Tang (2003) estimated trends for the individual seasons. He found that annual mean warming of **1.5 K** over the 1901-2003 period as not uniformly distributed over the seasons:

- winter:  $\mu_{2003} - \mu_{1901} = 1.2$  K
- spring:  $\mu_{2003} - \mu_{1901} = 1.8$  K
- summer:  $\mu_{2003} - \mu_{1901} = 1.4$  K
- autumn:  $\mu_{2003} - \mu_{1901} = 1.2$  K

Clearly, maximum warming occurred in spring, and to a lesser extent in summer. These conclusions were also drawn by Van Oldenborgh and Van Ulden (2003) and KNMI (2003). In the last reference explanations are given for the unusual warming in *winter* and spring.

Are these seasonal estimates contradictory to the results presented in Figure 4.2 and Table 4.1, where we conclude that warming is spread uniformly over the 12 months, and, consequently, uniformly over the seasons?

The discrepancy is easily understood if the uncertainty bands in seasonal warming are taken into account. These are as follows (Tang, 2003):

- annual:  $\mu_{2003} - \mu_{1901} = 1.5 \pm 0.6$  K
- winters:  $\mu_{2003} - \mu_{1901} = 1.2 \pm 1.3$  K
- spring:  $\mu_{2003} - \mu_{1901} = 1.8 \pm 0.9$  K
- summer:  $\mu_{2003} - \mu_{1901} = 1.4 \pm 0.6$  K
- autumn:  $\mu_{2003} - \mu_{1901} = 1.2 \pm 0.7$  K

Errors are  $2\text{-}\sigma$  confidence limits. Due to the large inter-annual variability the limits appear to be very wide. As a consequence, the difference between winter warming and spring warming is far from statistically significant. And winter warming *itself* is barely significant.

The conclusion is that there is indeed a *tendency* for non-uniform warming across seasons. However, these differences are far from statistically significant.

## 4.2 Precipitation

### 4.2.1 Annual totals

How did annual precipitation sums evolve in the Netherlands? From the structural time-series model for De Bilt, shown in **Figure 4.4**, it can be seen that the minimum precipitation in the annual data falls in 1921 (407 mm) and the maximum in 1998 (1307 mm).

Trend statistics are:

- $\mu_{1906} = 768$  [698, 838] mm
- $\mu_{2003} = 886$  [816, 956] mm
- $\mu_{2003} - \mu_{1906} = 118$  [20, 216] mm
- $\mu_{2003} - \mu_{2002} = 2.2$  [-1.0, 5.4] mm

The results show a gradually increasing precipitation series with a small acceleration in this increase since 1970. The trend value in 2003 is statistically greater than all the trend values in the 1901-1970 ( $\alpha = 0.05$ ) period. This conclusion is consistent with that drawn by Bruin (2002) and KNMI (2003).



*There is a significant increase in the annual amount of precipitation in the Netherlands. It has increased with 118 mm since 1901, i.e. an increase of 15%. Photo: C. Fetchmor.*

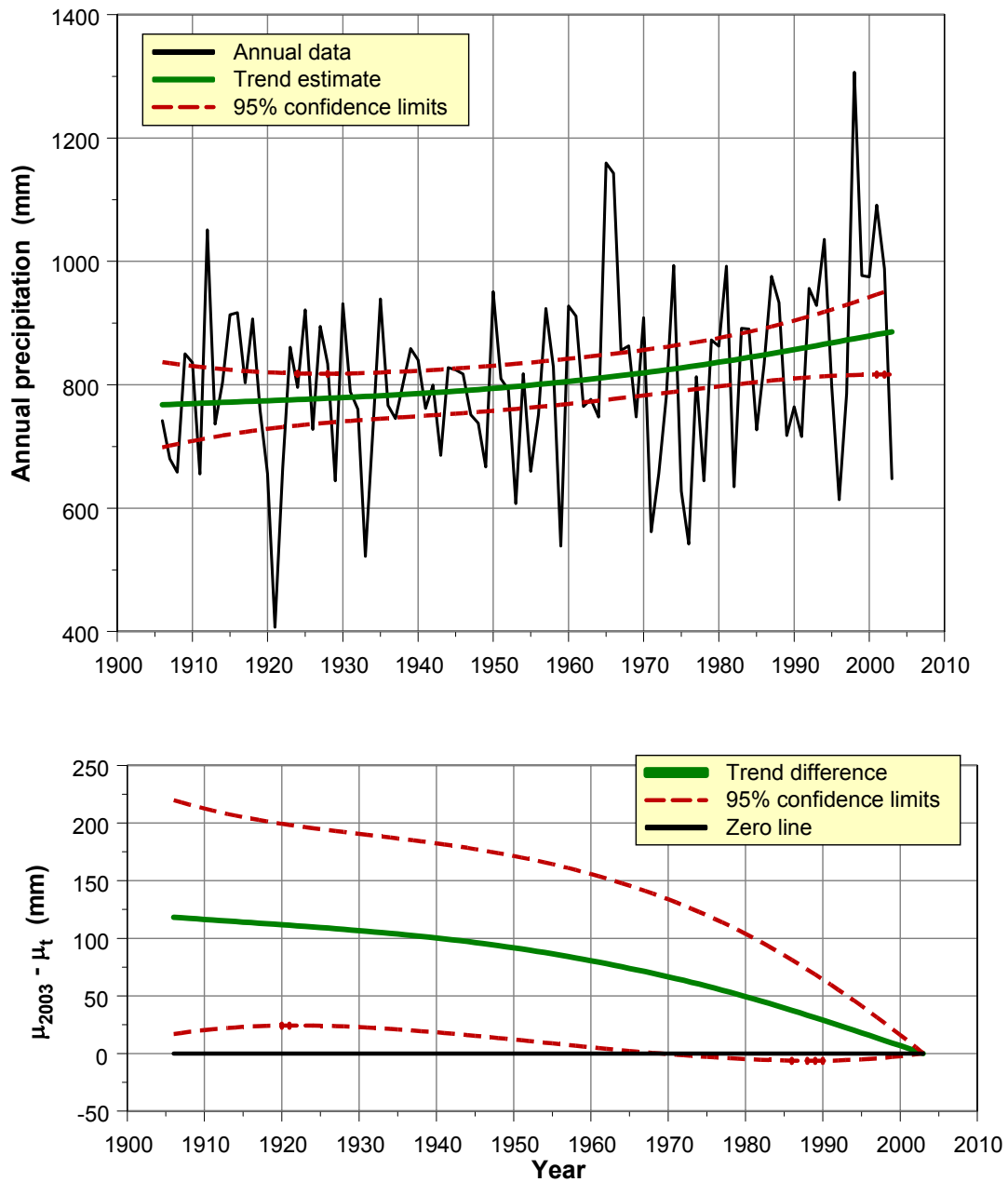


Figure 4.4 Annual precipitation sums from 1906 to 2003 for De Bilt (black line), the estimated trend (green line) and the corresponding 95% confidence limits (dashed red lines). The lower panel shows the trend differences  $\mu_{2003} - \mu_t$  (mm).

## 4.2.2 Annual cycle

We have also estimated the annual cycle along with the long-term trend to monthly precipitation sums. Because the residuals of the model directly estimated to the monthly data were skewed, we transformed the  $y_t$  series to  $y_t' = \log(15 + y_t)$ . The estimation results are given in **Figure 4.5**. Minimum monthly precipitation occurred in September 1959, summed to 3 mm, and in February 1986, summed to 1 mm. Maximum precipitation (226 mm) occurred in August 1912 and in September 2001 (230 mm).

The trend estimates equal those shown in Figure 4.4:

- $\mu_{\text{Jan } 1906} = 57 [52, 62]$  mm
- $\mu_{\text{July } 1950} = 58 [55, 61]$  mm
- $\mu_{\text{Dec } 2003} = 65 [59, 71]$  mm.

The structural time-series model allows the annual cycle to change over time. However, evaluation of the maximum likelihood function showed the best model for the data to be the one with a *constant* annual cycle. The annual cycle is given in **Table 4.2**. Due to the logarithmic transformation the shape of the cycle component changes slightly over time. Figure 4.5 shows the annual cycle to be small relative to the trend values, varying between 3% and 16% relative to  $\mu_t$ .

Figure 4.5 is also represented in **Figure 4.6**. The figure shows that all monthly precipitation sums have increased by approximately 7 mm since 1950.

*Table 4.2 Annual cycle in monthly total precipitation for 1906-1950 (upper table) and for 2003 (lower table).*

The average of the cycle is approximately 0 mm (due to model estimation on log-transformed data not being exactly 0 mm). The uncertainty in these estimates is negligible.

Jan.	Feb.	Mar.	April	May	June	July	Aug	Sept.	Oct.	Nov.	Dec.
4 mm	-15 mm	-11 mm	-13 mm	-9 mm	2 mm	8 mm	11 mm	3 mm	4 mm	8 mm	11 mm

Jan.	Feb.	Mar.	April	May	June	July	Aug.	Sept.	Oct.	Nov.	Dec.
2 mm	-17 mm	-11 mm	-15 mm	-10 mm	4 mm	8 mm	12 mm	3 mm	6 mm	9 mm	13 mm

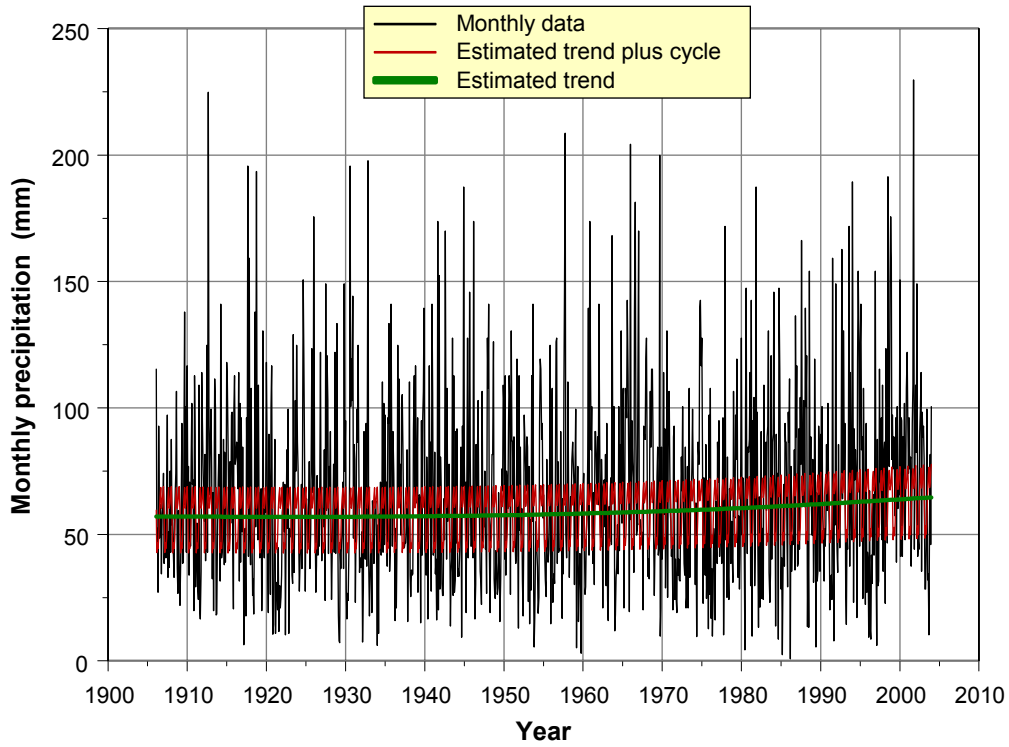


Figure 4.5 Structural time-series model with trend and cycle estimated for monthly precipitation sums at De Bilt. The model has been estimated using the transformation  $y_t' = \ln(15 + y_t)$ .

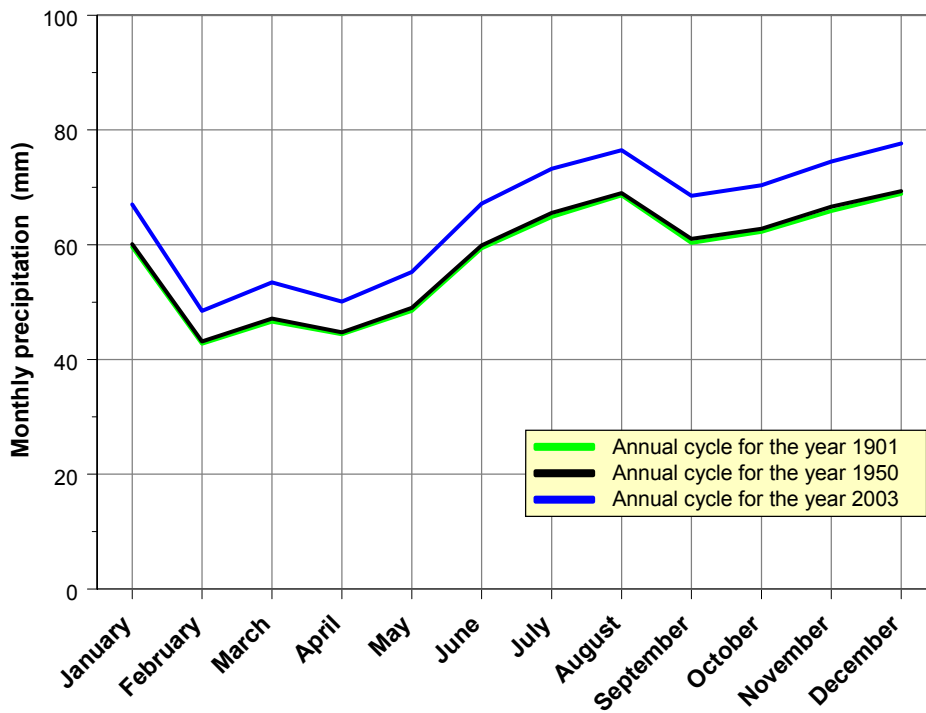


Figure 4.6 Annual precipitation cycles for three different years.

### 4.2.3 Are the results consistent with seasonal estimates?

Tang (2003) estimated trends for the individual seasons. He found that changes in annual precipitation totals over the 1906-2003 period not to be spread uniformly over the seasons (estimated on a slightly different precipitation series, based on daily pluviograph measurements):

- winter:  $\mu_{2003} - \mu_{1906} = 20$  mm
- spring:  $\mu_{2003} - \mu_{1906} = 28$  mm
- summer:  $\mu_{2003} - \mu_{1906} = -20$  mm
- autumn:  $\mu_{2003} - \mu_{1906} = 52$  mm

As for the temperature estimates discussed in section 4.1.3 these seasonal estimates seem contradictory to the results presented in Figure 4.5 and Table 4.2, where we conclude that the annual increase in precipitation is spread uniformly over the 12 months, and, consequently, uniformly over the seasons.

Again, the discrepancy is easily understood if the uncertainty bands are taken into account. These are as follows (Tang, 2003):

- winter:  $\mu_{2003} - \mu_{1906} = 20 \pm 40$  mm
- spring:  $\mu_{2003} - \mu_{1906} = 28 \pm 38$  mm
- summer:  $\mu_{2003} - \mu_{1906} = -20 \pm 50$  mm
- autumn:  $\mu_{2003} - \mu_{1906} = 52 \pm 50$  mm

Errors are  $2\text{-}\sigma$  confidence limits. Due to the large inter-annual variability the limits appear to be very wide. As a consequence, the difference between summer and autumn precipitation sums is not statistically significant. And only the autumn precipitation sum is just statistically significant - the other changes are not.

The conclusion is that there is indeed a *tendency* for non-uniform precipitation increases across seasons. However, these differences are far from statistically significant.



## 5. Extreme weather conditions

### 5.1 Temperature

#### 5.1.1 Absolute minimum temperatures

How did annual absolute minimum temperatures evolve in the Netherlands? In other words, what is the trend in the coldest moment in a year? **Figure A.1** in Appendix A, upper panel, shows these data for main observatory De Bilt along with the average of the stations Den Helder, Groningen, De Bilt and Vlissingen. The graph shows good correspondence between the two series apart from the outlier at  $-25^{\circ}\text{C}$ . It should be noted here that thermometers at all stations were lowered in height from 2.20 m to 1.50 m around 1961. Therefore, data before 1961 should be handled with some care (to correct for this inhomogeneity one should slightly lower temperatures before 1961, in the order of 0.1 K).



*There is hope for one of the most popular outdoor winter sports in the Netherlands. The increase in temperature of the coldest moment of the year is not statistically significant if compared with 1901 (Figure 5.1). Photo: H. Visser.*

The structural time-series model for De Bilt is shown in **Figure 5.1**. Because of the skewness of minimum temperatures, the minimum temperatures were transformed into  $y_t$  to  $y_t' = \ln(-y_t)$ .

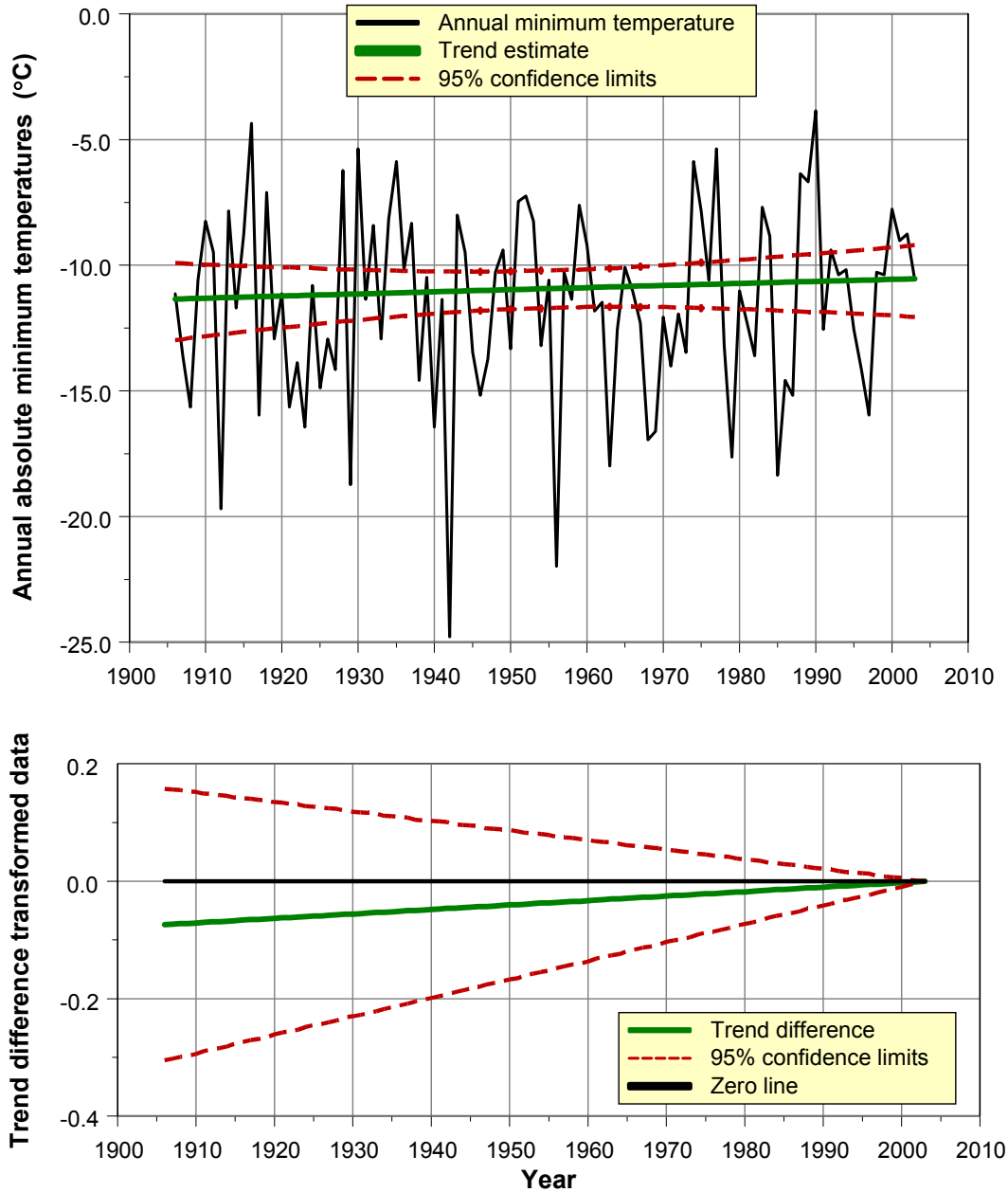


*Figure 5.1 Annual absolute minimum temperatures for De Bilt (black line), the estimated trend (green line) and the corresponding 95% confidence limits (dashed red lines).*

Period is 1901-2003. Because of the skewness of minimum temperatures the original temperatures,  $y_t$ , have been transformed to  $y_t' = \ln(-y_t)$ . Estimated results have been back-transformed in this panel. The lower panel shows the trend differences,  $\mu_{2003} - \mu_t$  ( $\ln(K)$ ), based on the transformed model  $y_t'$ .

The lowest annual minimum temperature is 24.8 °C (in 1942) and the maximum temperature is 3.9 °C (in 1990).

Trend statistics are:

- $\mu_{1901} = -11.4$  [-13.0, -9.9] °C
- $\mu_{2003} = -10.5$  [-12.1, -9.2] °C
- $\mu_{2003} - \mu_{1901} = 0.9$  [non significant] K
- $\mu_{2003} - \mu_{2002} = 0.01$  [non significant] K

The results show a slightly increasing temperature series. However, the trend in 2003 is not statistically larger than any of the trend values in the 1901-2002 period.

It is noted that the small inhomogeneity around 1961 would not change the result of a non-significant trend, as found above.

## 5.1.2 Absolute maximum temperatures

How did annual absolute maximum temperatures evolve in the Netherlands? In other words, what is the trend in the hottest moment in a year? As described in section 2.1 we have corrected daily data at De Bilt using *monthly* correction factors from Brandsma. However, these corrections may be too low for extremely warm days due to a ‘micro greenhouse effect’ under the roof of the pagoda type of screen (Figure 2.2). Also the change in height of the thermometer (1961) may play a role. Therefore, one should be careful with inferences on trends over the whole 1901-2003 period. Data before 1961 are less reliable.

**Figure A.2** in Appendix A, upper panel, shows the maxima for De Bilt along and the four station mean values. The graphs show reasonably good correspondence between the two series ( $R = 0.89$ ). This result is positive for the homogeneity of the De Bilt series with annual maxima, although some doubts remain for the first half of the series.

The structural time-series model for De Bilt is shown in **Figure 5.2**. The minimum temperature of the annual data falls in 1974 (26.4 °C) and the maximum in 1947 (36.4 °C).

Trend statistics:

- $\mu_{1906} = 30.4$  [28.9, 31.9] °C
- $\mu_{2003} = 32.9$  [31.5, 34.3] °C
- $\mu_{2003} - \mu_{1906} = 2.6$  [0.4, 4.8] K
- $\mu_{2003} - \mu_{2002} = 0.12$  [-0.04, 0.28] K



*Extremely hot days pose a serious health impact for elderly people.  
This aspect will be studied in more detail in section 6.1.*

The results show an overall increasing temperature series. However, the trend value in 2003 is not statistically larger than all trend values in the 1901-2002 period. The lower panel in **Figure 5.2** shows alternating periods of significance, 1906 - 1920 and 1951 - 1992.

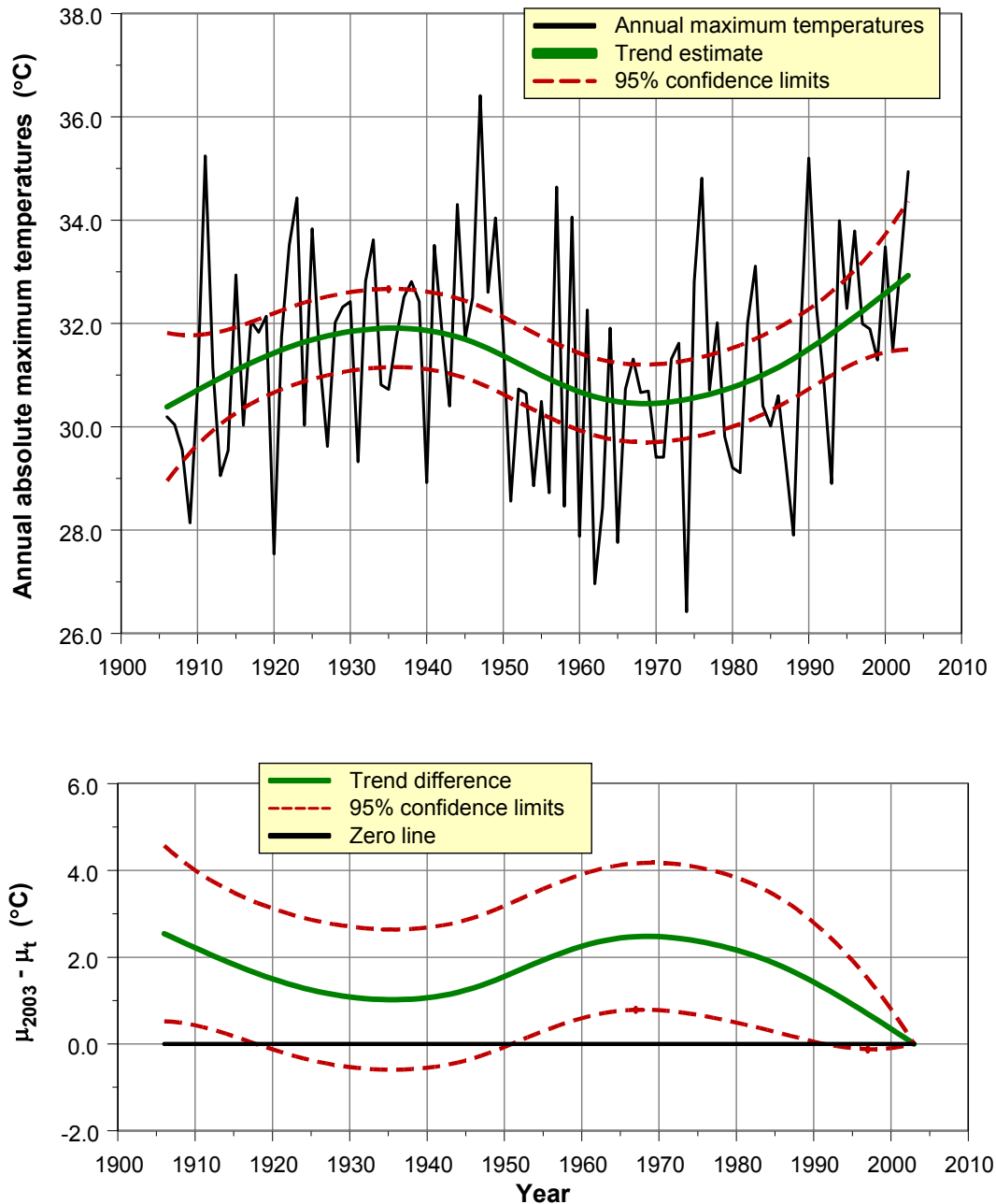


*Figure 5.2 Annual absolute maximum temperatures for De Bilt (black line), the estimated trend (green line) and the corresponding 95% confidence limits (dashed red lines). Data before 1961 are less reliable.*

Period is 1901-2003. The lower panel shows the trend differences,  $\mu_{2003} - \mu_t$  (K).

### 5.1.3 Number of summer days

How did the number of summer days evolve over the past 100 years? Summer days are defined as days with a maximum temperature above 25.0 °C. **Figure 5.3.**, upper panel, shows these data for De Bilt along with the four-station mean series. The graphs show a reasonable good correspondence between the two series ( $R = 0.93$ ).

The structural time-series model for De Bilt is also shown in Figure 5.3. The skewed residuals have led us to transform the original temperature maxima  $y_t$  to  $y_t' = \ln(y_t + 5)$ . The upper panel shows estimates that have been back transformed using the inverse relation. The lower panel is for the transformed data  $y_t'$ .

The minimum of annual summer days (3) falls in 1963, while the maximum (60 days) falls in 1947.



*The number of summer days shows a significant increase.*

*Photo: H. Visser.*

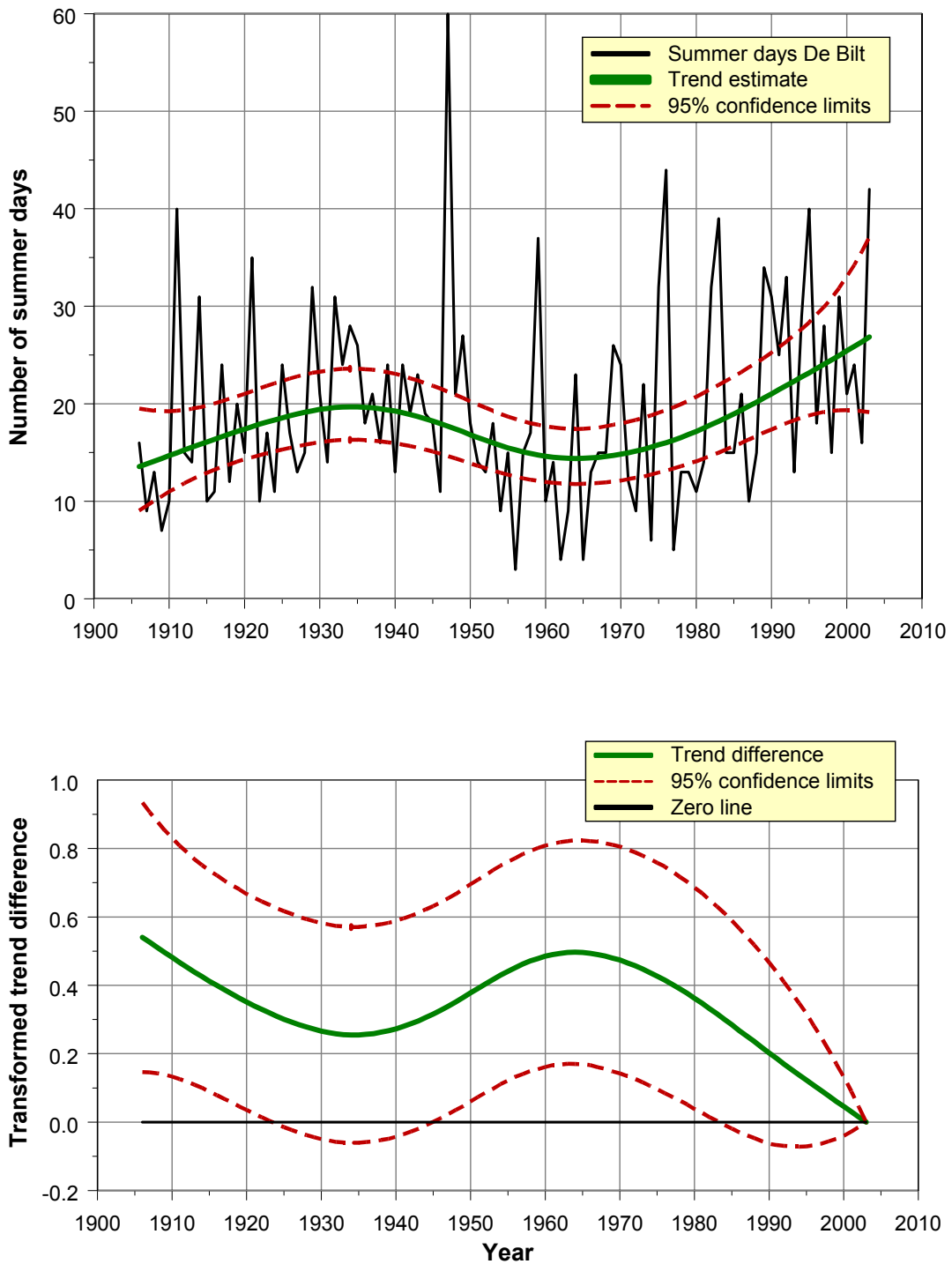


Figure 5.3 Annual number of summer days for De Bilt (black line) station, the estimated trend (green line) and the corresponding 95% confidence limits (dashed red lines).

The model was estimated on the transformed series,  $y_t' = \ln(y_t + 5)$ . The confidence limits are somewhat skewed due to the log-transform. Period is 1906-2003. The lower panel shows the transformed trend differences,  $\mu_{2003} - \mu_t$ .

Trend statistics:

- $\mu_{1906} = 13.5$  [9.0, 19.5] days
- $\mu_{2003} = 26.9$  [19.1, 37.1] days
- $\mu_{2003} - \mu_{1906} = 13.4$  [significant] days
- $\mu_{2003} - \mu_{2002} = 0.51$  [non-significant] days

The results show a gradually increasing trend for the 1906-1935 period, a decreasing one in 1935-1963, and an accelerated increase in the 1970-2003 period. The trend in summer days in 2003 is statistically smaller than in the 1906-1922 and 1943-1984 periods.

## 5.2 Precipitation

### 5.2.1 Maximum daily precipitation

How did the amount of rainfall on the wettest day in a year evolve? This wettest day, or maximum daily precipitation, is compared to the 13-station mean series in **Figure A.4**. The graphs show a *low* correspondence between the two series ( $R = 0.58$ ). However, this result is not surprising: the occurrence of large amounts of precipitation is a very local phenomenon and by no means representative for the Netherlands as a whole.

In the structural time-series model for De Bilt, shown in **Figure 5.4**, there is minimum precipitation in 1921 (17.6 mm). The maximum falls in 1952 (66.2 mm).



*Large amounts of rainfall in 1 or 2 days time may have positive implications for children. However, a lot of rainfall presents a serious danger for harvests in the months of August and September. Another implication is for the quality of swimming water along the Dutch coast. Sewage plants cannot handle the large amounts of water and part of the sewage flows directly to the coastal waters. Photo: H. Visser.*

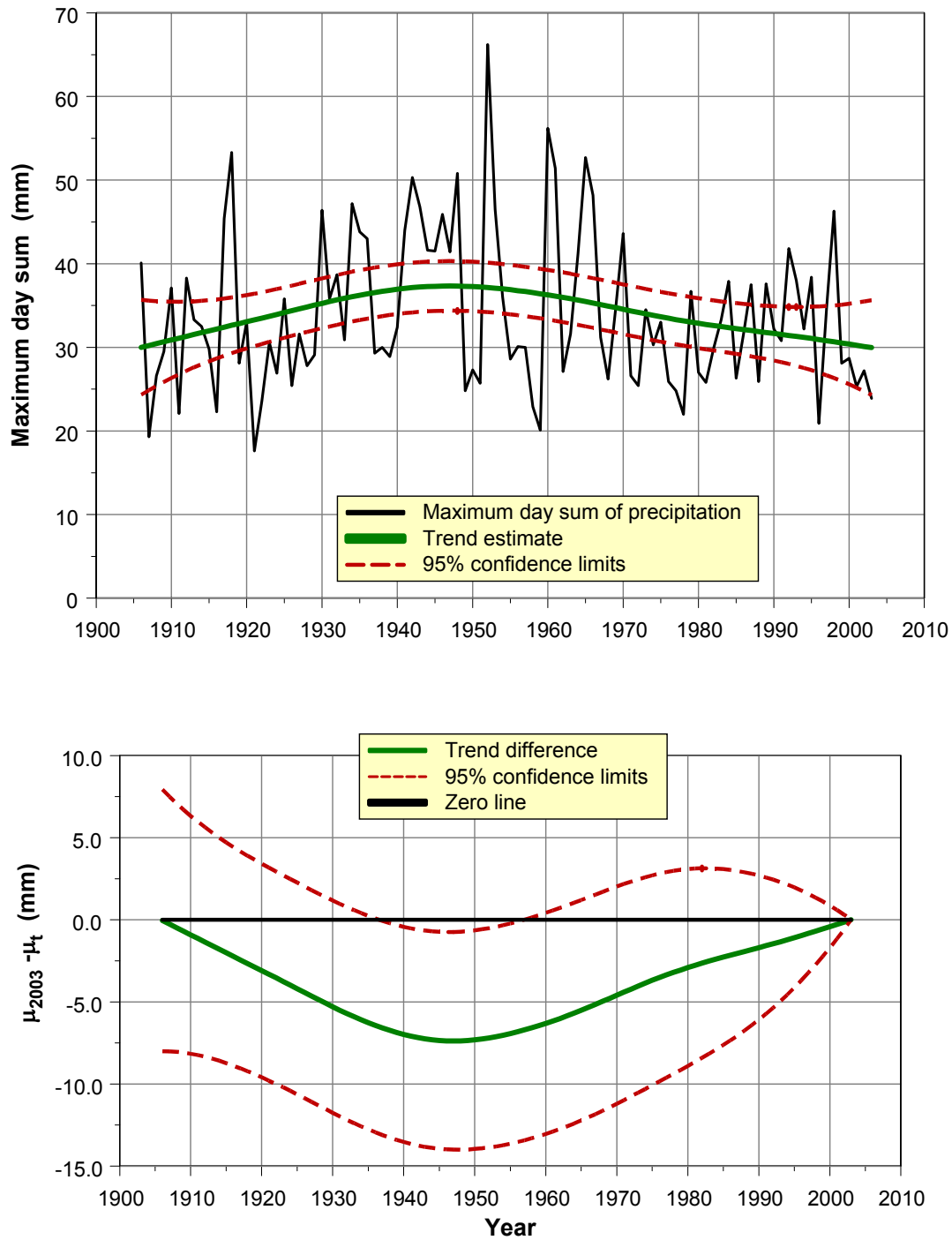


Figure 5.4 Annual maximum precipitation on one day summed for De Bilt (black line), the estimated trend (green line) and the corresponding 95% confidence limits (dashed red lines).

Period is 1906-2003. The lower panel shows the trend differences  $\mu_{2003} - \mu_t$  (°C).

## Trend statistics:

- $\mu_{1901} = 30.0$  [24.2, 35.8] mm
- $\mu_{2003} = 30.0$  [24.2, 35.8] mm
- $\mu_{2003} - \mu_{1901} = 0.0$  [-6.0, 6.0] mm
- $\mu_{2003} - \mu_{2002} = -0.14$  [-0.60, 0.31] mm

The results show increasing daily precipitation sums for 1906-1950 and decreasing precipitation sums for 1951-2003. The trend in precipitation in 2003 is statistically larger than in 1936-1957.

## 5.2.2 Number of extremely wet days

The annual number of extremely wet days is defined as the number of days with precipitation sums of 10 mm or more. How has this indicator evolved over the years?

**Figure A.5**, upper panel, shows these data for De Bilt, along with the 13-stations mean series. The graph shows a reasonable correspondence between the two series, given the variability of local precipitation.



*River flooding in recent years has led to intensive political discussions on mitigation measures. Here, boots have been put ready for visiting politicians.  
Photo: M. Wijnbergh.*

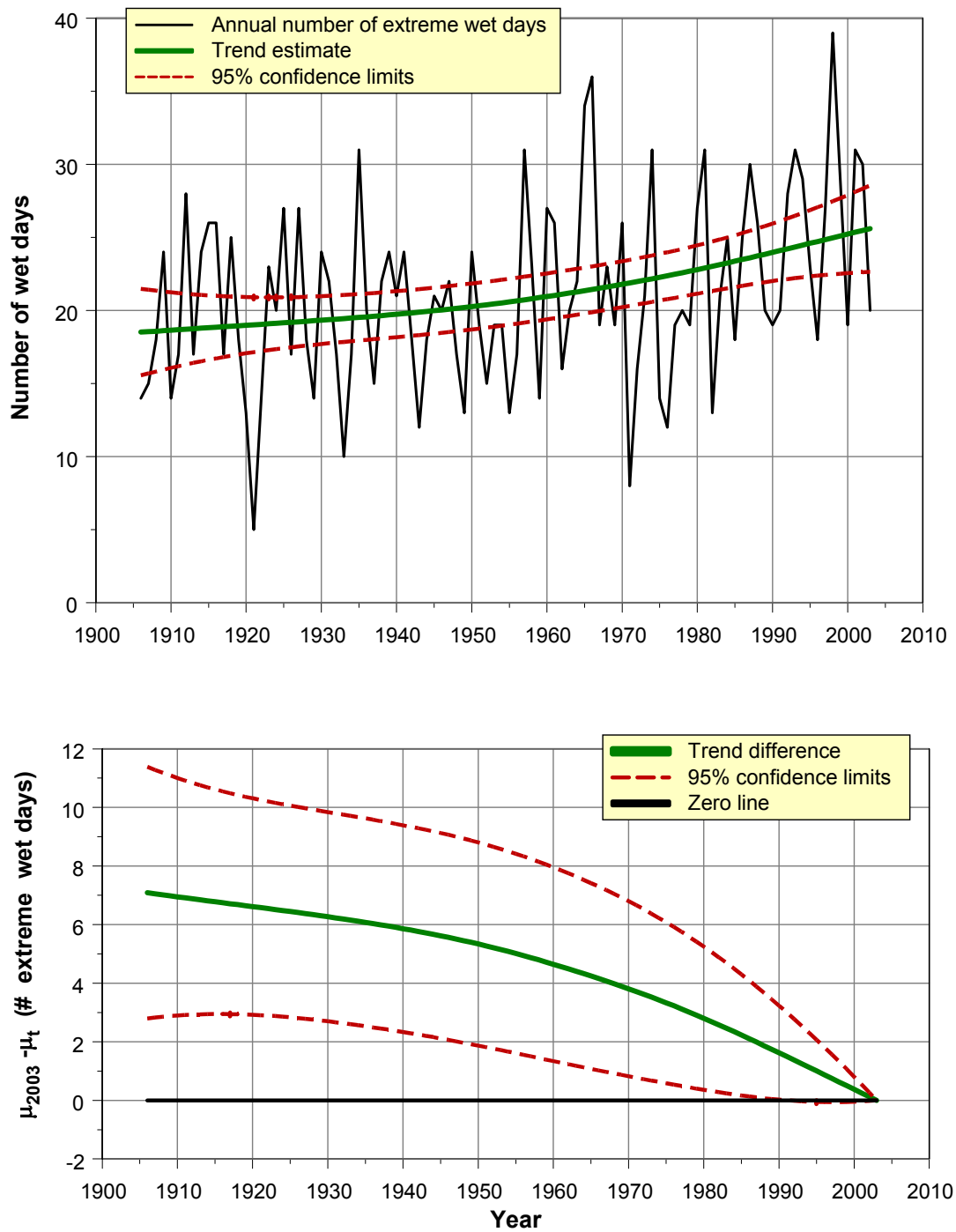


Figure 5.5 Annual number of extreme wet days for De Bilt (black line), the estimated trend (green line) and the corresponding 95% confidence limits (dashed red lines).

Period is 1906-2003. The lower panel shows the trend differences  $\mu_{2003} - \mu_t$  (days).

The structural time-series model for De Bilt is shown in **Figure 5.5**. The minimum of the annual data falls in the year 1921 (5 days). The maximum falls in the year 1998 (39 days).

Trend values are:

- $\mu_{1906} = 18.5$  [15.5, 21.5] days
- $\mu_{2003} = 25.6$  [22.6, 28.6] days
- $\mu_{2003} - \mu_{1906} = 7.1$  [2.8, 11.4] days
- $\mu_{2003} - \mu_{2002} = 0.13$  [-0.02, 0.28] days

The results show a gradually increasing number of wet days with a small acceleration of this increase since 1970. The trend value in 2003 is statistically larger than all trend values in the period 1906-1992.

### 5.2.3 Maximum number of consecutive dry days

How did periods of drought evolve in the Netherlands? Here we use the ECA definition for a dry day: a day is 'dry' if the total precipitation amounts less than 1.0 mm. We note that in the literature other definitions can be found, such as 0.3 or even 0.1 mm thresholds (Bruin, 2002). However, these last two thresholds are sensitive to measurement errors, so the threshold of 1.0 mm has been chosen. The definition used for 'dry period' is the maximum number of consecutive dry days. An impact of long dry periods is given in the inset at the next page.

**Figure A.6**, upper panel shows dry periods for De Bilt, along with the 13-station mean series. The graph shows a reasonable correspondence between the two series and for the trend. The actual year-to-year drought periods vary more, as reflected by the value of  $R$ : 0.66. However, this result is not surprising. One shower at one or two stations other than De Bilt may 'spoil' the length of the dry period for all 13 stations.

The structural time-series model for De Bilt is shown in **Figure 5.6**. The minimum of the annual dry days fall in 1979 (8 days) and the maximum in 1919 (30 days) and 2003 (29 days).

Trend statistics:

- $\mu_{1906} = 18.2$  [16.2, 20.2] days
- $\mu_{2003} = 18.6$  [16.6, 20.6] days
- $\mu_{2003} - \mu_{1906} = -0.4$  [-3.8, 3.0] days
- $\mu_{2003} - \mu_{2002} = -0.004$  [-0.038, 0.030] days

The results show the trend in drought to be constant over the 1906-2003 period. The trend value in 2003 does not differ statistically from any of the trend values in the 1906-2002 period.

### Peat dike failure, August 2003

There are more than 17,000 kilometres of dikes in the Netherlands. The Dutch are all familiar with the huge flood disaster of February 1953 on the islands of the province of Zeeland (Zeeland), in the southwest of the country. During this event 1836 people died. The sea dikes broke due to the combination of high tide and a heavy winds. The problems of *river dikes* during the high-water situations in March 1988, December 1993 and January-February 1995 have still not been forgotten. However, people were totally astonished at the dike breach along a canal in Wilnis, a town 30 km south of Amsterdam, at the end of the warm and very dry summer in 2003.

The water in the canal started to flow into a residential quarter of the town necessitating a dike closure by a local contractor . By the time the closure was completed, 600 houses were already half a metre under water. The 2000 residents were evacuated in the early morning. Almost all residents could return to their homes the same evening after the water has been pumped out of the area. The dike breach over 30 metres is shown below (Photo: ANP).



Like many other small dikes in the Netherlands, the complete dike consists of peat. Since peat has a relatively low specific weight, a peat dike has a higher risk of being pushed aside by water pressure than sand or clay dikes. This horizontal sliding is a rare type of failure mechanism. However, checking the stability of this dike using a simple computation makes clear how realistic the failure of a dike after a long dry period is.

*For more information and further reading see: S. van Baar,  
<http://dutgeo.ct.tudelft.nl/vanbaars/research/Wilnis/Wilnis.pdf>.*

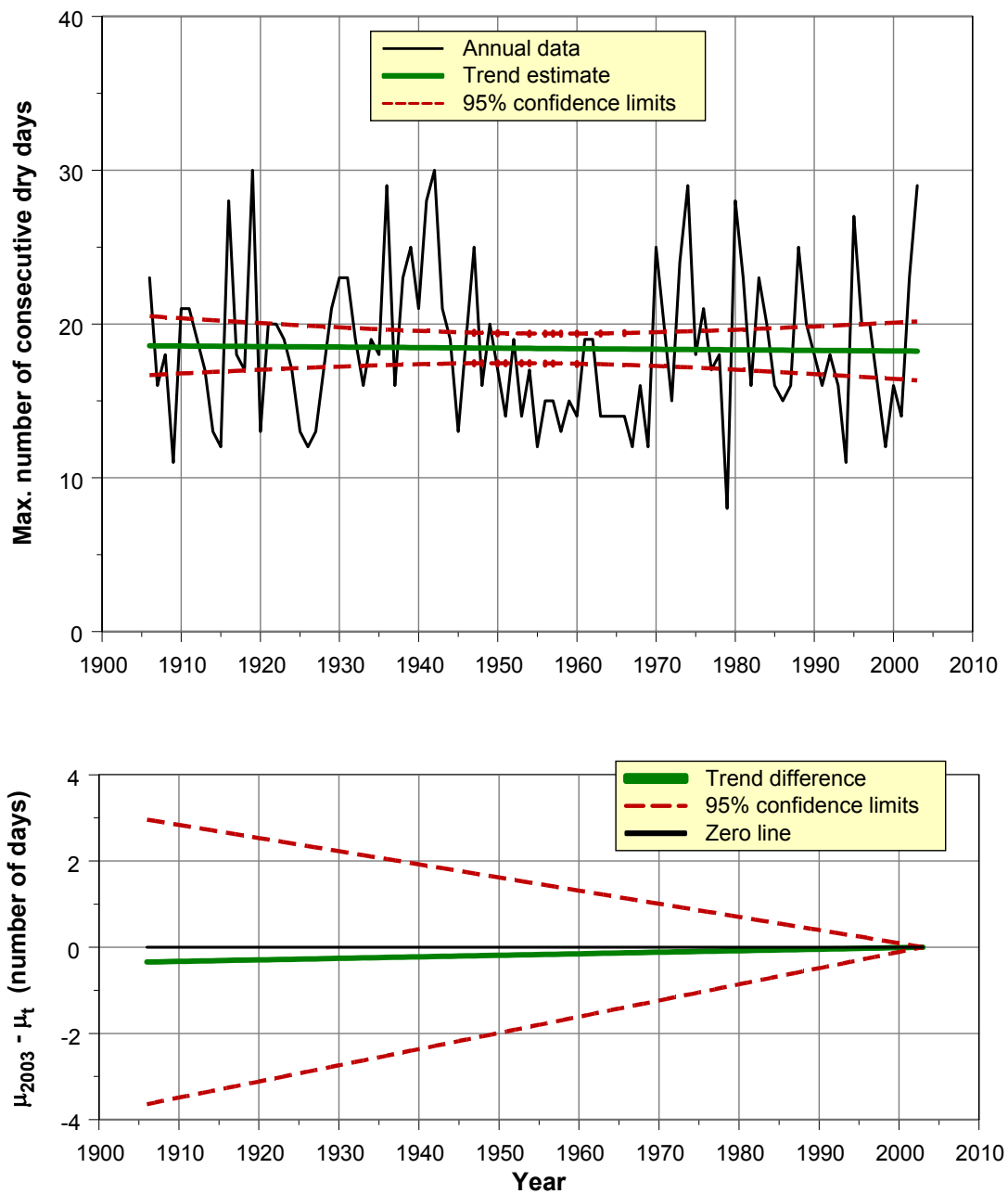


Figure 5.6 Maximum number of consecutive dry days for De Bilt (black line), the estimated trend (green line) and the corresponding 95% confidence limits (dashed red lines).  
 Period is 1906-2003. The lower panel shows the trend differences  $\mu_{2003} - \mu_t$  (days).



## 6. Temperature-related impacts

### 6.1 Premature deaths during heat waves

The heat wave in the summer of 2003 led to a great number of heat-related deaths all over Europe. See inset on the next page. In the Netherlands, 1000 to 1400 heat-related deaths, or to be more precise 'premature deaths', was estimated by Statistics Netherlands (CBS, 2003).

Statistics Netherlands has also deduced an equation to predict heat-related deaths on a weekly basis:

$$y_{t, \text{week } i} = (T_{\text{max},i} - 22.3) * [25, 35]$$

The variable  $T_{\text{max},i}$  is the weekly average of daily maximum temperatures, with week  $i$  falling in the months of June, July and August. The range  $[25, 35]$  stands for the number of deaths per degree, ranging from 25 to 35. Variable  $y_{t, \text{week } i}$  stands for the number of premature deaths in year  $t$  and week  $i$ . The variable  $y_{t, \text{low}}$  is the low estimate for the annual number of premature deaths in year  $t$ , and  $y_{t, \text{high}}$  is the high estimate.

In the following  $y_{t, \text{low}}$  and  $y_{t, \text{high}}$  are calculated for the weather conditions over the 1901-2003 period using the semi-homogenized data of De Bilt station. Both series,  $y_{t, \text{low}}$  and  $y_{t, \text{high}}$ , are interpreted to ask what the number of deaths,  $y_t$ , would be for the weather conditions of year  $t$ , and the healthcare/population of the year 2003.

Italy -- The high numbers of elderly Italians who apparently died as a result of this summer's (2003) scorching heat wave will not have died in vain, the country's health minister has pledged. The Health Ministry said on Thursday that 34,071 people over the age of 65 had died between July 16 and August 15, compared with 29,896 in 2002, a 14 percent increase. 'Nobody is looking for scapegoats, but all of this research helps to avoid problems in the future,' Health Minister Girolamo Sirchia told a news conference. In some cities, including Turin and Genoa, the increase in deaths on the previous year was as high as 40 percent during the heat wave, Reuters reported. Temperatures soared as high as 40 degrees Celsius during the period. The heat wave clearly had a role in the high numbers, according to officials from the Ministry's Superior Health Institute, which compiled the figures.

'There is a relationship between heat peaks and mortality,' the Associated Press quoted institute official Dr Donato Greco as saying. But officials said they could not blame the deaths entirely on the heat without further study. It was Italy's first official figures related to the heat. The government had first balked at releasing any figures but changed course following a public outcry in response to France's startling toll.

An estimated 11,435 people died in France from the heat, the French government has said. The country's leading undertaker put the number at 15,000 on Tuesday. The French toll sparked a political uproar in Paris over who was to blame, with calls for the health minister to resign. But Jean-Francois Mattei told lawmakers Thursday he had no plans to step down. A government report this week blamed hospitals for letting doctors leave during the August vacation and faulted health authorities for being too slow to realize how serious the situation was.

Spain reported 100 heat-related deaths, while Portugal scrapped its initial estimate of 1300 deaths and lowered it to just four. In Amsterdam, Dutch authorities estimated 1000 to 1400 victims, while in Britain officials said there were 907 more deaths registered during the week ending August 15 compared to the average from the same period over the previous five years.

The UK Health Department said it was 'fair to assume' that some of those deaths resulted from high temperatures. German authorities have reported about 40 heat-related deaths this summer, and in Belgium initial hospital reports indicate 150 more deaths between July 1 and August 15 than in the same period last year. In Serbia-Montenegro, three people were believed to have died from the heat wave in the Montenegrin capital, Podgorica, AP said. (CNN news.)



*Coffins are prepared in France, summer 2003.*

### 6.1.1 Low estimates

How did the annual number of premature deaths (low estimate) evolve in the Netherlands? To answer this question we had to transform the deaths numbers,  $y_{t, \text{low}}$ , through the following transformation:  $y_{t, \text{low}}' = \ln(20 + y_{t, \text{low}})$ . The structural time-series model is shown in **Figure 6.1**. The minimum of the annual deaths falls in 1907 (no deaths) and the maximum falls in 1947 (1077 deaths), and 2003 (878 deaths). In the graph transformed trend estimates have been back-transformed by the inverse transformation. Because of this transformation upper confidence limits are broader than lower confidence limits.

Trend values:

- $\mu_{1901} = 163$  [75, 334] deaths
- $\mu_{2003} = 438$  [217, 869] deaths
- $\mu_{2003} - \mu_{1901} = 275$  [border of significance] deaths
- $\mu_{2003} - \mu_{2002} = 17$  [not significant] deaths

The result shows an overall increased number of deaths since 1901, with an acceleration of this increase since 1970. The trend value in 2003 is larger than all the trend values in the 1901-2002 period. However, the trend value is only statistically significant for 1901-1921 and 1946-1981 (given  $\alpha = 0.05$ ).

### 6.1.2 High estimates

How did the annual number of premature deaths (high estimate) evolve? Again, the deaths numbers  $y_t$  were transformed with the transformation:  $y_{t, \text{high}}' = \ln(20 + y_{t, \text{high}})$ . The structural time-series model is shown in **Figure 6.2**. The minimum of the annual deaths falls in 1907 (no deaths) and the maximum in 1947 (1505 deaths). In the graph transformed trend estimates have been back-transformed by the inverse transformation.

Trend values:

- $\mu_{1901} = 223$  [100, 475] deaths
- $\mu_{2003} = 615$  [292, 1270] deaths
- $\mu_{2003} - \mu_{1901} = 392$  [border of significance] deaths
- $\mu_{2003} - \mu_{2002} = 25$  [not significant] deaths

The result shows an overall increasing number of deaths, with an acceleration of this increase since 1970. The trend value in 2003 is greater than all trend values in for 1901-2002. However, the trend value is only statistically significant for 1901-1921 and 1946-1981 (given  $\alpha = 0.05$ ).

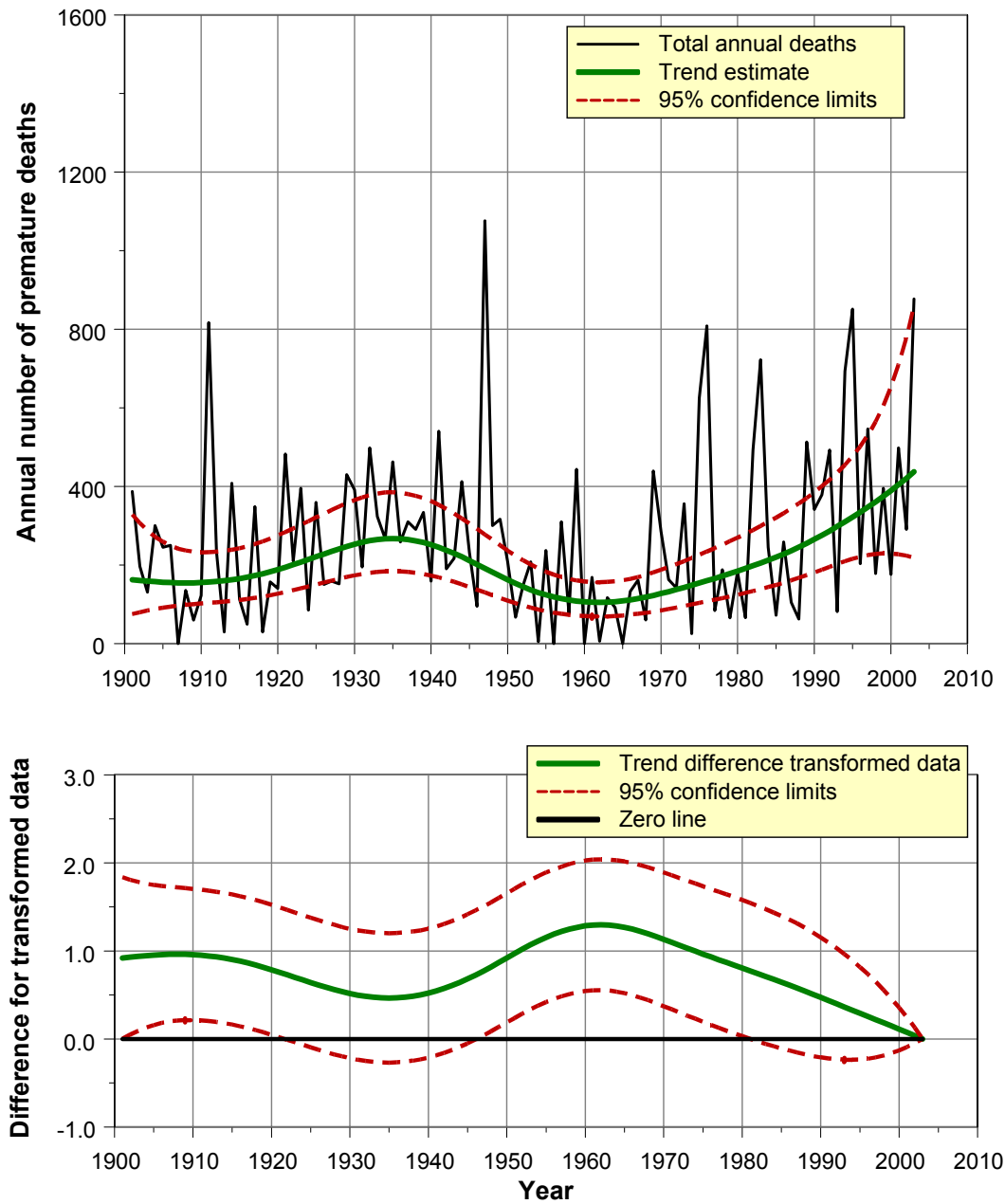


Figure 6.1 *Low estimate of heat-related deaths in the Netherlands, based on maximum temperatures at De Bilt (black line), the estimated trend (green line) and the corresponding 95% confidence limits (dashed red lines). Period is 1901-2003. The lower panel shows the trend differences  $\mu_{2003} - \mu_t$  (log(deaths)).*

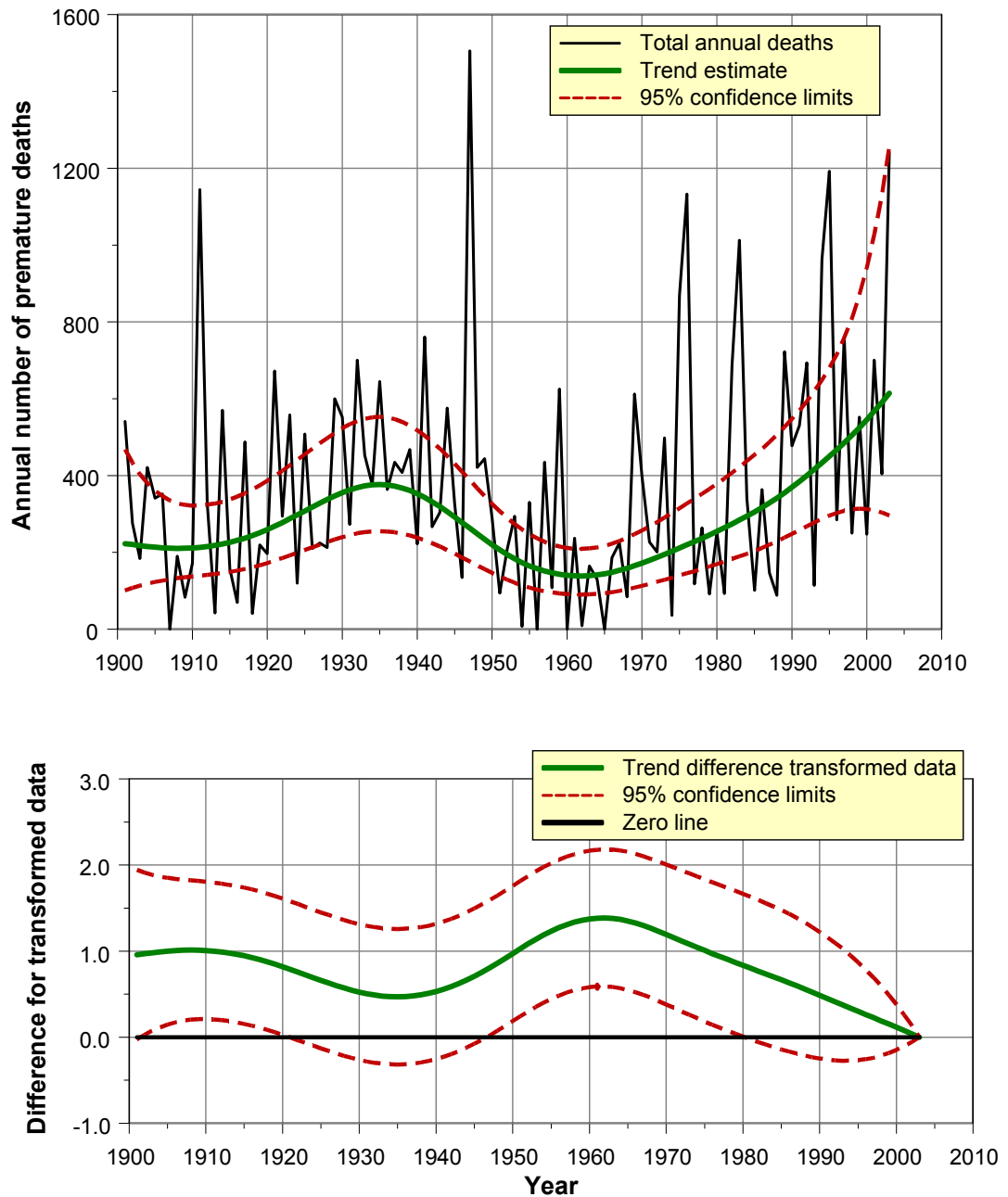


Figure 6.2 *High estimate of heat-related deaths in the Netherlands, based on maximum temperatures at De Bilt (black line), the estimated trend (green line) and the corresponding 95% confidence limits (dashed red lines). Period is 1901-2003. The lower panel shows the trend differences  $\mu_{2003} - \mu_t$  (log(deaths)).*

### 6.1.3 Combination of estimates

Combining the low and high estimates for sections 6.1.1 and 6.1.2 yields the following ranges:

- $\mu_{1901} = [75, 475]$  deaths
- $\mu_{2003} = [217, 1270]$  deaths
- $\mu_{2003} - \mu_{1901} = [275, 392]$  deaths (increment at the border of significance)
- $\mu_{2003} - \mu_{2002} = [17, 25]$  deaths (increment non-significant)

Furthermore, we note that the number of deaths has had a positive acceleration since the 1960s.

Fisher *et al.* (2003) analysed the premature data of CBS and drew the conclusion that these deaths were only partially due to extremely high temperatures. They state that an excess of around 400 to 600 deaths is related to air pollution (PM<sub>10</sub> and ozone). Their conclusion does not influence the patterns shown in **Figures 6.1** and **6.2**. Only the interpretation of the cause of these deaths is different.

Note that the impact of hot periods in the Netherlands will grow because of the sharp increase in the number of elderly people expected for 2010-2020. This phenomenon is due to the 'baby boom' just after World War II.

### 6.1.4 Fewer premature deaths in winter

Clearly, the number of premature deaths in summer will increase considerably in a warming climate. On the other hand, premature deaths during extreme cold periods will *decrease*. We do not have models to predict the size of this beneficial effect, but deriving such models could form an important research topic.

## 6.2 Changes in the start of the growing season

How has the start of the growing season evolved in the Netherlands? The definition of ECA has been chosen to determine the initiation date, with the starting date represented by the day number on which daily averaged temperatures reach 5 °C on 6 *consecutive* days (variable ‘GSL’). **Figure 6.3**, upper panel, shows these data for De Bilt.

The minimum day number is 6, and occurs in a number of years: i.e. 1902, 1916, 1921, 1926, 1988, 1992, 1998 and 1999. The maximum day number (115) falls in 1917.

Trend statistics:

- $\mu_{1901}$  = day number 63 [50, 76]
- $\mu_{2003}$  = day number 34 [21, 47]
- $\mu_{2003} - \mu_{1901}$  = -28.6 [-48.2, -9.0] days
- $\mu_{2003} - \mu_{2002}$  = -0.35 [-0.75, 0.05] days

The results show a linearly decreasing day-number series. The trend value in 2003 is statistically significant smaller than all trend values in the 1901-1985 period.

The impact of the shift in initiation day to earlier dates, which accounts for 29 days since 1901, has been reported in a number of publications. As temperatures rise sooner in the spring, interdependent species in ecosystems may shift dangerously out of sync. For references see Both and Visser (2001), Fitter and Fitter (2002), Moraal *et al.* (2004), and Grossman (2004a,b). An illustration of earlier flowering of plants is given in **Table 6.1**.



*Changes in the initiation of the growing season will seriously affect the stability of ecosystems (Grossman, 2004a,b; Moraal et al., 2004).*

*Photo: H. Visser.*

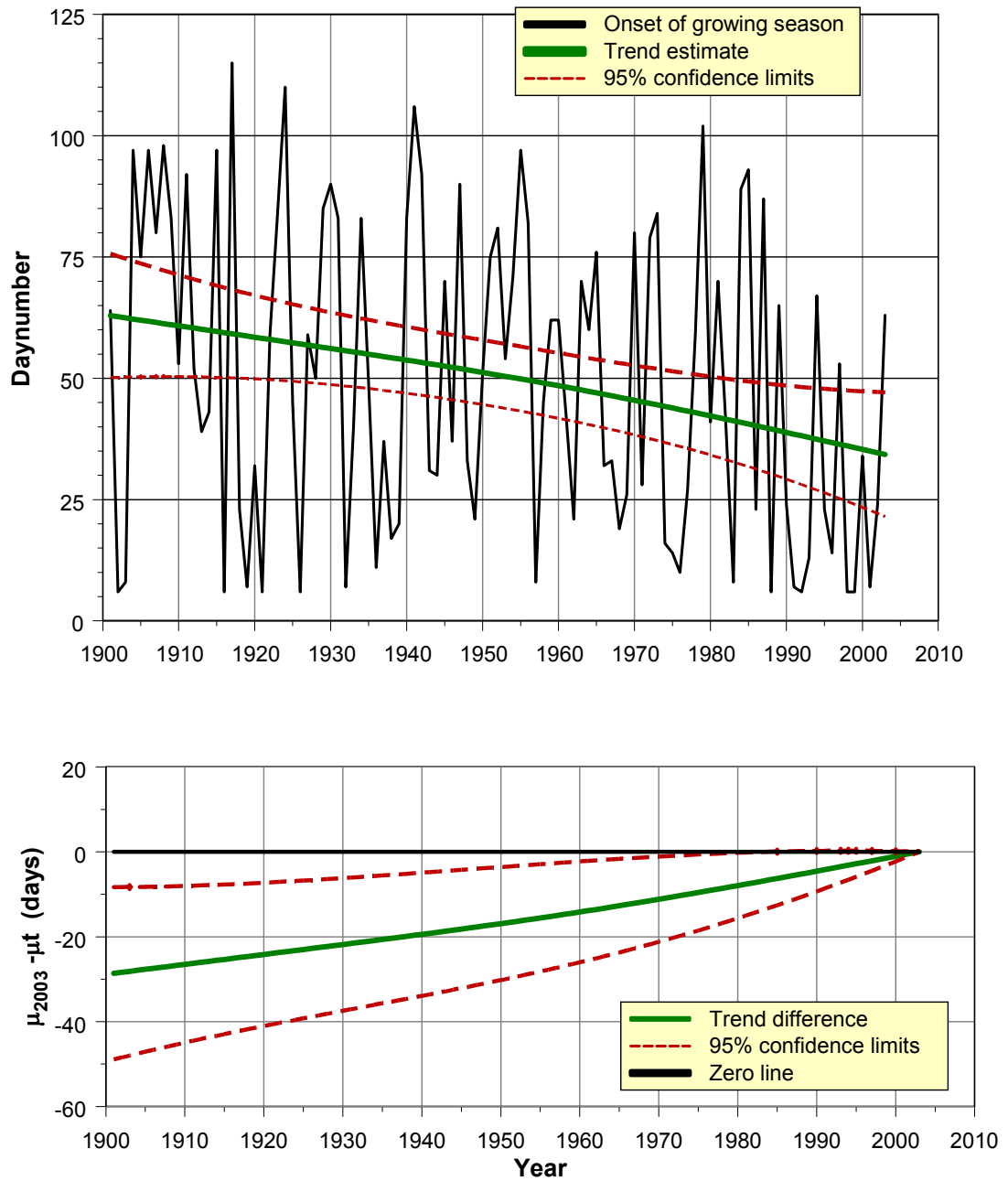


Figure 6.3 Start of the growing season in the Netherlands, based on daily averaged temperatures at De Bilt (black line), the estimated trend (green line) and the corresponding 95% confidence limits (dashed red lines). Period is 1901-2003. The lower panel shows the trend differences  $\mu_{2003} - \mu_t$  (days).

Table 6.1 *Early flowering in the Netherlands. Source: Zwart (2000) and [www.knmi.nl/voorl/nader/](http://www.knmi.nl/voorl/nader/).*

Onset of leaf flourishing or Flowering of trees and other plants	Average date 1975-1988	Average date 1988-2002	Difference in days
Old beeches in the KNMI park	1 May	22 April	9
Oaks in the KNMI park	3 May	24 April	9
Earliest chestnut in the KNMI park*	7 April	19 March	19
Idem (start of flowering)*	4 May	15 April	19
Apple	7 May	23 April	14
Peer	22 April	11 April	11
Prunus serrulata (cherry)	25 April	17 April	8
Magnolia	18 April	3 April	15
Hamamelis	14 January	4 January	10
Forsythia	25 March	5 March	20
Cornus mas (Cornelian cherry)	1 March	10 February	19
Hazel (onset of dispersion)	7 February	19 January	19
Black Elm (onset of dispersion)	2 March	13 February	17
Trumpet narcissus (Dutch Master)	30 March	11 March	19
Pilewort	29 March	2 March	27
Cow parsley	25 April	8 April	17
Coltsfoot	24 March	26 February	26
Dandelion	15 April	13 March	33

\* Cut in the year 2000

## 6.3 Heating- and cooling-degree days

### 6.3.1 Heating-degree days

Heating-degree days for year  $t$  are defined as the sum of the differences ( $18.0\text{ }^{\circ}\text{C} - \text{TG}_{i,t}$ ), with  $\text{TG}_{i,t}$ , a day with average temperatures below  $18.0\text{ }^{\circ}\text{C}$  and the index  $i$  running through all the days in year  $t$ . Days with average daily temperatures above  $18.0\text{ }^{\circ}\text{C}$  make no contribution. Heating-degree days have an important economic component. The use of fuels for household warming is strongly coupled to this indicator.

How did these heating-degree days evolve? **Figure A.7**, upper panel, shows these data for De Bilt along with the four-station average series (Den Helder, Groningen, De Bilt and Vlissingen). Both graphs show good correspondence ( $R = 0.99$ ).

The structural time-series model for De Bilt is shown in **Figure 6.4**. The minimum of the annual days falls in the years 1990 (2709) and 2000 (2695). The maximum falls in 1963 (3746).

Trend statistics:

- $\mu_{1906} = 3333 [3193, 3470]\text{ }^{\circ}\text{C}$
- $\mu_{2003} = 2887 [2747, 3027]\text{ }^{\circ}\text{C}$
- $\mu_{2003} - \mu_{1906} = -446 [-630, -262]\text{ }^{\circ}\text{C}$
- $\mu_{2003} - \mu_{2002} = -13.6 [-25.5, -1.7]\text{ }^{\circ}\text{C}$

The result shows a gradually decreasing series with a rapid acceleration after 1970. The trend value in 2003 is statistically smaller than all trend values in the 1906-2002 period.

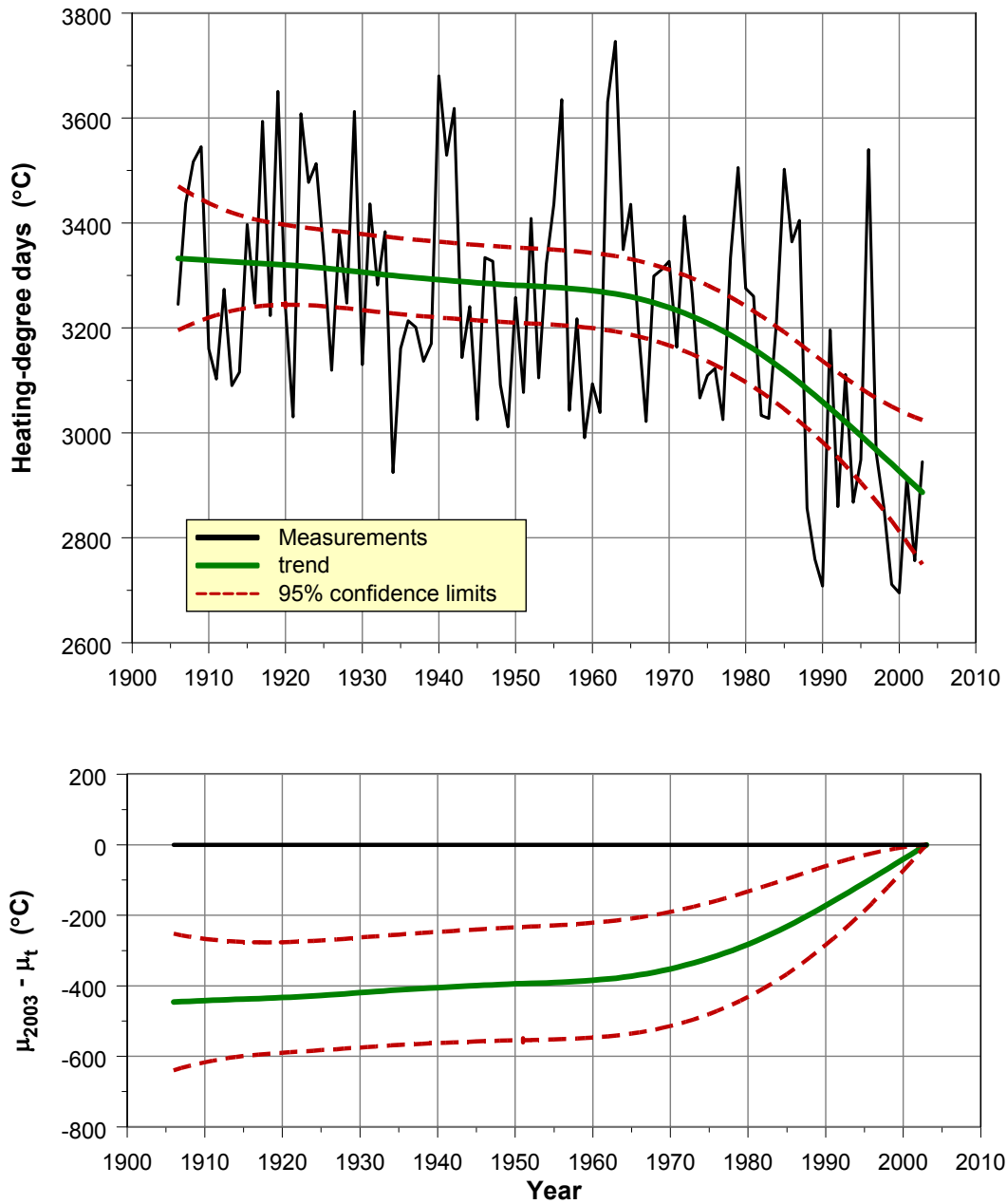


Figure 6.4 Number of heating-degree days the Netherlands, based on daily averaged temperatures at De Bilt (black line), the estimated trend (green line) and the corresponding 95% confidence limits (dashed red lines).

Period is 1906-2003. The lower panel shows the trend differences  $\mu_{2003} - \mu_t$  (°C).

### 6.3.2 Cooling-degree days

Annual cooling-degree days for year  $t$  are defined as the sum of the differences ( $TG_{i,t} - 18.0\text{ }^{\circ}\text{C}$ ), with  $TG_{i,t}$  a day with average temperatures *above*  $18.0\text{ }^{\circ}\text{C}$  and the index  $i$  running over all days in year  $t$ . Days with  $TG$ 's under  $18\text{ }^{\circ}\text{C}$  are omitted. Thus, cooling-degree days are the complement of heating-degree days. They have an important economic component. The use of airco's for households, commercial buildings and cars is strongly coupled to this indicator. Subsequently, temperature corrections for national  $\text{CO}_2$  emissions can be modelled using this indicator.

The structural time series model for De Bilt is shown in **Figure 6.5**. The minimum of the annual data falls in the years 1956 (5.0), 1962 (4.4) and 1965 (4.6). The maximum falls in the year 1947 (198).

Trend statistics are

- $\mu_{1906} = 25.9$  [15.4, 40.8] ( $^{\circ}\text{C}$ )
- $\mu_{2003} = 92.1$  [62.0, 134.7] ( $^{\circ}\text{C}$ )
- $\mu_{2003} - \mu_{1906} = 66.2$  [significant] ( $^{\circ}\text{C}$ )
- $\mu_{2003} - \mu_{2002} = 2.32$  [non significant] ( $^{\circ}\text{C}$ )



*The demand for air conditioning systems is related to the cooling-degree indicator defined here. This demand will increase as cooling-degree days will rise in the near future (Appendix D.2).*

The result shows a gradually increasing series up to 1940, a plateau from 1940 to 1970 and a rapid acceleration since 1970. The trend value in 2003 is statistically larger than all trend values in the period 1906-1990. In other words all trend differences  $(\mu_{2003} - \mu_{1990})$ ,  $(\mu_{2003} - \mu_{1989})$ ,  $(\mu_{2003} - \mu_{1988})$ , .....,  $(\mu_{2003} - \mu_{1906})$  are statistically significant positive.

It is noted that the upper confidence limits are wider than the lower limits due to the log transformation.

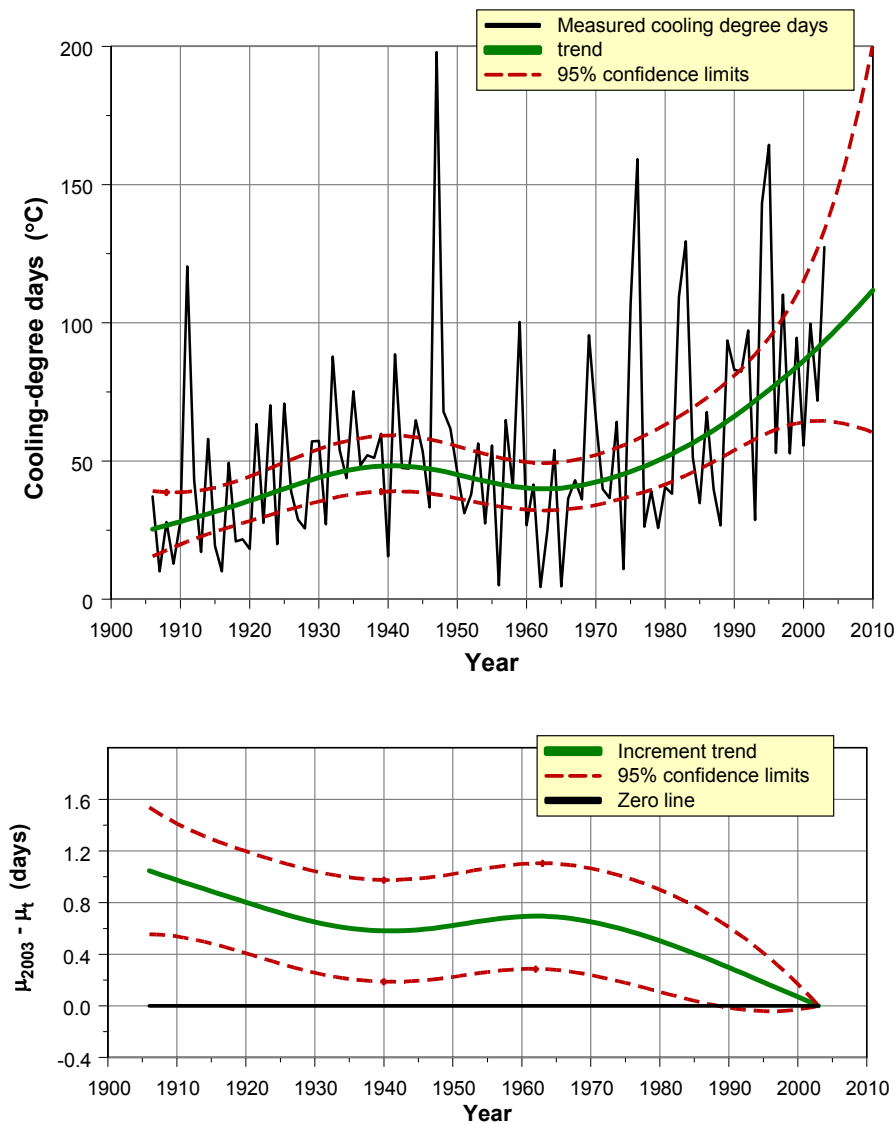


Figure 6.5 Annual number of cooling-degree days in the Netherlands, based on daily averaged temperatures at De Bilt (black line), the estimated trend (green line) and the corresponding 95% confidence limits (dashed red lines).

Period is 1906-2003. Data have been transformed using the formula  $y_t' = \ln(10 + y_t)$ . As for the upper panel estimates have been **backtransformed**. This is **not the case** for the increment of the trend in the lower panel.

## 6.4 Outdoor skating and the ‘Elfstedentocht’

Outdoor skating is a popular sport in the Netherlands. During cold periods a great number of tours are organized throughout the country. The ‘tour of all tours’ is the ‘Elfstedentocht’, the 11-city marathon, held in the province of Friesland. In this section we explore how climate warming has influenced the conditions for holding such a marathon since the beginning of the 20th century. In other words, how evolved the chance of holding an annual ‘Elfstedentocht’ in the 1901-2004 period (see the history of this event in the next subsection).

The derivation of the chance of an ‘Elfstedentocht’ is more complex than the examples given in the preceding sections. The annual chances will be estimated in three steps by asking the following questions:

- What is a simple indicator for maximum ice thickness? (section 6.4.2)
- How does the trend in this indicator evolve over 1901-2004? (section 6.4.3)
- What is the chance of holding an annual ‘Elfstedentocht’? (section 6.4.4)

The contents of this section is also given by Visser (2005). The history of the ‘Elfstedentocht’ is shortly given in the next section.

### 6.4.1 History

For a long time the ‘Elfstedentocht’ has been considered an impressive opportunity in the Netherlands to skate along eleven Friesian cities on the water in one day, covering a distance of almost 200 km (see inset). The names of dozens of successful skaters from the last century are still familiar, their stories being proudly passed on within their family circles from generation to generation. The ‘Elfstedentocht’ offers both competitive and non-competitive marathons for the same route on the same day. This event has taken place 15 times since 1909.

The marathon is highly dependent on specific weather conditions. For the marathon to actually take place, the ice needs to be at least 15 cm thick along virtually the whole route. During prolonged freezing, the regional organizing committee goes out every day at least once to measure the thickness of the ice. Sometimes ice is transplanted to places where the natural ice layer is thin. Once the marathon committee has given the green light, ‘klünen’ (skate-walking) facilities are constructed along the vulnerable parts of the route. Please refer to [www.elfstedentocht.pagina.nl](http://www.elfstedentocht.pagina.nl) for more information.

The 'Elfstedentocht' covers a course of almost 200 kilometres, going from town to town, over lakes and ditches, between fields and under bridges. Hundreds of thousands of spectators cheer the skaters along the route. Leeuwarden, the capital of Friesland, has always been the start and finish. The marathon takes the participants from Leeuwarden (Ljouwert) to Sneek (Snits), IJlst (Drylts), Sloten (Sleat), Stavoren (Starum), Hindeloopen (Hynljippen), Workum (Warkum), Bolsward (Boalsert), Harlingen (Harns), Franeker (Frentsjer), Dokkum and back to Leeuwarden. At registration, every participant gets a card which has to be stamped in each town and at a number of checkpoints located in hidden places along the route.



For the route of the 11-city marathon see [www.elfstedentocht.nl](http://www.elfstedentocht.nl) (choose English version).

## 6.4.2 Indicator for maximum ice thickness

In principle the marathon is organized if ice thickness exceeds **15 cm**, according to the Elfsteden committee<sup>1)</sup>. This criterion necessitates a simple indicator to reasonably predict ice thickness in Friesland. Brandsma (2001) used the average winter temperature as an indicator. He compared the indicator with *calculated* maximal annual ice thickness for the province of Friesland, and found a reasonable linear relation between ice thickness and average winter temperature.

Maximal ice thickness can be calculated by an ice-grow model developed at KNMI (De Bruin and Wessels 1988, 1990; Wessels, 1999). These calculations have been performed by Wessels and were published by Brandsma (2001) for the 1901-2000 period. Maximal ice thickness and the years in which the ‘Elfstedentocht’ has been held are shown in **Figure 6.6A**. Four years in which the marathon *could have been organized* (maximal ice thickness of more than 30 cm) have been added. These potential years are 1939, 1979, 1987 and 1996.

Average winter temperature is quite a rough indicator. One could imagine a winter with one extremely cold month, one average month and one extremely warm month. The average of this winter will be ‘normal’. However, it could have very well been a winter with an ‘Elfstedentocht’. In the search for a more accurate indicator eight simple indicators were formulated and correlated with the 100 years with maximal ice thickness. The data set with ice thickness was kindly supplied by T. Brandsma from the KNMI.

The indicator  $I_t$  ≡ ‘the coldest period of 15 consecutive days in winter’ was found to perform best (in terms of the highest squared correlation). A scatterplot between maximal ice thickness and  $I_t$  is shown in **Figure 6.6B**. Green bullets denote years with a marathon organized (15 times) or a year with a potential marathon (4 years). The vertical orange line shows the best threshold, based on calculated ice thickness, for making a decision to organize a marathon. The optimal threshold is **20 cm**. The horizontal orange line shows the corresponding optimal threshold for  $I_t$ : **- 4.2 °C**.

The performance of the indicator is good. In the 81 years in which no marathon was organized (black bullets in Figure 6.6B) only four years came *below* the threshold of - 4.2 °C. In the 19 years with a (potential) marathon (green bullets in Figure 6.5B) only two years came *above* the threshold. In fact, the indicator is almost as good as the model-based ice-thickness predictions.

---

<sup>1)</sup> Other factors also play a role, such as the amount of open water due to drainage or occurring under bridges, and organizational factors

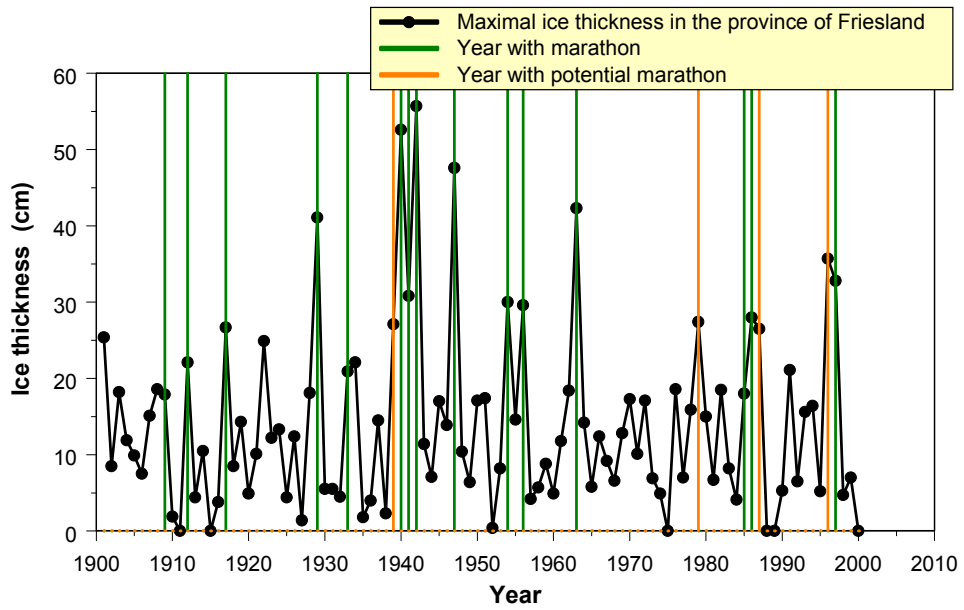


Figure 6.6A Maximal ice thickness 1901-2000, as computed by the ice-grow model from De Bruin and Wessels (1988), along with the years showing a (potential) 'Elfstedentocht' (19 in total).

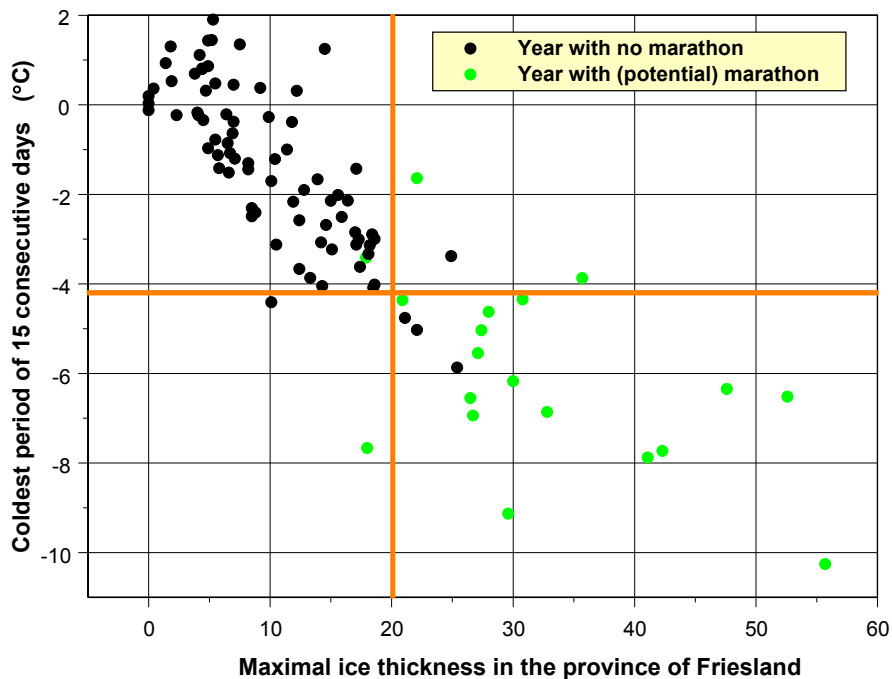


Figure 6.6B Scatterplot between annual maximal ice thickness and the corresponding indicator. Green dots represent years for a potential marathon.

### 6.4.3 Trend estimate ‘Elfstedentocht’ indicator

A trend model has been estimated for the indicator described in the preceding section. Because the residuals of the estimated trend model appeared to be skewed, the annual indicator values have been transformed by taking logarithms:  $I_t' = \ln(5.0 - I_t)$ .

**Figure 6.7** shows the estimation results. The upper panel shows the estimated trend after back transformation of the logarithmic model. The lower panel shows the differentiated trend  $\mu_{2004} - \mu_t$ , with corresponding uncertainties for the transformed model (these estimation results cannot simply be back transformed to the original metric).

Minimum thickness of the indicator falls in 1942 (-10.18 °C) and 1956 (-9.01 °C). Maximum thickness falls in 1989 (2.49 °C) and 2000 (3.03 °C).

Trend statistics:

- $\mu_{1901} = -1.52 [-2.82, -0.44]$  °C
- $\mu_{2004} = -0.29 [-1.34, 0.59]$  °C
- $\mu_{2004} - \mu_{1901} = 1.23$  [non significant] K
- $\mu_{2004} - \mu_{2003} = 0.05$  [non significant] K

The results show a slightly decreasing indicator series up to 1950 and an increasing trend thereafter. A statistical test on significance can be performed with the following  $H_0$  and  $H_1$  hypotheses:

$H_0$  : the indicator  $I_t$  is increasing over ‘first year’-2004

$H_1$  : the indicator is constant or even decreasing over ‘first year’-2004

If we choose  $\alpha = 0.05$  and a one-sided test, it can be read from the lower panel of Figure 6.7 that the trend value in 2004 is not significantly larger than values over the 1901-1913 and 1987-2003 periods. However, a significant increase was concluded for 1914-1986.

We note that the increase in  $I_t$  of 1.2 K over the whole century is only slightly smaller than the trend increment in annual averaged temperatures (1.5 K, section 4.1). Taking into account the large uncertainties, we can conclude that changes in this indicator closely follow the pattern of annual averaged temperatures.

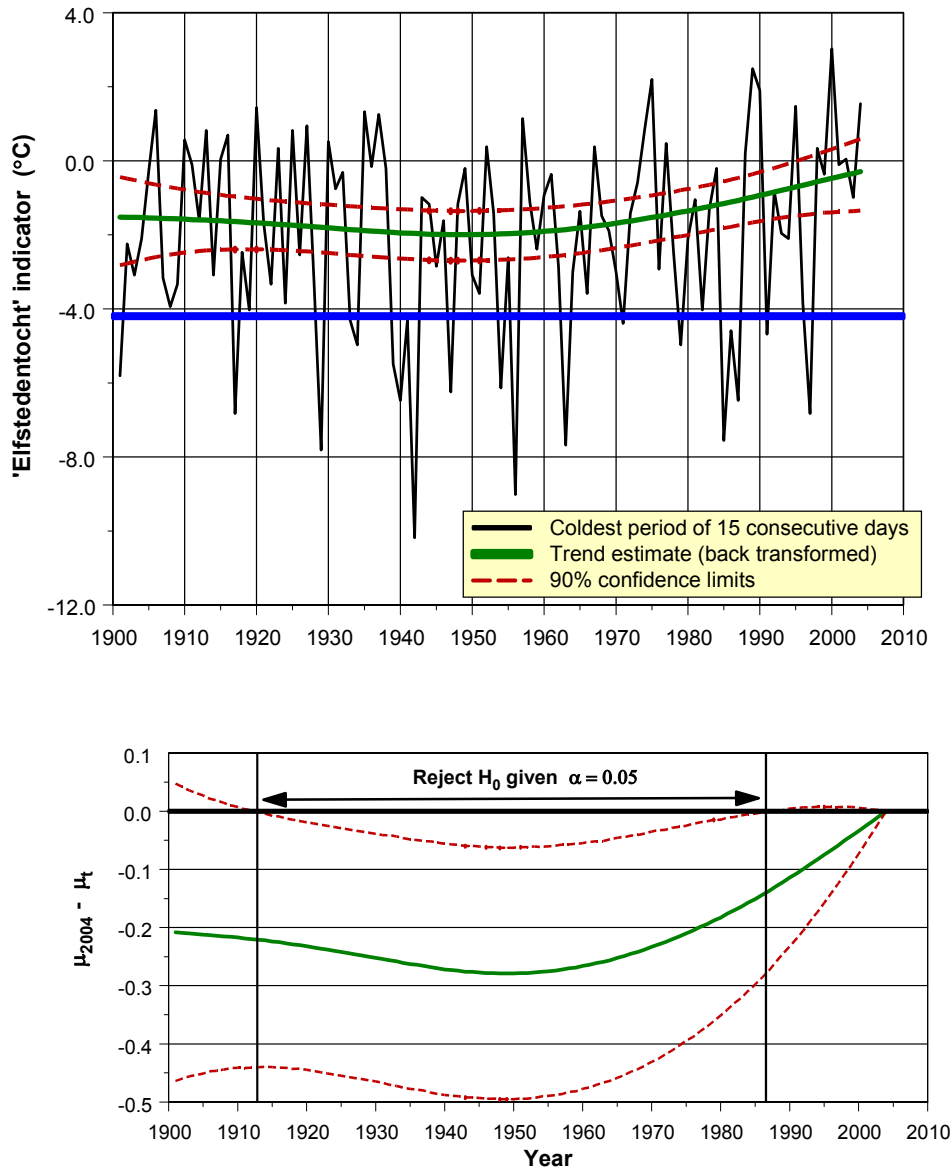


Figure 6.7 Annual 'Elfstedentocht' indicator based on daily temperatures at De Bilt (black line), the estimated trend (green line) and the corresponding 95% confidence limits (dashed red lines).

Period is 1901-2004. Because of the skewness of minimum temperatures the original temperatures  $y_t$  have been transformed to  $I_t' = \ln(5.0 - I_t)$ . Estimation results have been back transformed in this panel. The lower panel shows the trend differences  $\mu_{2004} - \mu_t$  based on the transformed model  $I_t'$ .

However, due to the larger variability in extreme cold periods the increment of 1.2 K over 1901-2004 is not significant (lower panel Figure 6.7,  $\alpha = 0.05$  and one-sided test). For the near future the indicator will become significant as the warming through the year will continue to rise (section 7.2). Thus the message here is a pessimistic one for those who love outdoor skating.

#### 6.4.4 Chance for an ‘Elfstedentocht’

Given the transformed indicator trend estimates  $\mu_t$ , its uncertainty  $\sigma_t$  and the uncertainty of the residuals  $\sigma_\varepsilon$  we can calculate for each year  $t$  the probability of having an Elfstedentocht organized (the ln-transformed indicator  $I_t$  is normally distributed with mean  $\mu_t$  and variance  $\sigma_t^2 + \sigma_\varepsilon^2$ ). Thus, we can calculate the chance  $P(I_t < -4.2 \text{ }^\circ\text{C})$ , with  $-4.2 \text{ }^\circ\text{C}$  being the threshold shown in Figure 6.6B. As an illustration the probability density functions of  $I_{1901}$  (green line) and  $I_{2004}$  (red line) are plotted in **Figure 6.8** (cf. the illustration in Figure 3.3). The densities follow a log-normal distribution due to the transformation. The

The chance  $p_t$  of having a marathon organized is equal to the surface of the tail of the density function right of the vertical decision line at  $-4.2 \text{ }^\circ\text{C}$ , shown in Figure 6.8. For 1901 the chance  $p_{1901}$  accounts for 0.21, for 2004 we find  $p_{2004} = 0.10$ . The complete function  $p_t$  is shown in **Figure 6.9**. The graph shows that the chance for organizing the marathon accounts for 0.22 in 1901, slightly increasing to 0.26 in 1950, and decreasing to 0.10 in the final year, 2004. These chances can also be expressed in terms of average return periods,  $r_t$ . A return period is simply the inverse of the annual chance ( $r_t = 1/p_t$ ). Thus, we have  $r_{1901} = 5$  years,  $r_{1950} = 4$  years and  $r_{2004} = 10$  years.

Section 6.4.3 concluded that the rise in the Indicator  $I_t$  is not significant relative to the first year, 1901. Consequently, the chance shift from  $p_{1901} = 0.22$  to  $p_{2004} = 0.10$  is not significant either.

The latter result seems contradictory to the halving of the chance or, equivalently, to the doubling of the return period. The reason is illustrated in Figure 6.9, where a relative small shift in the average of  $I_t$  (from  $-1.6 \text{ }^\circ\text{C}$  in 1901 to  $-0.3 \text{ }^\circ\text{C}$  in 2004, green and red vertical lines) results in a much larger change in chances on for extreme cold periods.

Are the results found here then hopeful for those who love outdoor skating? The answer is ‘no’. There is a tendency for increasing temperatures in the historical temperature records that are on the edge of significance. Moreover, temperatures, and thus the ‘Elfstedentocht’ indicator  $I_t$ , are expected to rise in the near future (see Chapter 7). This conclusion is consistent with that drawn by Brandsma (2001).

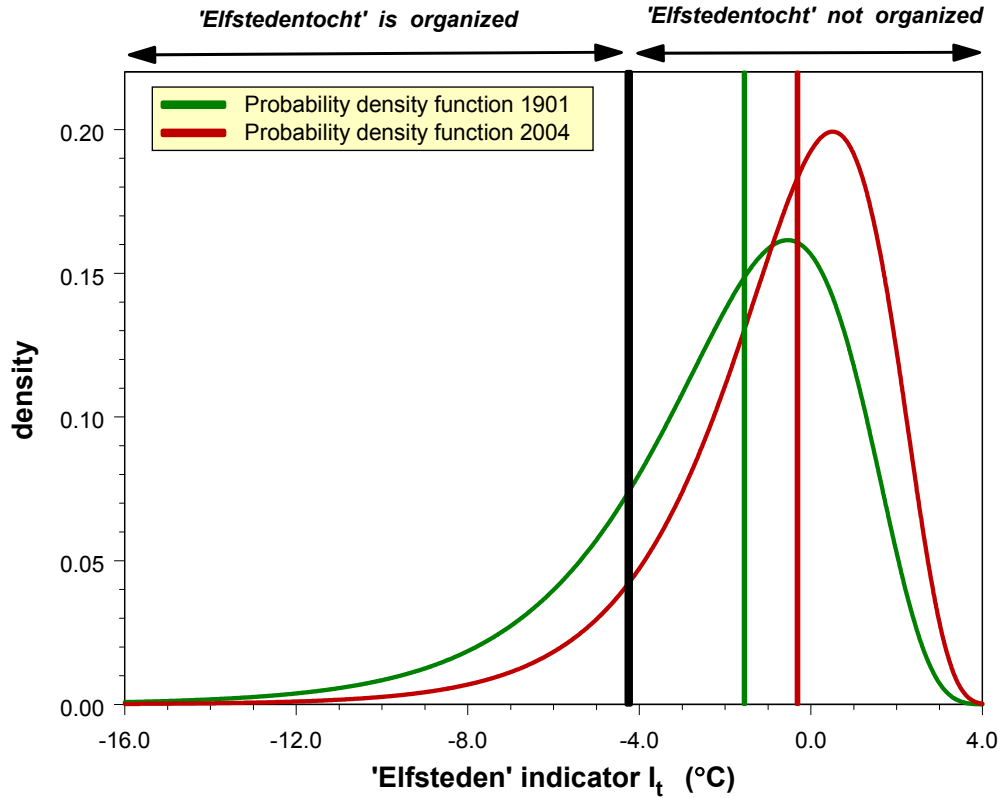


Figure 6.8 Probability density functions for the 'Elfsteden' indicator  $I_{1901}$  (green lines) and  $I_{2004}$  (red lines). Vertical lines are the mean values. The probability functions are shifted log-normal with long tails to the left (due to the transformation  $I_t' = \ln(5.0 - I_t)$ ).

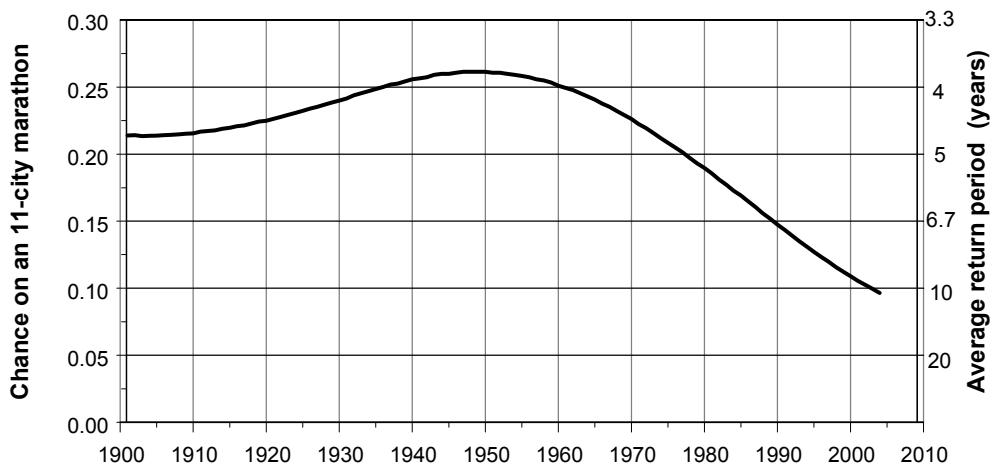
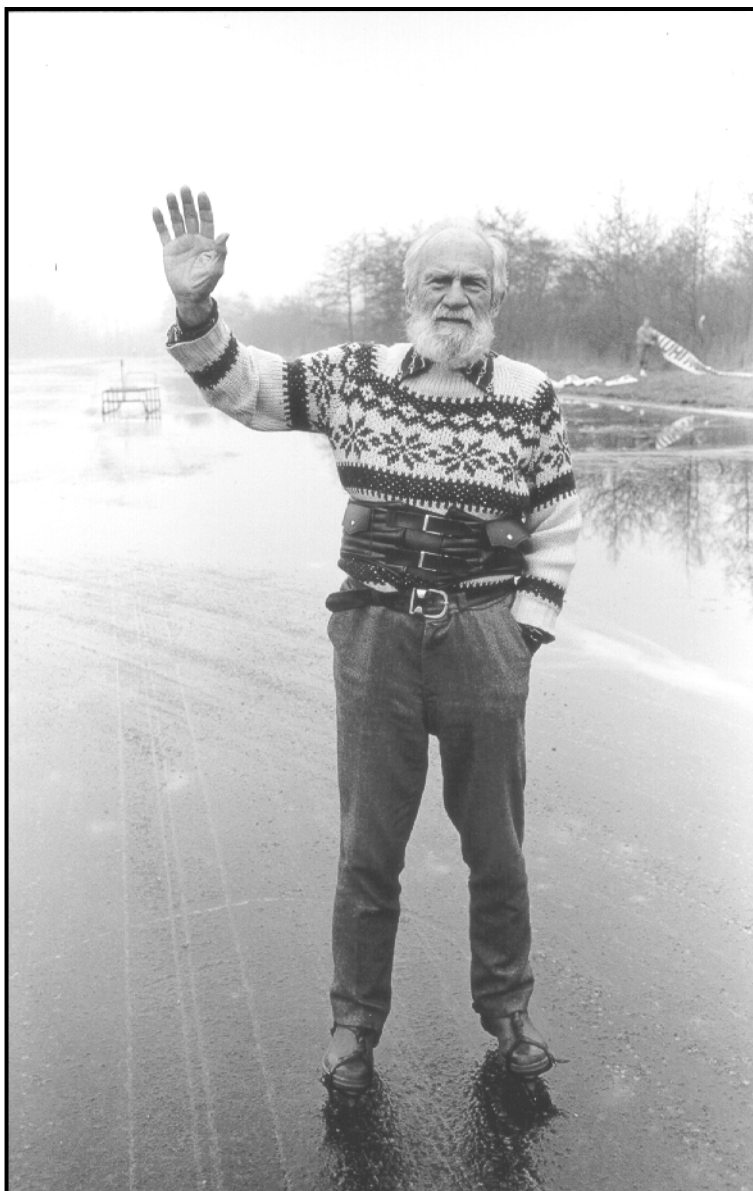


Figure 6.9 Annual chance for organizing an 'Elfstedentocht'. The right y-axis shows the corresponding return periods, which are simply the inverse of the annual chances.



*One of the conclusions from this study is that cold extremes show a less intense rise over the century than warm extremes. This also holds for the ice thickness indicator derived here. Yet, the chance for a large outdoor skating tour such as the 'Elfstedentocht', has decreased from once every five years in 1901 to once every ten years in 2004.*

*As annual (and monthly) averaged temperatures are projected to increase over the years to come, meteorological conditions favourable for outdoor skating will occur less frequently in the near future.*

*Photo: H. Visser.*



## 7. Future weather conditions: a two-way approach

This Chapter deals with temperature predictions for the near future: 2004-2020. This time horizon is important for a range of short-term policy measures for coping with the impacts of climate change.

Climate will be predicted on the basis of *two* approaches. The first approach followed is based on combining Global Climate Model (GCM) predictions for 2004-2020. The ratio between global and local warming yields another approximation for warming in the Netherlands that is *model-based*. For background information please see IPCC (2001), and the inset on the next pages.

The second approach is a simple one, but one that proved very powerful in many applications: i.e. to simply extrapolate historical trends (based on the 1901-2003 period) to the future (2004-2020). As a rule of thumb, in time-series analysis one should not go further into the future than ~20% of the existing series. This heuristic rule has been complied with by extending predictions no further than the year 2020. The method of extrapolation is purely *data-based*. It does not make any assumptions on climate change due to anthropogenic emissions of greenhouse gases.

Both approaches yield predictions which will be derived here. The rationale here is that trend estimates from state-of-the-art GCMs are regarded as giving the most reliable predictions for the near future. At the other hand, GCMs are still not able to generate reliable estimates for the year-to-year variability on a regional or even a local scale (i.e. the scale of the Netherlands). Therefore, the historical-extrapolation method yields additional information.

We note that *statistical extrapolation* is not a prediction method generally accepted amongst climatologists. There even exist two ‘schools’: those who feel that GCMs are the **only** tools for predicting and projecting future climate, and those who stress the weaknesses of GCMs, and therefore advocate more data-based methods. We refer to Shackley *et al.* (1998) for further discussions and arguments.

Conclusions drawn by IPCC (2001) on the attribution of climate change:

**There is new and stronger evidence that most of the warming observed over the last 50 years is attributable to human activities.**

The conclusion of IPCC in 1997 was that: 'The balance of evidence suggests a discernible human influence on global climate'. That report also noted that the anthropogenic signal was still emerging from the background of natural climate variability. Since 1997, progress has been made in reducing uncertainty, particularly with respect to distinguishing and quantifying the magnitude of responses to different external influences.

Although many of the sources of uncertainty identified in 1997 still remain to some degree, new evidence and improved understanding support an updated conclusion:

- There is a longer and more closely scrutinized temperature record and new model estimates of variability. The warming over the past 100 years is very unlikely to be due to internal variability alone, as estimated by current models. Reconstructions of climate data for the past 1000 years also indicate that this warming was unusual and is unlikely to be entirely natural in origin.
- There are new estimates of the climate response to natural and anthropogenic forcing, and new detection techniques have been applied. Detection and attribution studies consistently find evidence for an anthropogenic signal in the climate record of the last 35 to 50 years.
- Simulations of the response to natural forcings alone (i.e., the response to variability in solar irradiance and volcanic eruptions) do not explain the warming in the second half of the 20th century (see **Figure 7.1a**). However, they do indicate that natural forcings may have contributed to the observed warming in the first half of the 20th century.
- The warming over the last 50 years due to anthropogenic greenhouse gases can be identified despite uncertainties in forcing due to anthropogenic sulphate aerosol and natural factors (volcanoes and solar irradiance). The anthropogenic sulphate aerosol forcing, while uncertain, is negative over this period and therefore cannot explain the warming. Changes in natural forcing during most of this period are also estimated to be negative and are unlikely to explain the warming.
- Detection and attribution studies comparing model simulated changes with the observed record can now take into account uncertainty in the magnitude of modelled response to external forcing, in particular that due to uncertainty in climate sensitivity.
- Most of these studies find that, over the last 50 years, the estimated rate and magnitude of warming due to increasing concentrations of greenhouse gases alone are comparable with, or larger than, the observed warming. Furthermore, most model estimates that take into account both greenhouse gases and sulphate aerosols are consistent with observations over this period.
- The best agreement between model simulations and observations over the last 140 years has been found when all the above anthropogenic and natural forcing factors are combined, as shown in **Figure 7.1c**). These results show that the forcings included are sufficient to explain the observed changes, but do not exclude the possibility that other forcings may also have contributed.

In the light of new evidence and taking into account the remaining uncertainties, most of the observed warming over the last 50 years is likely to have been due to the increase in greenhouse gas concentrations.

*continued*

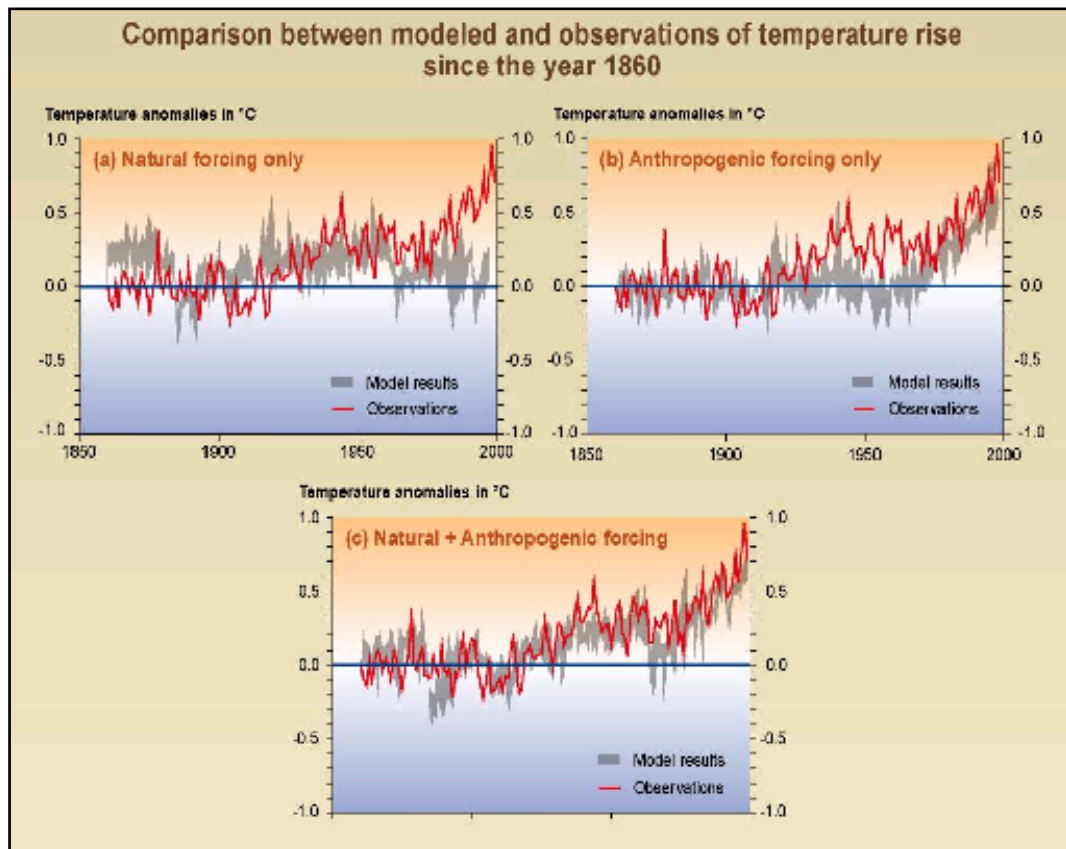


*Figure 7.1 A climate model can be used to simulate the temperature changes that occur as a result of natural and anthropogenic causes.*

The simulations represented by the band in (a) were done with only natural forcings: solar variation and volcanic activity. Those encompassed by the band in (b) were done with anthropogenic forcings: greenhouse gases and an estimate of sulphate aerosols, and those encompassed by the band in (c) were done with both natural and anthropogenic forcings. From (b), it can be seen that inclusion of anthropogenic forcings provides a plausible explanation for a substantial part of the observed temperature changes over the past century, but the best match with observations is obtained in (c), where both natural and anthropogenic factors are included. These results show that the forcings included are sufficient to explain the observed changes, but do not exclude the possibility that other forcings may also have contributed. The bands of model results presented here are for four runs from the same model. Similar results to those in (b) are obtained with other models using anthropogenic forcing. Source: graphs based on Chapter 12, Figure 12.7 from IPCC (2001).

## 7.1 Predicting global warming up to 2020

### *Model-based approach*

For model-based predictions we follow the approach set out in IPCC, as summarized in the introduction of this Chapter. GCM-based predictions and corresponding uncertainties are derived in Appendix C, section C.1 (equation C4). These predictions are:

$$- T_{\text{Global - GCM, 2010}} = 0.65 [0.41, 0.99] \text{ } ^\circ\text{C} \quad (4a)$$

$$- T_{\text{Global - GCM, 2020}} = 0.80 [0.06, 1.79] \text{ } ^\circ\text{C} \quad (4b)$$

### *Data-based approach*

Section 3.2.3 (compare Figure 3.3) shows that predictions by extrapolation of the estimated trend will lead to the following global temperatures:

- $\mu_{1901} = -0.39 [-0.47, -0.31] \text{ } ^\circ\text{C}$
- $\mu_{2003} = 0.47 [0.39, 0.55] \text{ } ^\circ\text{C}$
- $\mu_{2010} = 0.61 [0.42, 0.80] \text{ } ^\circ\text{C}$
- $\mu_{2020} = 0.81 [0.39, 1.23] \text{ } ^\circ\text{C}$
- $\mu_{2020} - \mu_{2000} = 0.41 [0.00, 0.81] \text{ K}$

Thus we have:

$$- T_{\text{Global - extapol, 2010}} = 0.61 [0.42, 0.80] \text{ } ^\circ\text{C} \quad (5a)$$

$$- T_{\text{Global - extapol, 2020}} = 0.81 [0.39, 1.23] \text{ } ^\circ\text{C} \quad (5b)$$

### *Comparing both approaches*

Clearly, estimates (4) and (5) are very similar as for the best guess values. However, the uncertainty bands for the GCM approach are much wider. The explanation is simple. The GCM uncertainty ranges are *absolute minimum and maximum values*, which themselves are very unlikely to occur (3- $\sigma$  or alike). On the other hand, the ranges in (5) are 95% (2- $\sigma$ ) confidence limits.

Both prediction methods and corresponding uncertainties are summarized in **Figure 7.2**.

### Overall conclusions

The conclusion from Appendix C and the results derived here, is that:

- global warming in the historical period of 1901-2003 is 0.86 [0.74 – 0.98] K. About [0.6 - 1.0] K is due to human emissions of greenhouse gases and [-0.2 - 0.2] K is due to natural variability.
- all future projections for human-induced warming are approx. linear over the period 2004-2100, and show an annual increase in the range 0.025 [0.005 – 0.060] K/y.
- model-based and data-based predictions are consistent. As for statistical extrapolation of the trend in global temperatures, the following warming is found for the years 2010 and 2020:  $T_{\text{global}, 2010} = 0.61$  [0.42, 0.80] °C and  $T_{\text{global}, 2020} = 0.81$  [0.39, 1.23] °C.

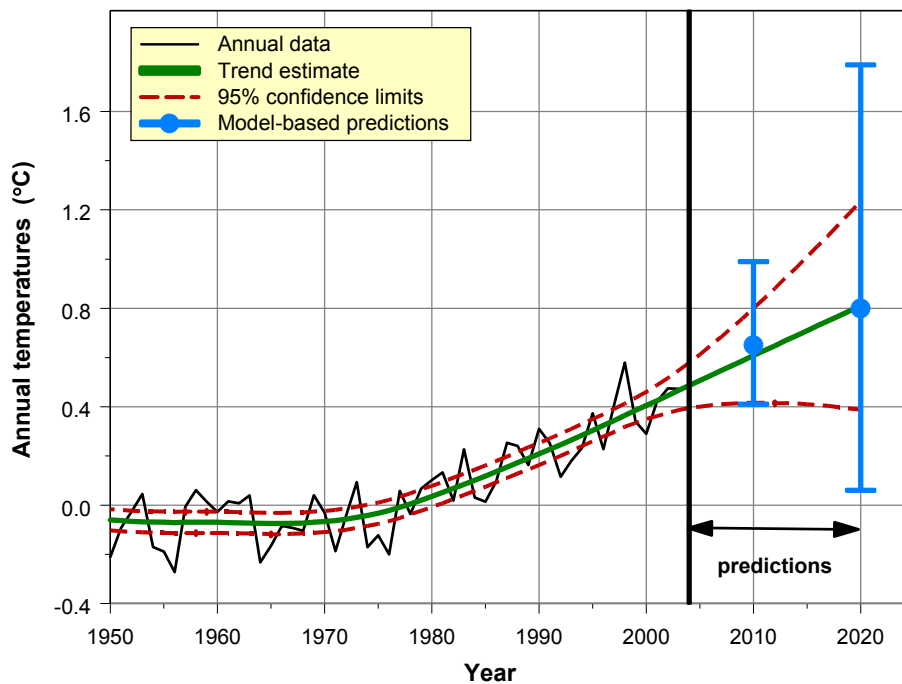


Figure 7.2 Model-based and data-based predictions for global annual temperatures, over the period 2004 – 2020.

## 7.2 Predicting local warming up to 2020

How will future temperatures evolve in the Netherlands up to the year 2020? Again, two approaches, data-based and model-based, have been followed.

### *Model-based approach*

The model-based approach uses the results found in Appendix C, which were deduced from GCM predictions. The ratio  $\Delta T_{\text{local}}/\Delta T_{\text{global}}$  for local and global future human-induced warming, respectively, has been found to account for **1.3 [1.1 – 1.5]**.

Furthermore, it was found for global temperatures that (equation C3):

$$- \Delta T_{\text{global - GCM, 2010}} \approx 0.18 [-0.06, 0.52] \text{ K} \quad (6a)$$

$$- \Delta T_{\text{global - GCM, 2020}} \approx 0.33 [-0.41, 1.32] \text{ K} \quad (6b)$$

As previously stated, the large negative lower bounds are due to natural variability.

If we combine global warming and the downscaling ratio for the Netherlands, we gain a warming prediction for De Bilt of:

$$- \Delta T_{\text{DeBilt - GCM, 2010}} = 1.3 [1.1 - 1.5] * \Delta T_{\text{global - GCM, 2010}} = 0.23 [< -0.06, 0.78] \text{ K} \quad (7a)$$

$$- \Delta T_{\text{DeBilt - GCM, 2020}} = 1.3 [1.1 - 1.5] * \Delta T_{\text{global - GCM, 2020}} = 0.43 [< -0.41, 1.98] \text{ K} \quad (7b)$$

Here, the notation '< -0.06' and '< -0.41' means that the lower bounds might be somewhat lower <sup>1)</sup>.

---

<sup>1)</sup> The KNMI designed a number of climate scenarios for the Netherlands. For annual averaged temperatures they foresee an anthropogenic-induced increase of 2.0 [1.0, 4.0-6.0] K, over the period 1990–2100. This is approx. equal to an annual rate of 0.018 [0.009, 0.055] K/year. This leads to the following increases for 2010 and 2020:

$$- \Delta T_{\text{DeBilt - GCM, 2010}} = 0.13 [0.06, 0.39] \text{ K}$$

$$- \Delta T_{\text{DeBilt - GCM, 2020}} = 0.31 [0.15, 0.94] \text{ K}$$

Best guess values are a tenth of a degree lower and uncertainty bands are narrower. However, natural variability has not been incorporated in the KNMI predictions. Because the KNMI ranges fall completely within the ranges presented in (7), the estimates in (7) will be used here.

Again we note that the uncertainty bands are minima and maxima, which themselves are very unlikely to occur. They are closer to 3- $\sigma$  confidence limits than the 2- $\sigma$  limits given for the extrapolated trend estimates. Furthermore, minimum values in (7a) and (7b) could not be calculated exactly due to the fact that the downscaling range was not calculated for relative *cooling*.

Given the trend estimate of 10.4 °C for the year 2003, the following predictions for De Bilt result :

$$- T_{\text{DeBilt - GCM, 2010}} = 10.6 \text{ [} < 10.3, 11.2 \text{]} \text{ } ^\circ\text{C} \quad (8a)$$

$$- T_{\text{DeBilt - GCM, 2020}} = 10.8 \text{ [} < 10.0, 12.4 \text{]} \text{ } ^\circ\text{C} \quad (8b)$$

### ***Data-based approach***

**Figure 7.3**, upper panel, shows estimates over the 1901-2020 period for the observatory at De Bilt. Trend statistics are:

- $\mu_{1901} = 8.8 \text{ [} 8.4, 9.2 \text{]} \text{ } ^\circ\text{C}$
- $\mu_{2003} = 10.4 \text{ [} 10.0, 10.8 \text{]} \text{ } ^\circ\text{C}$
- $\mu_{2010} = 10.7 \text{ [} 10.1, 11.3 \text{]} \text{ } ^\circ\text{C}$
- $\mu_{2020} = 11.1 \text{ [} 10.1, 12.1 \text{]} \text{ } ^\circ\text{C}$
- $\mu_{2020} - \mu_{2000} = 0.90 \text{ [} 0.10, 1.70 \text{]} \text{ K}$

The results show a gradually increasing temperature series with an acceleration of this increase since 1970. The trend value in 2020 is statistically larger than all trend values in the period 1901-2005.

Thus, using the notation from section 7.1, we have:

$$- T_{\text{DeBilt - extrapol, 2010}} = 10.7 \text{ [} 10.1, 11.3 \text{]} \text{ } ^\circ\text{C} \quad (9a)$$

$$- T_{\text{DeBilt - extrapol, 2020}} = 11.1 \text{ [} 10.1, 12.1 \text{]} \text{ } ^\circ\text{C} \quad (9b)$$

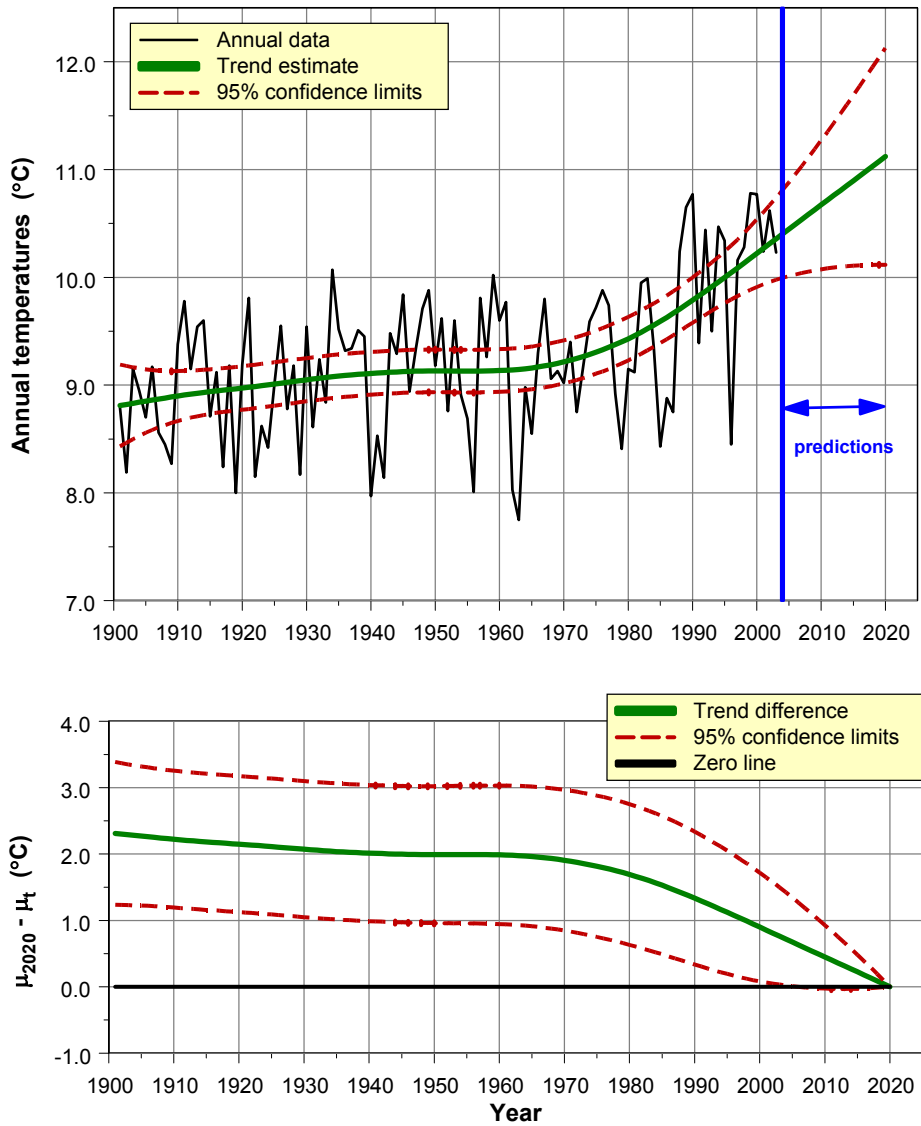
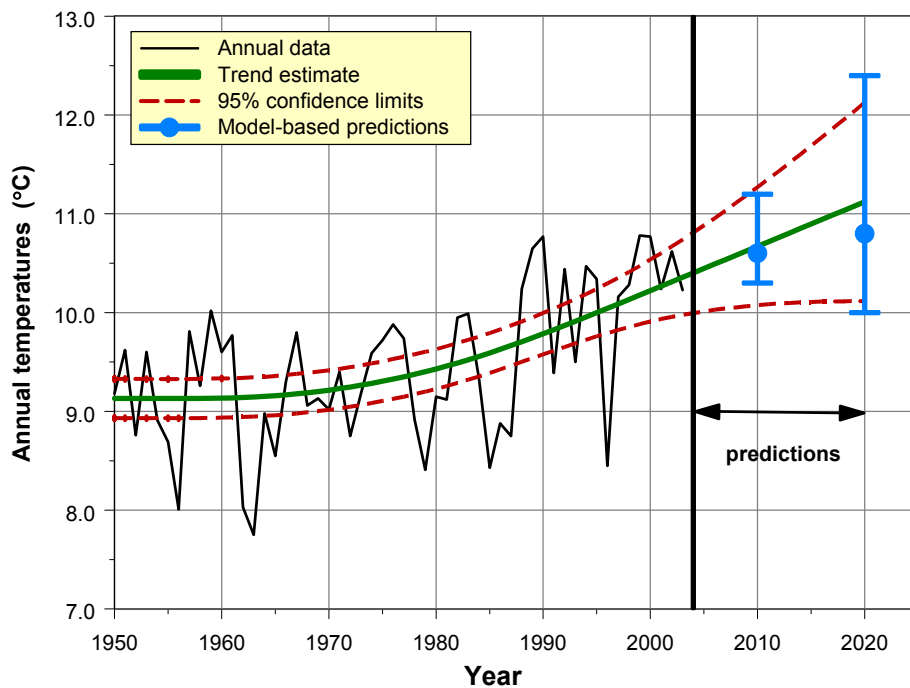


Figure 7.3 Analysis of annual averaged temperatures at De Bilt for 1901-2003. Estimates are extrapolated over the 2004-2020 period. The upper panel shows the data and the trend with 95% confidence limits. The lower panel shows the difference function,  $\mu_{2020} - \mu_t$  with 95% confidence limits.

### Comparing both approaches

It turns out that the GCM-based predictions (equations 8a and 8b) are very similar to those found by extrapolating the historical trend (equations 9a and 9b). This holds in the first place for the best-guess values. Remarkable here is that the GCM-based confidence limits are only slightly wider than the data-based limits, while a result similar to that found in section 7.1 for global temperatures was expected. Predictions and uncertainties are summarized in **Figure 7.4**).

The explanation for the latter result lies in the signal/noise ratio. If we compare Figures 3.2 (global temperatures) and 4.1 (temperatures De Bilt), it appears that the signal/noise ratio for De Bilt is much smaller. As a consequence the uncertainty bands for future data will be much wider.



*Figure 7.4 Model-based and data-based predictions for temperatures at De Bilt, over the period 2004 – 2020, appear to be very similar.*

**Overall conclusions**

It can be concluded that:

- model-based and data-based predictions are consistent. As for statistical extrapolation of the trend in global temperatures, the following warming is found for the years 2010 and 2020:  $T_{\text{De Bilt, 2010}} = 10.7 [10.1, 11.3] \text{ } ^\circ\text{C}$  and  $T_{\text{De Bilt, 2020}} = 11.1 [10.1, 12.1] \text{ } ^\circ\text{C}$ .



*Advertisement campaign for public awareness of the greenhouse effect ('a better environment starts with yourself'). Photo: H. Visser.*

### 7.3 Consequences for weather-related indicators

Are extrapolations of indicators other than the annual mean temperatures shown in Figure 7.1, allowed? Extending the period up to 2020 would represent an important extension of the analyses in Chapters 5 and 6. For some indicators the answer is ‘yes’, for others ‘no’. The answer will depend on the relation between the indicator  $I_t$  and  $T_{De\ Bilt, t}$ . If this relation is **linear**, we may extrapolate  $I_t$  as well. This can simply be seen in the following equations.

Suppose we have linear increasing temperatures, or:

$$T_{De\ Bilt, t} = a + b * t \quad (10a)$$

where indicator  $I_t$  is linearly coupled to  $T_{De\ Bilt, t}$ , or:

$$I_t = c + d * T_{De\ Bilt, t} \quad (10b)$$

Substitution of (10a) into (10b) yields a linear increasing indicator  $I_t$ :

$$I_t = c + a * d + b * d * t = \alpha + \beta * t \quad (10c)$$

with  $\alpha$  and  $\beta$  constants.

If we want to approximate predictions for  $I_t$  over the period 2004 – 2020, we can simply estimate the linear regression model:

$$I_t = \alpha + \beta * T_{De\ Bilt, t} + \varepsilon_t \quad (11)$$

with  $t$  any time in the historic period. Now, we can compute any future  $I_t$  value using (11). Predictions for  $T_{De\ Bilt, t}$ , with  $t > 2003$ , could be *data-based* or *model-based*. The standard errors for the fitted regression line can be used to incorporate the uncertainty in the estimates for  $\alpha$  and  $\beta$ . Upper and lower estimates for  $T_{De\ Bilt, t}$  could also be substituted in (11).

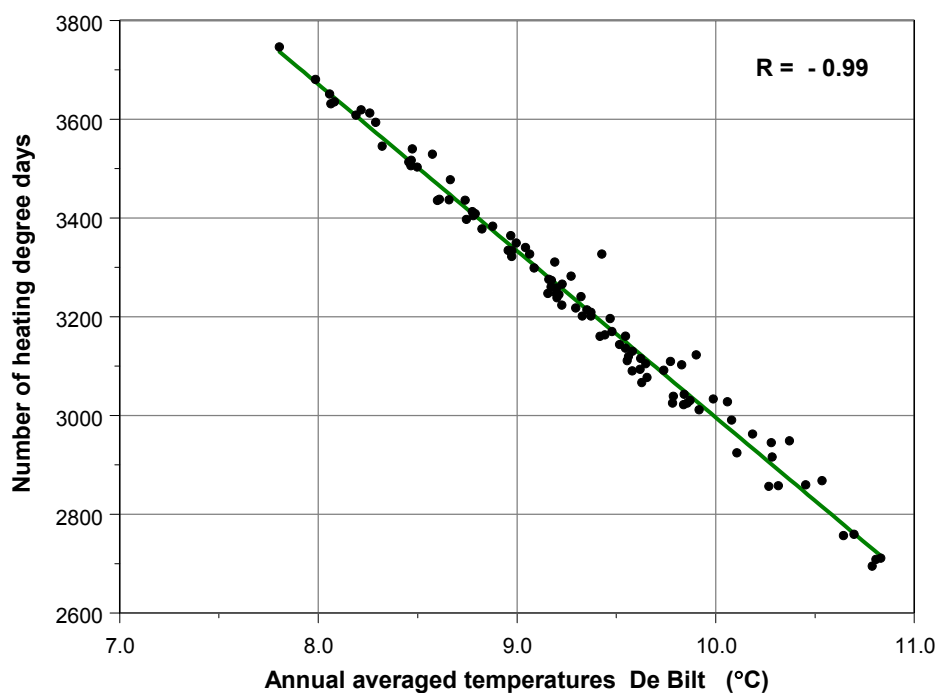
### 7.3.1 Heating-degree days

Heating-degree days and annual temperatures appear to be highly correlated, as shown in **Figure 7.5**. The correlation between the two series is -0.99. This is an important result which allows us to predict heating-degree days without actually having daily data for future years!

Based on the reasoning in (10), heating-degree days may be extrapolated up to the year 2020. These extrapolations are shown in **Figure 7.6**.

Trend statistics are:

- $\mu_{1906} = 3333$  [3193, 3470] heating-degree days
- $\mu_{2003} = 2887$  [2762, 3011] heating-degree days
- $\mu_{2010} = 2792$  [2604, 2979] heating-degree days
- $\mu_{2020} = 2656$  [2352, 2960] heating-degree days
- $\mu_{2020} - \mu_{1906} = -677$  [-1004, -349] heating-degree days



Coefficients regression line:

	Value	Std. Error	t value	Pr(> t )
(Intercept)	6368.8193	41.5535	153.2679	0.0000
Annual temp.	-337.2489	4.4433	-75.9001	0.0000

Figure 7.5 Scatterplot between annual mean temperatures and heating-degree days.

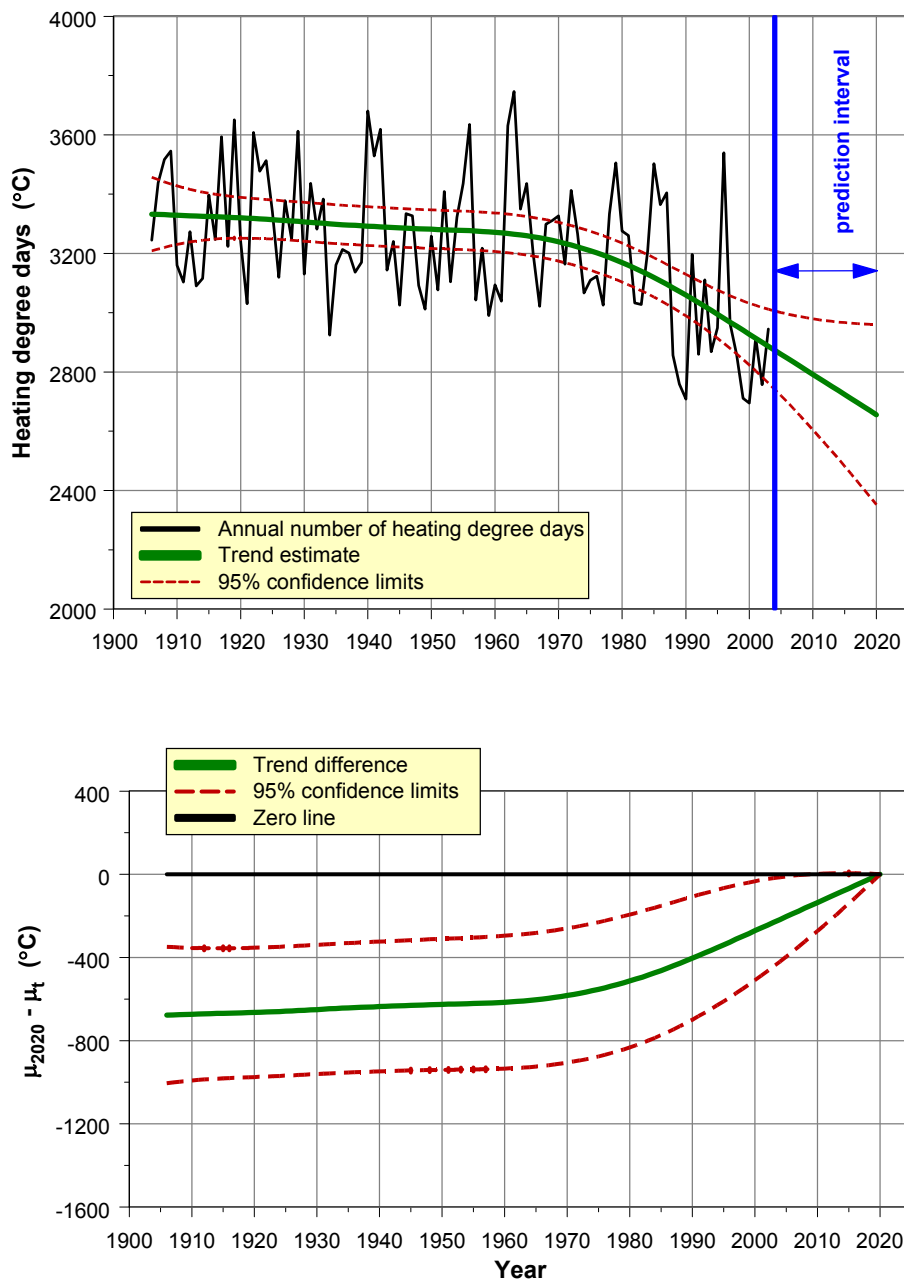


Figure 7.6 Heating-degree days for the 1906-2020 period. The mathematical model is identical to that shown in Figure 6.5.

Alternatively, we can calculate **model-based predictions** for heating-degree days by using the regression equation:

$$I_t = 6369 - 337 * T_{DeBilt-GCM,t} + \varepsilon_t \quad (12)$$

with  $T_{DeBilt-GCM,t}$  given by equation (8):

$$- T_{DeBilt-GCM,2010} = 10.6 [ < 10.3, 11.2 ] \text{ } ^\circ\text{C} \quad (13a)$$

$$- T_{DeBilt-GCM,2020} = 10.8 [ < 10.0, 12.4 ] \text{ } ^\circ\text{C} \quad (13b)$$

By substitution of these values in (12) and calculating the standard errors for regression model (12) (calculation details not shown) the following model-based estimates for  $I_t$  are gained:

$$- I_{DeBilt-GCM,2010} = 2797 [ 2573, 2906 ] \text{ } ^\circ\text{C} \quad (14a)$$

$$- I_{DeBilt-GCM,2020} = 2727 [ 2157, 3005 ] \text{ } ^\circ\text{C} \quad (14b)$$

Both model-based and data-based predictions are summarized in **Figure 7.7**.

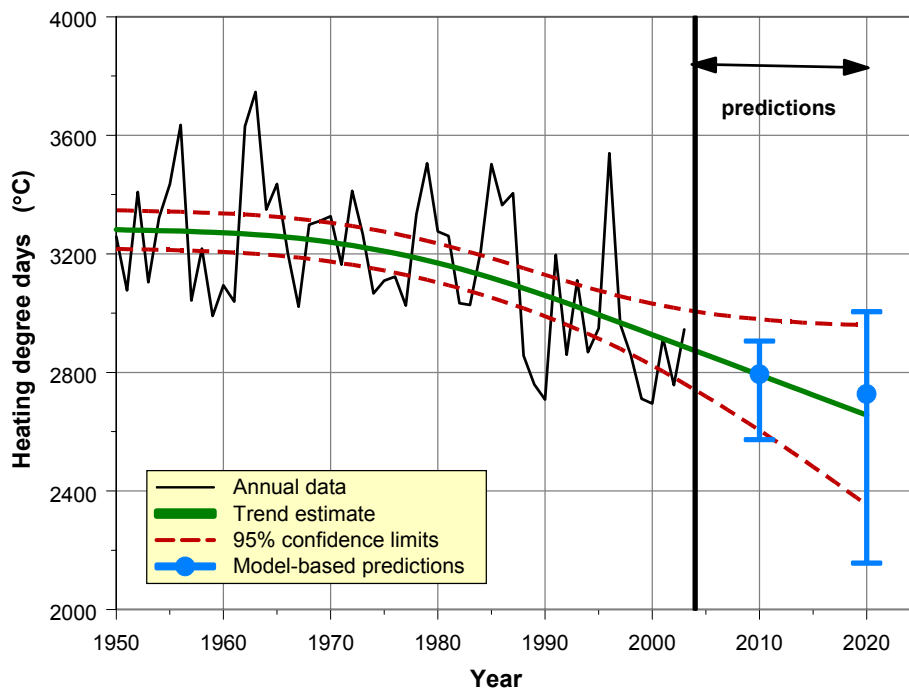


*Figure 7.7 Heating-degree days for the 1950-2020 period. Both predictions by statistical extrapolation and GCM-based calculations are shown.*

The conclusion from Figure 7.7 is that the best guess values are very similar. Even the uncertainty bands are reasonable consistent.

Predictions up to the year 2040 are derived in **Appendix D**.



*Heating of house holds and buildings is related to the heating-degree day indicator.  
Due to a warmer climate emissions of CO<sub>2</sub> and other greenhouse gases  
will level off significantly.*

*Photo: H. Visser.*

### 7.3.2 Premature deaths

A high correlation between the premature-deaths series (section 6.1) and *annual temperatures* is not to be expected. Therefore, we correlated this series with summer temperatures. GCM predictions such as those from the Dutch Challenge Project, suggest linear increasing seasonal temperatures.

The scatterplot given in **Figure 7.8** shows that the correlation is much lower than that shown in Figure 7.2. The scatterplot also suggests a more quadratic relation between the two variables at higher values. Therefore, we cannot be sure that the premature-deaths series can be extrapolated up to the year 2020, as we did for heating-degree days in the preceding section.

A better verification might be gained by using *daily data* from GCM output and the formula for the premature-deaths indicator. We will discuss this approach in section 8.

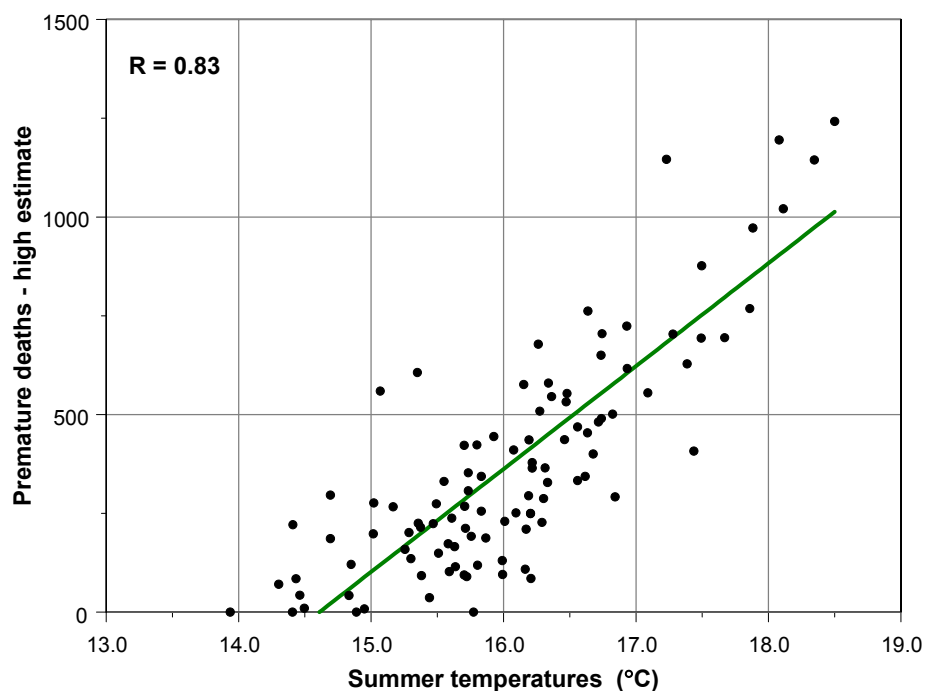


Figure 7.8 Scatterplot between summer temperatures for De Bilt and the indicator for premature deaths due to heat waves.

## 8. Summary and conclusions

This report has endeavoured to provide an answer to the question on how trends in weather conditions and weather-related impacts have evolved over the past century. Our main focus has been the estimation of uncertainty around the trends and trend differences.

First of all, application of structural time-series models has proven to be a very valuable tool (Tang, 2003; Visser, 2004a). Second, a two-step approach for predicting variables over the 2004-2020 period was followed. One method is 'data based' and uses a statistical extrapolation of the historical trends identified. The second approach is 'model based' and makes use of GCM projections for annual global temperatures, which are then downscaled to conditions in the Netherlands. Both natural warming and the human-induced warming have been projected for the second approach, along with their respective uncertainties.

These two items summarize how this report may be compared to the wealth of reports and articles on: (i) global climate change (IPCC, 2001 as a main reference), (ii) climate change on a European scale (Klein Tank, 2002; EEA, 2004 as main references) and (iii) climate change in the Netherlands (KNMI, 2003; Van Oldenborgh and Van Ulden, 2003, as main references). Most of the studies documented in the literature lack a rigorous time-series approach in their analyses of historical data. As for future predictions, the literature relies solely on the second approach (and in some cases without the inclusion of natural variability with corresponding uncertainty).

The conclusions of this study have been clustered under the following topics:

- homogeneity of data
- time-series approach
- annual temperatures and temperature extremes, 1901 - 2003
- annual precipitation sums and extremes, 1906 - 2003
- temperature-related impacts, 1901 - 2004
- predictions 2004 - 2020
- future work

Please note that all figures used forthwith apply to the estimated *trends* in the data. All uncertainties given denote *95% confidence limits*.

### ***Homogeneity of data***

For drawing inferences on the increase or decrease of trends, we have to be certain that weather series are **homogeneous**. This was achieved in this study using the following sources:

- the monthly *temperature* series for De Bilt, as published by Brandsma (KNMI): found to be of high quality. The same holds for daily temperature data, although one should be careful when analysing extremely hot days, which may be biased for data before 1950. Registrations are probably slightly too *high*.
- the daily *precipitation* series for 13 stations in the Netherlands: homogenized within the context of the ECA project and of high quality.
- measurements of *wind direction* and *wind speed*: appeared to be non-homogeneous over the 1901-2003 period. These data were not analysed.

### ***Time-series approach***

The time-series approach, as given in Visser (2004a), has been followed throughout this report. This approach was chosen not because trend estimates by structural time-series models are necessarily better than other trend models – such as moving averages (frequently applied in IPCC, 2001, or KNMI, 2003) – but because models from this class of time-series models yield the *uncertainty information* we need.

Another advantage is demonstrated in the estimation of the annual cycle in monthly temperatures and precipitation sums. Using the maximum likelihood criterion, the model ‘tells’ us whether this cycle is constant over time, or rather, if it evolves over time.

In all cases, the Integrated Random Walk (IRW) trend model was used. For some models the original data had to be transformed by a logarithmic transformation. The residuals appeared to be normally and independently distributed for all models considered.

In none of the cases were there signs of strong serially correlated residuals (‘unit root errors’, see Visser 2004a, Appendix B). Furthermore, no indications could be for using extreme value distributions, such as the Gumbel distribution, for modelling the noise processes. Such distributions can be expected when analysing extreme weather conditions.

The analysis of climate data revealed the need for an important extension for the TrendSpotter software: the incorporation of individual weights for measurements. If we know that data in early periods are less certain than more recent data, we could quantify this aspect. An example is the global temperature series shown in Figure 3.2 where it is known how reliability changes over time. This extension will be programmed early 2005.

***Annual temperatures and temperature extremes, 1901 - 2003***

- Annually averaged temperatures show an increasing pattern over the 1901-2003 period. There is an acceleration of warming since 1970. The increase since 1901 is statistically significant and accounts for 1.5 [0.9 - 2.1] K.
- Warming appears to be homogeneous over the months (and seasons) of the year, a result that seems contradictory to earlier findings that spring temperatures have risen 1.8 K over the same period; summer temperatures rose 1.4 K, and autumn/winter temperatures rose only 1.2 K. The explanation is that uncertainties in these seasonal increments are very large. For example, warming in winter since 1901 has been  $1.2 \pm 1.3$  K, with spring yielding a warming of  $1.8 \pm 0.9$  K. Given such wide margins the best model that can be presented is that of *constant warming* throughout the year.
- As for temperature extremes, the series with the hottest moment in each year was found to show a significant increasing tendency after 1906 at 2.6 [0.4 - 4.6] K. This warming seems higher than the warming in annual averaged temperatures (1.5 K). However, uncertainty bands are too wide for drawing inferences in this sense.
- The coldest moment in each year shows a small and *non-significant* increase of 0.9 K over the 1906-2003 period.
- The pattern of the number of summer days per year is analogous to that of annual temperatures: i.e. accelerated increase after 1970. The number has roughly doubled, from 14 days in 1906 to 27 days in 2003.
- The last three conclusions show trends in warm extremes to follow the trend in annual averages more closely than trends in cold extremes. This conclusion is consistent with that drawn by Klein Tank and Können (2003) for a range of temperature records within Europe, although on a shorter time scale (1946-1999).

***Annual precipitation sums and extremes, 1906 - 2003***

- Annual precipitation sums for De Bilt show an increase throughout the 20th century. The increase since 1906 is statistically significant and accounts for 118 [20, 216] mm. There is a small acceleration seen after 1970. The annual increase in precipitation amounts appears to be homogeneous throughout the year (in the same way as temperature).
- The length of longest dry period per year appears constant after 1906. Thus, there is no conclusive proof in the data that the extreme long drought in the summer of 2003 is an indication of a systematic change towards longer drought periods in the near future.
- As for precipitation extremes, the maximum daily amount of precipitation per year was found to be more or less constant over the 1906-2003 period.
- However, the annual number of extremely wet days shows a steady and significant increase 7.1 [2.8 - 11.4] days in the course of the century: from 19 days in 1906 to 26 days in 2003.
- Klein Tank and Können (2003) conclude that wet extremes (annual number of moderate and very wet days) increase throughout Europe (period 1946-1999), although the spatial coherence between trends is low. Their conclusion is consistent with our conclusion on trends in the number of extreme wet days.

***Temperature-related impacts, 1901 - 2004***

The four temperature-related impacts analysed yield the following conclusions:

- The annual number of heat-related premature deaths were modelled using a formula published by Statistics Netherlands and based on the deaths registered in the summer of 2003. This formula can be applied to the weather conditions over 1901-2003, to get an impression how weather conditions and probable changes in weather conditions in the near future might alter the number of premature deaths. The historical reconstruction shows a significant increase from [75, 475] deaths due to heat waves in 1906 to [217, 1270] deaths in 2003.
- The length of the (meteorological) growing season is an important plant-related impact indicator. The ECA definition for this indicator was found not to suffice for the Netherlands: the initiation of the growing season in spring is relevant but the termination of it is not. For some years the growing season did not end before 31 December of the current year, explaining the lengths of growing seasons of more than 310 days (RIVM, 2004b, p. 140) or over 360 days per year (KNMI 2003, p. 9). An alternative approach is given in section 4.1.2, where it was found that the length of the growing season since 1901 has been prolonged; it now starts 16 days earlier and ends 14 days later. It is also shown that, if annual temperatures were to increase another 2.0 degrees since 2003, the growing season would last all year round.
- Heating-degree days have an economic component. This indicator functions as a measure for heating of houses and buildings. The indicator is also important for the weather correction of CO<sub>2</sub> emissions. The indicator was found to evolve as a mirror image of annual temperatures: i.e. it significantly decreases over the whole period from 1906 to 2003, with a rapid acceleration from 1970 onwards. The indicator decreases from 3333 in 1906 to 2887 in 2003, representing a decrease of -446 [ -630, -262] heating degree days since 1906. The decrease has implications for the prediction of CO<sub>2</sub> emissions in the year 2010 and likewise for meeting the Dutch Kyoto target. The net climate effect is expected to be a lowering of future Dutch greenhouse-gas emissions by 3.5 Mton CO<sub>2</sub> equivalents. One can expect outdoor skating in the Netherlands to disappear when monthly and annual temperatures increase. As a case study, a temperature indicator was derived to represent a measure for maximum ice thickness in the province of Friesland (with the coldest period of 15 consecutive days within a particular winter). A threshold of -4.2 °C was found to be decisive for organizing the famous ‘Elfstedentocht’ (11-city marathon). The indicator was found to significant increasing over the period 1912 - 1987. In other words, the indicator trend value in 2004 was seen to be significantly higher than trend values in the 1912-1987 period. However, the difference relative to 1906-1911 is not significant. This result is consistent with the finding that the rise in warm extremes tends to exceed that of cold extremes. Using trend estimates and their respective probability distributions allows us to calculate the actual chance of an ‘Elfstedentocht’. This was found to be 0.21 in 1901 (return period of once every four years), increasing to 0.26 around 1950 (idem) and decreasing to a chance of 0.10 in 2004 (return period of once every ten years).

### ***Predictions 2004 - 2020***

One of the main findings here was that annually averaged temperatures can be predicted up to 2020 following *two* different approaches: data-based and model-based, both yielding consistent trend estimates and uncertainty bands.

Predictions for global and local temperature are as follows (synthesis of GCM and statistical predictions):

- global temperatures rose from  $-0.39$  [ $-0.47$ ,  $-0.31$ ] °C in 1901 to  $0.47$  [ $0.39$ ,  $0.55$ ] °C in 2003. Predictions for 2010 account for  $0.55$  [ $0.36$ ,  $0.74$ ] °C and  $0.80$  [ $0.38$ ,  $1.22$ ] °C in 2020.
- local temperatures in the Netherlands rose from  $8.8$  [ $8.4$ ,  $9.2$ ] °C in 1901 to  $10.4$  [ $10.0$ ,  $10.8$ ] °C in 2003. Predictions for 2010 account for  $10.6$  [ $10.0$ ,  $11.2$ ] °C and  $10.8$  [ $9.8$ ,  $11.8$ ] °C in 2020.

Thus far, it is not clear if the annual cycle in local temperatures will stay constant in the future, as it did over the historic period (cf. Table 4.1). However, for short-term predictions up to the year 2020, it is not unreasonable, to expect this cycle to stay constant.



*The projection of future warming, both by natural and anthropogenic causes can be predicted by following two different paths: data-based and model-based. Both approaches lead to consistent estimates up to the year 2020, a conclusion valid for both for global annual temperatures and annual temperatures in the Netherlands.*

*Photo: H. Visser*

Furthermore, weather indicators have been shown to lend themselves to extrapolation in the same way as for annual temperatures, as long as they are linearly connected to annual temperatures. This applies to **heating-degree days**, which decreased from 3333 [3193, 3470] in 1906 to 2887 [2747, 3027] in 2003. Predictions for 2010 are 2792 [2604, 2979] and 2656 [2352, 2960] in 2020.

The latter result has implications for the Dutch emission estimates of CO<sub>2</sub>-equivalents in the Kyoto period, 2008-2012. Tentative calculations, based on predictions shown in Figures D.1 and D.4 from this report, show that climate-change corrected emission estimates, based on heating-degree days for 2004-2010, will be 3-4 Mton lower than estimates without such a correction (Van Dril and Elzenga, 2005). The increasing use of air conditionings for cooling, which is related to the **cooling-degree day indicator**, and lower investments for isolation of buildings has been taken into account here. It is noted that the Kyoto commitments for the Netherlands account for 199 Mton CO<sub>2</sub> equivalents by the period 2008-2012.

### ***Future work***

For impact variables such as premature deaths during warm periods, we can only rely on statistical extrapolation. It would be an important extension of the work presented here to simulate the behaviour of these indicators using *daily* predictions from GCMs. An example is the database from the Dutch Challenge Project. Using the data set from the project we could devise a model-based approach for the near future which will, hopefully, be consistent with statistical extrapolation. A recent example of such an approach for European data was given by Klein Tank, Können and Selten (2004).

Within the Dutch Challenge Project 62 similar likely simulations were generated over the 1940-2080 period. Future warming and natural variability were simulated by the National Center for Atmospheric Research Community Climate System Model (NCAR-CCSM, version 1.4) in the Challenge ensemble experiment. The model is a fully-coupled global climate model. By taking the grid box which is most representative for the Netherlands we can calculate the indicators of interest for each of the 62 simulations based on daily data. Beforehand one should check if GCM 'predictions' over the historical period of 1940-2003 match the actual measurements over the same period.



## References

- Allen, K., Francey, R., Michael, K., Nunez, M., 1999. A structural time series approach to the reconstruction of Tasmanian maximum temperatures. *Environmental Modelling & Software* 14, 261-274.
- Both, C., Visser, M.E., 2001. Adjustment to climate change is constrained by arrival date in a long-distance migrant bird. *Nature* 441, 296-298.
- Brandsma T., 2001. Hoeveel Elfstedentochten in de 21e eeuw?, *ZENIT*, 28, 194-197.
- Brandsma T., Koek F., Wallbrink H., Können G., 2000. Het KNMI programma HISKLIM (historisch klimaat), KNMI-publicatie 191.
- Brandsma T., Können G. P., Wessels H. R. A., 2002. Empirical estimation of the effect of urban heat advection on temperature series of De Bilt, KNMI-rapport 2002-19.
- Bruin A.T.H., 2002. Verandering in neerslagkarakteristieken in Nederland gedurende de periode 1901-2001. *Klimatologische Dienst KNMI*.
- Buishand T. A., Velds C.A., 1980. Neerslag en verdamping. *Klimaat van Nederland* 1, KNMI.
- Cleveland, R.W., Grosse, E., 1991. Computational methods for local regression. *Statistics and Computing* 1, 47-62.
- De Bruin, H.A.R., Wessels, H.R.A., 1988. A model for the formation and melting of ice on surface waters. *J. of Applied Meteorology* 27, 164-173.
- De Bruin, H.A.R., Wessels, H.R.A., 1990. IJs in de Lage Landen. *Zenit* 17, 437-444.
- De Jong, P., 1988. The likelihood for a state space model. *Biometrika* 75, 165-169.
- Dekkers A.L.M., 2001. S-PLUS voor het RIVM. Krachtig statistisch software-gereedschap. RIVM rapport 442516001.
- Durbin J., Koopman, S.J., 2001. *Time series analysis by state space methods*. Oxford Statistical Science Series, Oxford.

- Eickhout, B., den Elzen, M.G.J., Kreileman, G.J.J., 2004. The atmosphere-ocean system of IMAGE 2.2. RIVM report 48150801.
- EEA, 2004. Impacts of Europe's changing climate. An indicator-based assessment. EEA report no 2.
- Fitter, A.H., Fitter, R.S.R., 2002. Rapid changes in flowering time in British plants. *Science* 296, 1689-1691.
- Grossman, D., 2004a. Spring forward. *Scientific American*, January issue, 74-81.
- Grossman, D., 2004b. Vroege lente. *Scientific American/eos* maart, 36-44.
- Harvey, A.C., 1984. A unified view of statistical forecasting procedures. *Journal of Forecasting* 3, 245-275.
- Harvey, A.C., 1989. Forecasting, structural time series models and the Kalman filter. Cambridge University Press, UK.
- Harvey, A.C., 2001. Testing in unobserved component models. *J. of Forecasting* 20, 1-19.
- Heijboer D., Nellestijn J., 2002. *Klimaatatlas van Nederland*. Elmar B.V.
- Hess, A., Iyer, H., Malm, W., 2001. Linear trend analysis: a comparison of methods. *Atmospheric Environment* 35, 5211-5222.
- IPCC, 2001 (eds. J.T. Houghton, Y. Ding, D.J. Griggs, M. Noguer, P.J. van der Linden, X. Dai, K. Maskell, C.A. Johnson). *Climate Change 2001, The Scientific Basis. Contribution of Working Group I to the third Assessment Report of the IPCC*. Cambridge University Press.
- Kitagawa, 1981. A non stationary time series model and its fitting by a recursive filter. *Journal of Time Series Analysis* 2(2), 103-116.
- Kalman, R.E., 1960. A new approach to linear filtering and prediction problems. *Trans. ASME D*, 82, 95-108.
- Katz R.W. and Brown B.G., 1992. Extreme events in a changing climate: variability is more important than averages. *Clim. Change*, 21.

- Klein Tank, A.M.G., 2004. Changing temperature and precipitation extremes in Europe's climate of the 20th century. Ph.D. thesis, University of Utrecht.
- Klein Tank, A.M.G., Wijngaard, J., van Engelen, A., 2002a. Climate of Europe. Assessment of observed daily temperature and precipitation extremes. ECA report (see [www.knmi.nl/samenw/ECA](http://www.knmi.nl/samenw/ECA)).
- Klein Tank, A.M.G. *et al.*, 2002b. Daily series of temperature and precipitation observations. *Int. J. Climatol.* 22, 1441-1453.
- Klein Tank, A.M.G., Können, G.P., 2003. Trends in daily temperature and precipitation extremes. *J. Climate* 16, 3665-3680.
- Klein Tank, A.M.G., Können, G.P., Selten, F.M., 2004. Signals of anthropogenic influence on European warming. *Int. J. Climatology* (in press).
- Klok E.J., 1998. Indices die de variabiliteit en de extremen van het klimaat beschrijven. KNMI-rapport, TR-211.
- KNMI, 2003 (Verbeek K., red.). De toestand van het klimaat in Nederland 2003. KNMI-rapport.
- Lenten, L.J.A., Moosa, I.A., 2003. An empirical investigation into long-term climate change in Australia. *Environmental Modelling & Software* 18, 59-70.
- Millard S.P., Neerchal N.K., 2001. *Environmental Statistics with S-Plus*. CRC Press.
- Moraal, L.G., Jagers op Akkerhuis, G.A.J.M., Siepel, H., Schelhaas, M.J., Martakis, G.F.P., 2004. Verschuivingen van insectenplagen bij bomen sinds 1946 in relatie met klimaatverandering. *Alterra-rapport 856*.
- National Geographic, 2004a. Special issue on climate change impacts. July issue.
- National Geographic, 2004b. Special over gevolgen klimaatverandering. Juli nummer Nederlands-Belgische uitgave.
- Petersen, A.C., Janssen, P.H.M., Van der Sluijs, J.P., Risbey, J.S., Ravetz, J.R., 2003. RIVM/MNP guidance for uncertainty assessment and communication. RIVM brochure.
- RIVM, 2003. Milieubalans 2003. RIVM-rapport, Kluwer, 2003.

- RIVM, 2004a. Milieubalans 2004. RIVM-CBS-rapport.
- RIVM, 2004b. Milieucompendium 2004. Milieu in cijfers. RIVM-rapport, Kluwer.
- Shackley, S., Young, P., Parkinson, S., Wynne, B., 1998. Uncertainty, complexity and concepts of good science in climate change modelling: are GCMs the best tools? *Climatic Change* 38, 159-205.
- Smits, A., Klein Tank, A.M.G., Können, G.P., 2004. Trends in storminess over the Netherlands, 1962-2002. *Int. J. Climatology* (submitted).
- Stern, D.I. and Kaufmann, R.K., 2000. Detecting a global warming signal in hemispheric temperature series: a structural time series analysis. *Climatic Change* 47, 411-438.
- Tang, J., 2003. Veranderingen in klimaatextremen en weergeerelateerde indicatoren in Nederland. Trends en onzekerheden in historische klimaatdata (1901-2003). RIVM/KNMI/TU Delft rapport.
- Van Boxel J., Cammeraat E., 1999. Wordt Nederland steeds natter? Een analyse van de neerslag in deze eeuw. *Meteorologica* 1-99.
- Van den Brakel, J., Visser, H., 1996. The influence of environmental conditions on tree-ring series of Norway Spruce for different canopy and vitality classes. *Forest Science* 42(2), 206-219.
- Van der Wal, J.T., Janssen, L.H.J.M., 2000. Analysis of spatial and temporal variations of PM<sub>10</sub> concentrations in the Netherlands using Kalman filtering. *Atmospheric Environment* 34, 3675-3687.
- Van Dril, A.W.N., Elzenga, H., 2005. Referentieraming energie, klimaat en verzurende emissies 2004-2020. ECN-RIVM rapport, in druk.
- Van Oldenborgh, G.J., van Ulden, A., 2003. On the relationship between global warming, local warming in the Netherlands and changes in circulation in the 20th century. *Int. J. of Climatology* 23, 14, 1711-1724.
- Verkaik, J.W., 2001. Documentatie windmetingen in Nederland. KNMI-rapport.
- Visser, H., 1994. Regression models with time-varying parameters: applications in the environmental sciences. Ph.D. Thesis, University of Amsterdam.

- Visser, H., 2003. Detection of environmental changes. An application of structural time series models and the Kalman filter. RIVM report 550002002, Bilthoven, the Netherlands (in Dutch).
- Visser, H., 2003. Een beschrijving van de TrendSpotter-software: detectie van milieuveranderingen, RIVM Memo 550002002.
- Visser, H., 2004a. Estimation and detection of flexible trends. *Atm. Environment* 38, 4135-4145.
- Visser, H., 2004b. Description of the TrendSpotter software. RIVM Memo 007/2004 IMP.
- Visser, H., 2005. Neemt de kans op een elfstedentocht af? *STAtOR*, January issue, in press.
- Visser H., Molenaar, J., 1990. Estimating trends in tree-ring data. *Forest Science* 36(1), 87-100.
- Visser H., Molenaar, J., 1995. Trend estimation and regression analysis in climatological time series: an application of structural time series models and the Kalman filter. *J. of Climate* 8(5), 969-979.
- Visser, H., Folkert, R.J.M., Hoekstra, J., De Wolff, J.J., 2000. Identifying key sources of uncertainty in climate change projections. *Climatic Change* 45, 421-457.
- Wessels, H.R.A., 1999. Ijsbedekking in Friesland gedurende de 20e eeuw. *Zenit* 26, 60-63.
- Wieringa, J., Rijkoort, P.J., 1983. Windklimaat van Nederland. KNMI uitgave - Staatsuitgeverij, Den Haag.
- Young, P.C., Lane, K., Ng, C.N., Palmer, D., 1991. Recursive forecasting, smoothing and seasonal adjustment of nonstationary environmental data. *Journal of Forecasting* 10, 57-89.
- Zwart, B., 2000. Wat doet de natuur als het klimaat verandert. *Meteorologica*, March issue.



## Appendix A Comparison of historical station data

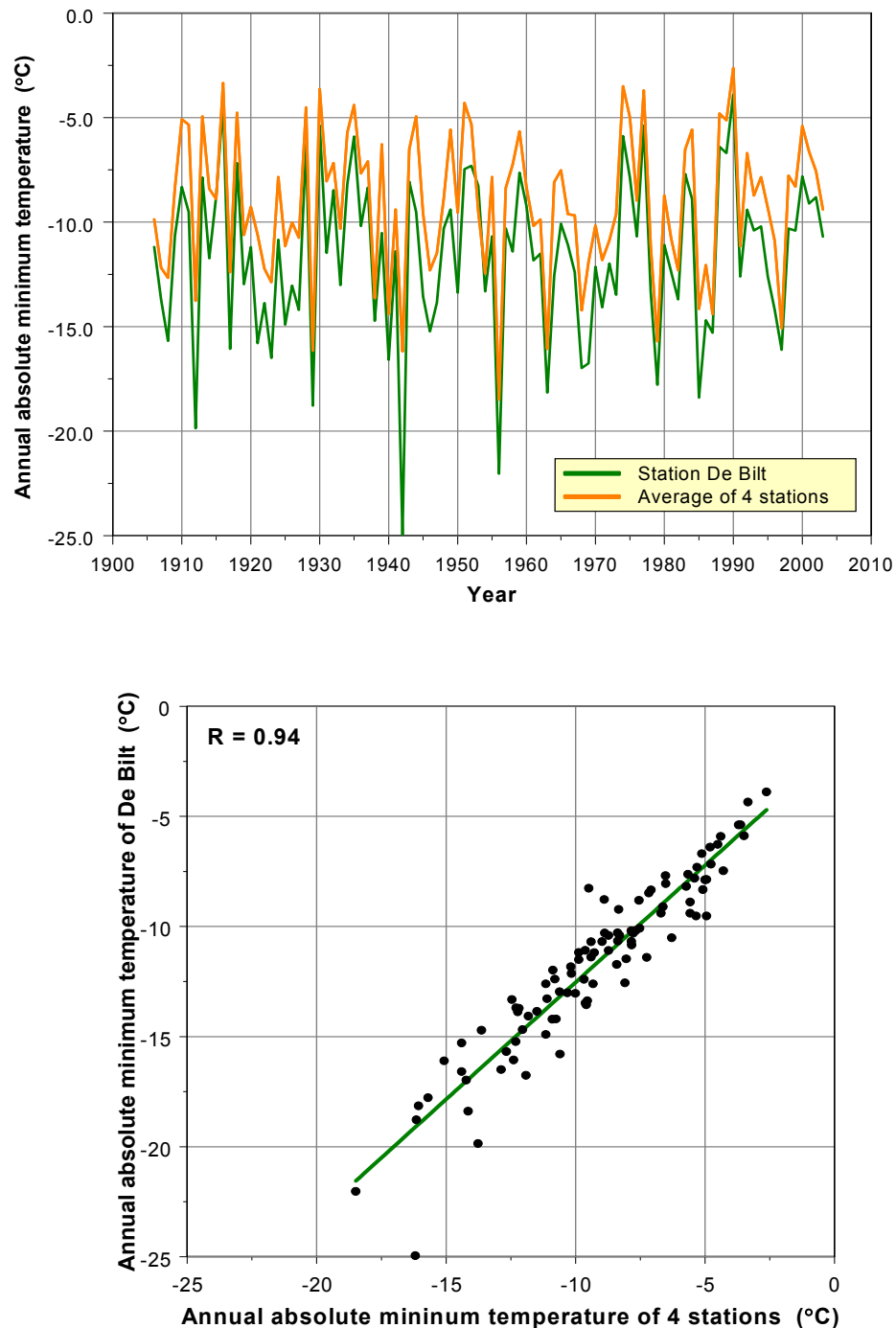


Figure A.1 Time series of annual absolute minimum temperatures for De Bilt (green line) and annual averages for four stations, Den Helder, Groningen, De Bilt and Vlissingen (orange line). The lower panel shows the scatter plot between the two series.

The correlation coefficient is 0.94. Period is 1901 – 2003.

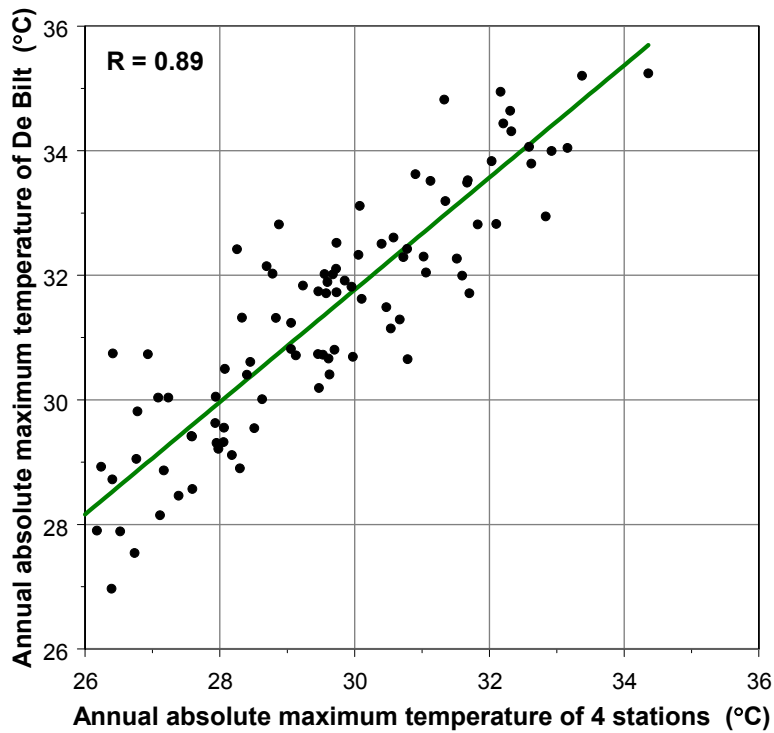
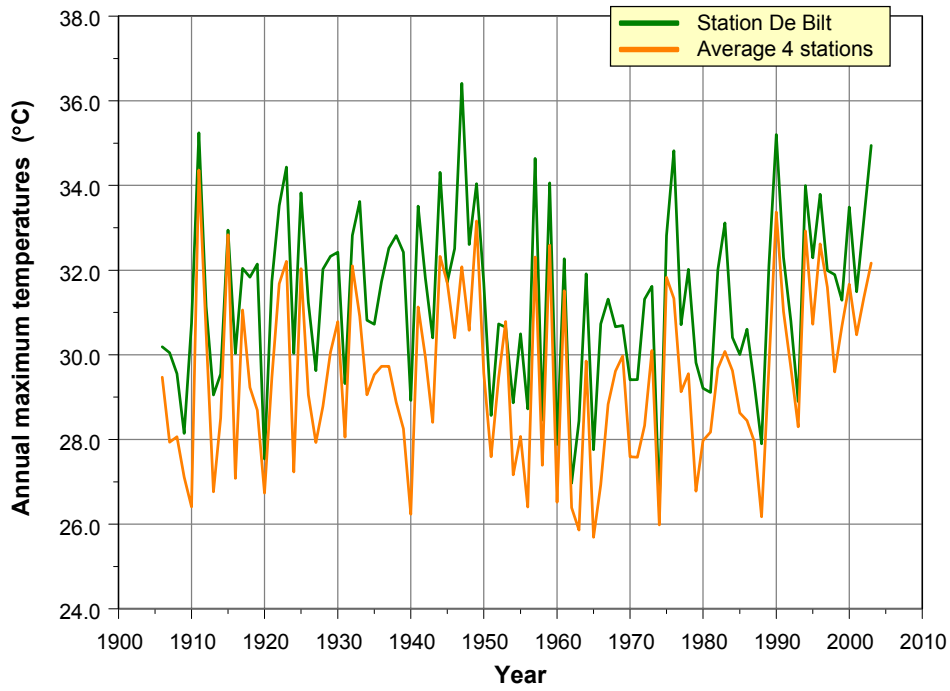


Figure A.2 Time series of annual absolute maximum temperatures for De Bilt (green line) and annual averages of four stations, Den Helder, Groningen, De Bilt and Vlissingen (orange line). The lower panel shows the scatter plot between the two series.

The correlation coefficient is 0.89. Period is 1901 – 2003.

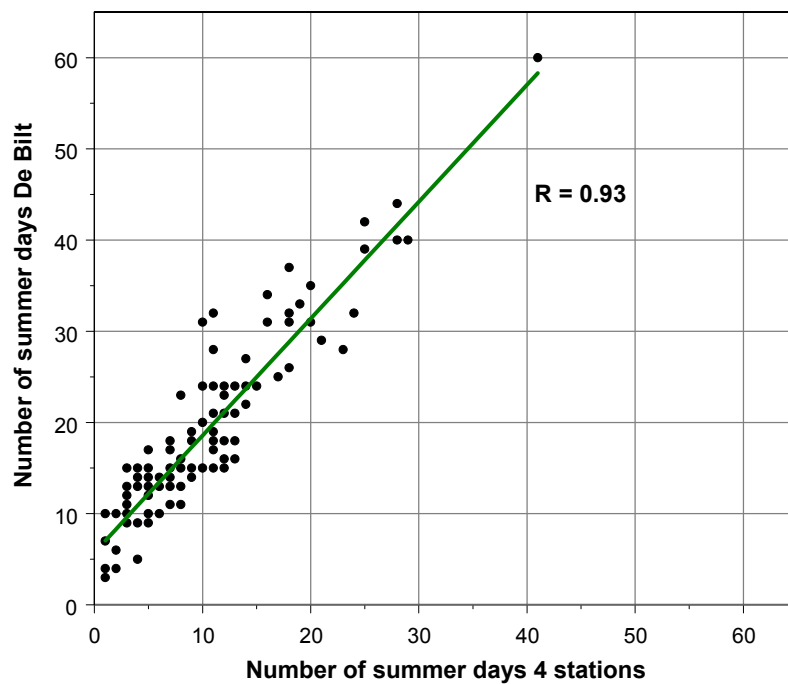
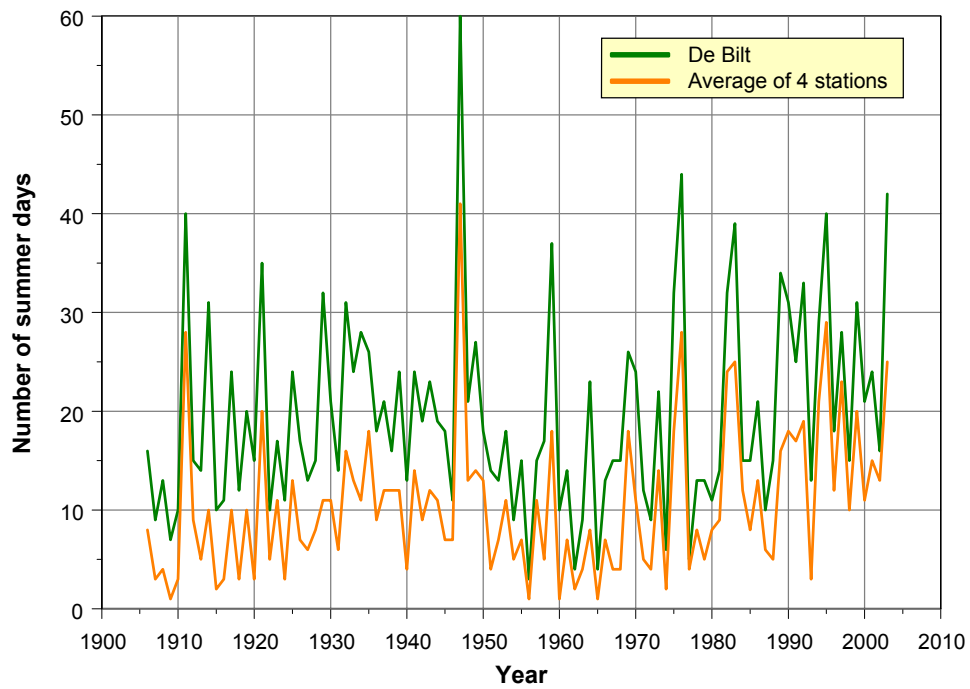


Figure A.3 Time series of annual number of summer days for De Bilt (green line) and idem for averages of four stations, Den Helder, Groningen, De Bilt and Vlissingen (orange line). The lower panel shows the scatterplot between the two series.

The correlation coefficient is 0.93. Period is 1906 – 2003.

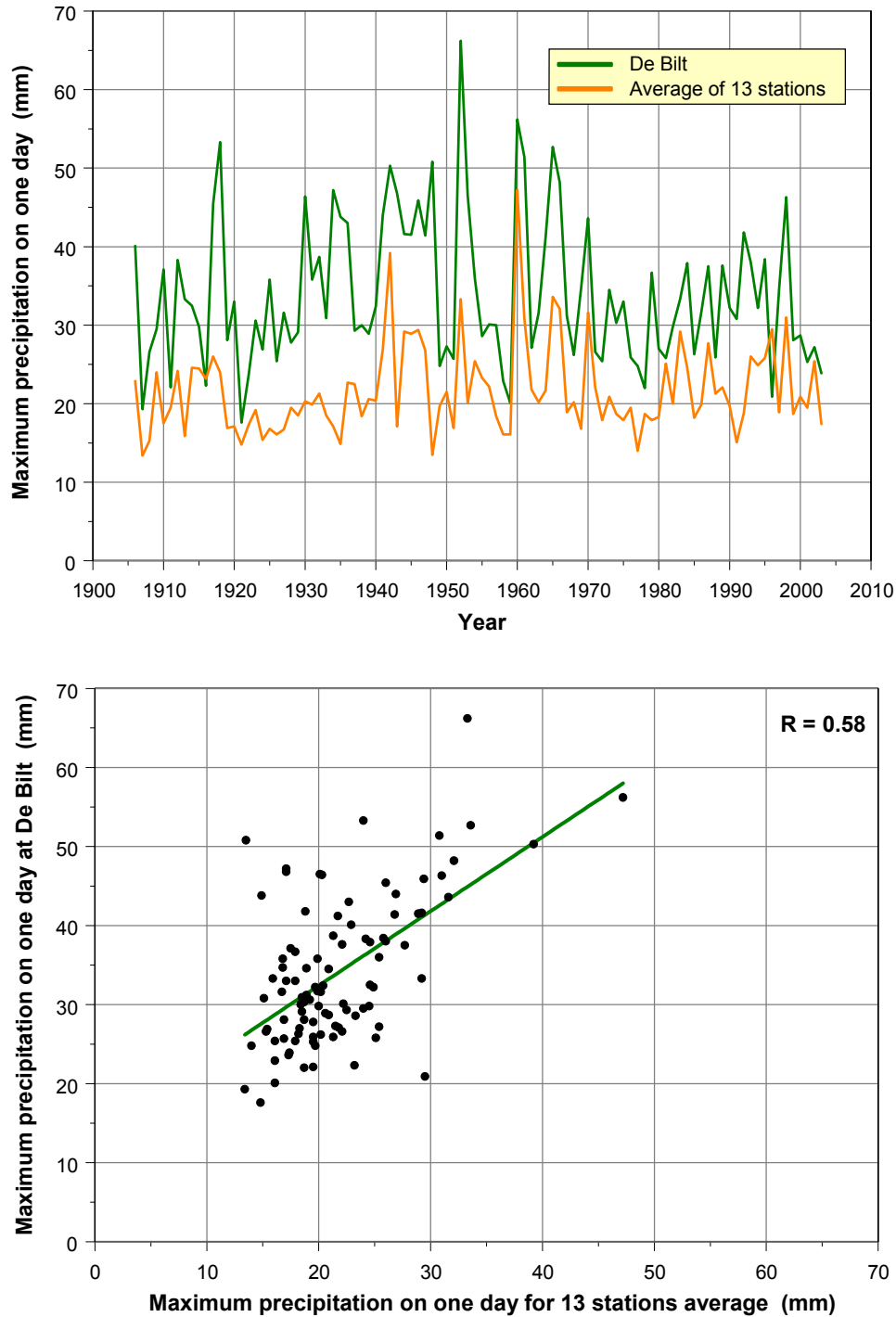


Figure A.4 Time series of the wettest day in a year for De Bilt (green line) and annual averages of 13 stations, with location given in Figure 2.6 (orange line). The lower panel shows the scatterplot between the two series. The correlation coefficient is 0.58. Period is 1906 – 2003.

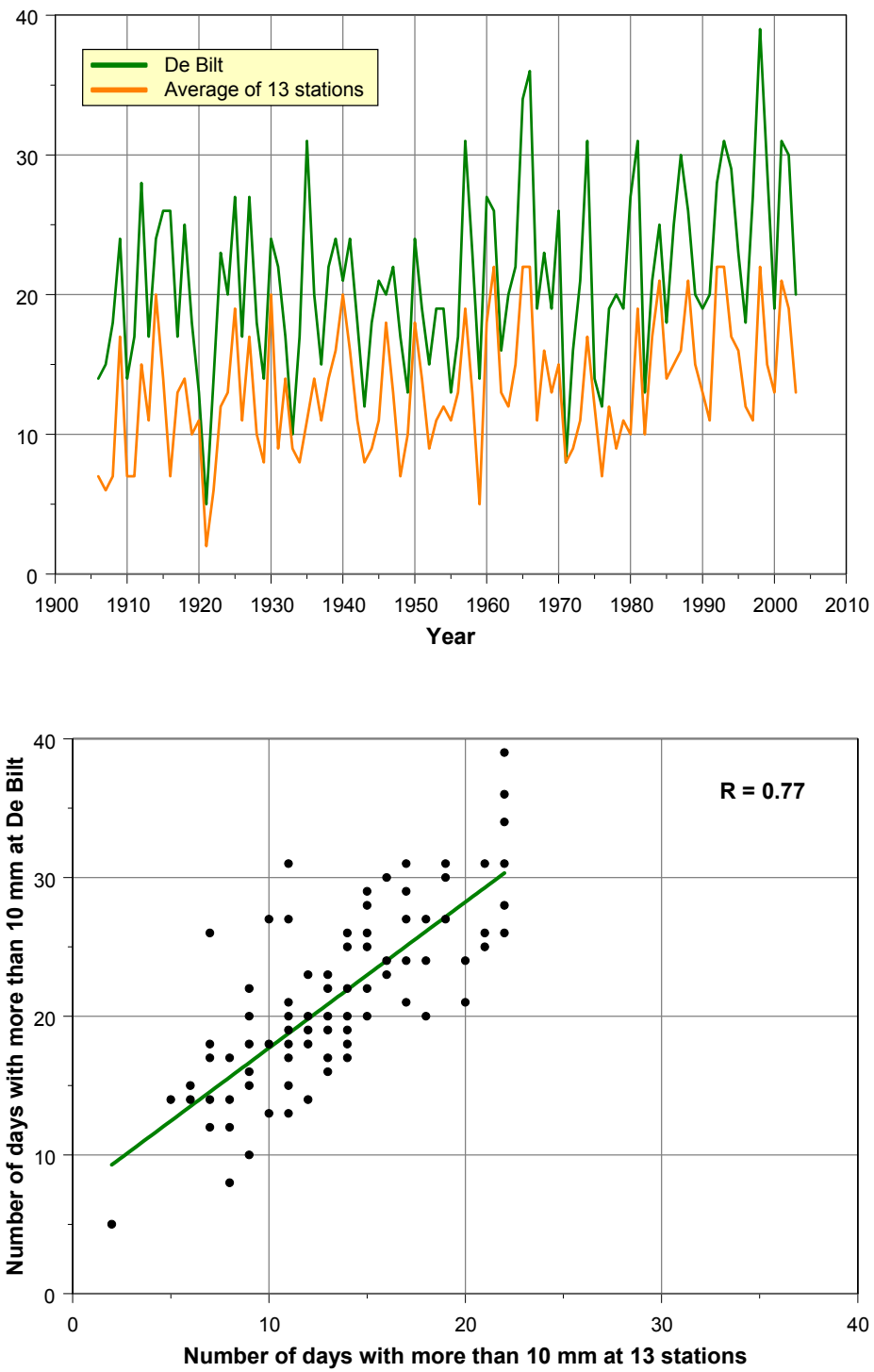


Figure A.5 Time series of annual number of extreme wet days for De Bilt (green line) and annual averages of 13 stations (location given in Figure 2.6). The lower panel shows the scatterplot for the two series.

The correlation coefficient is 0.77. Period is 1901 – 2003.

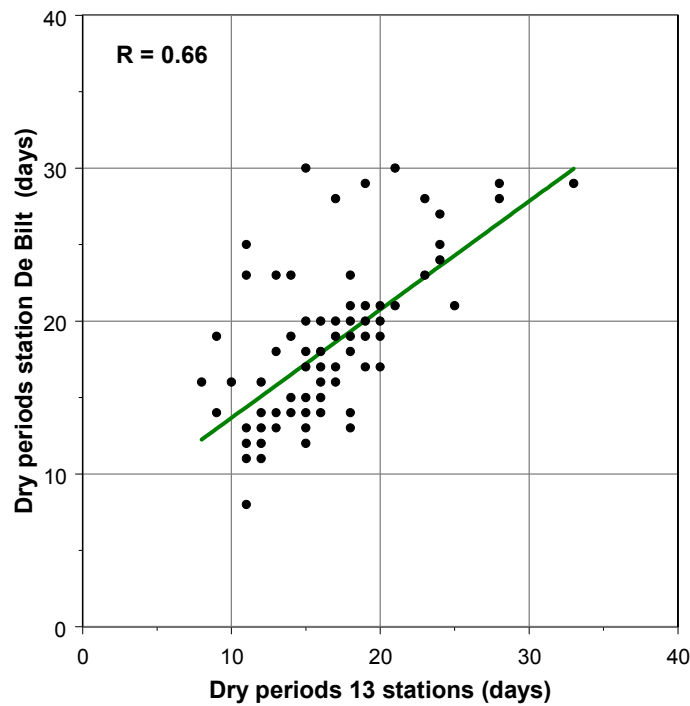
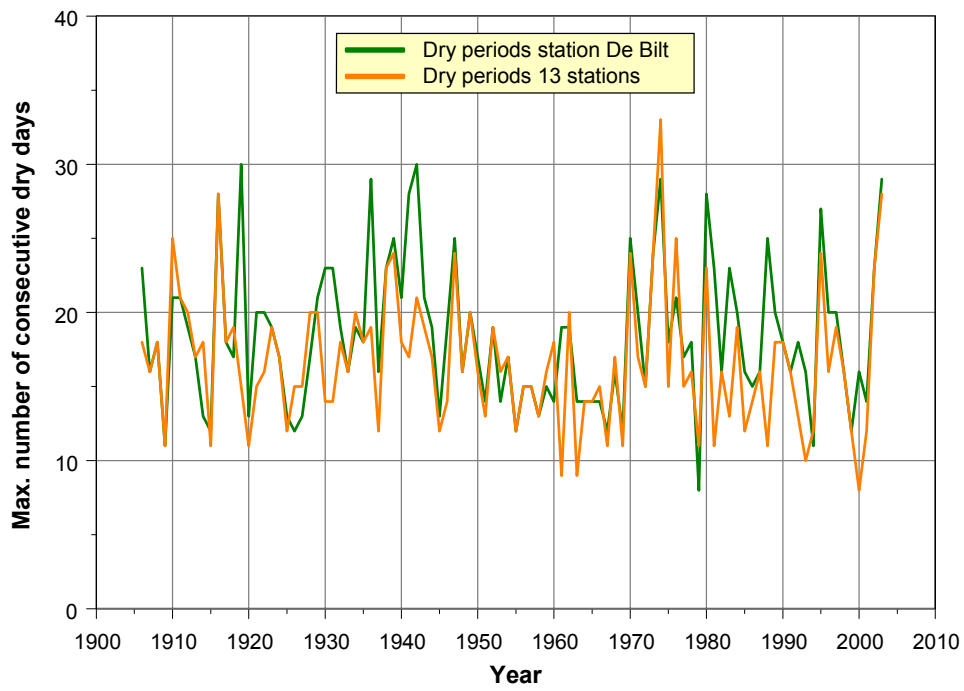


Figure A.6 Time series of annual longest dry period for De Bilt (green line) and annual averages of 13 stations (location given in Figure 2.6; orange line). The lower panel shows the scatterplot between both series. The correlation coefficient is 0.66. Period is 1906 – 2003.

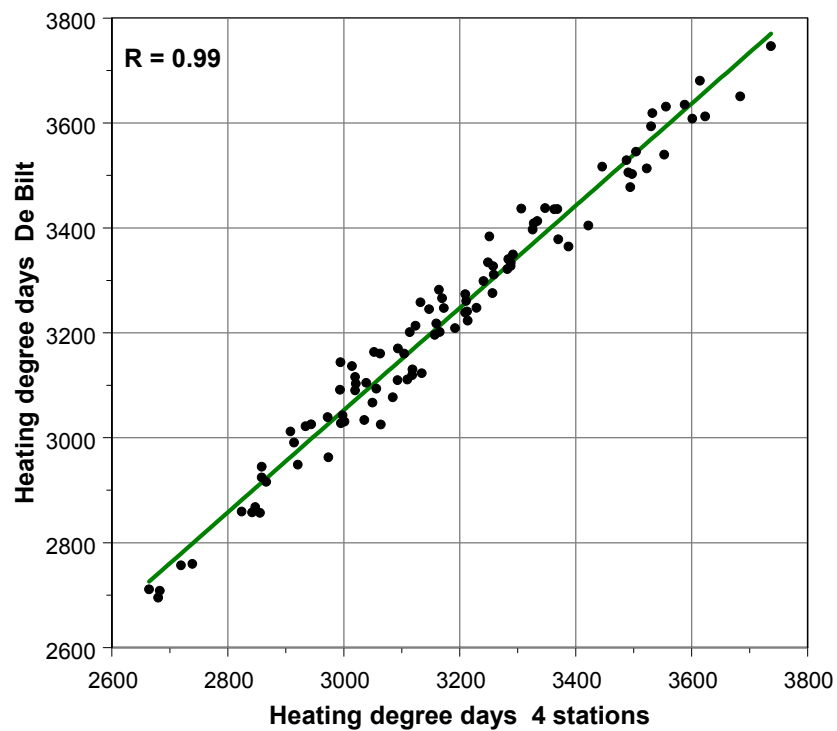
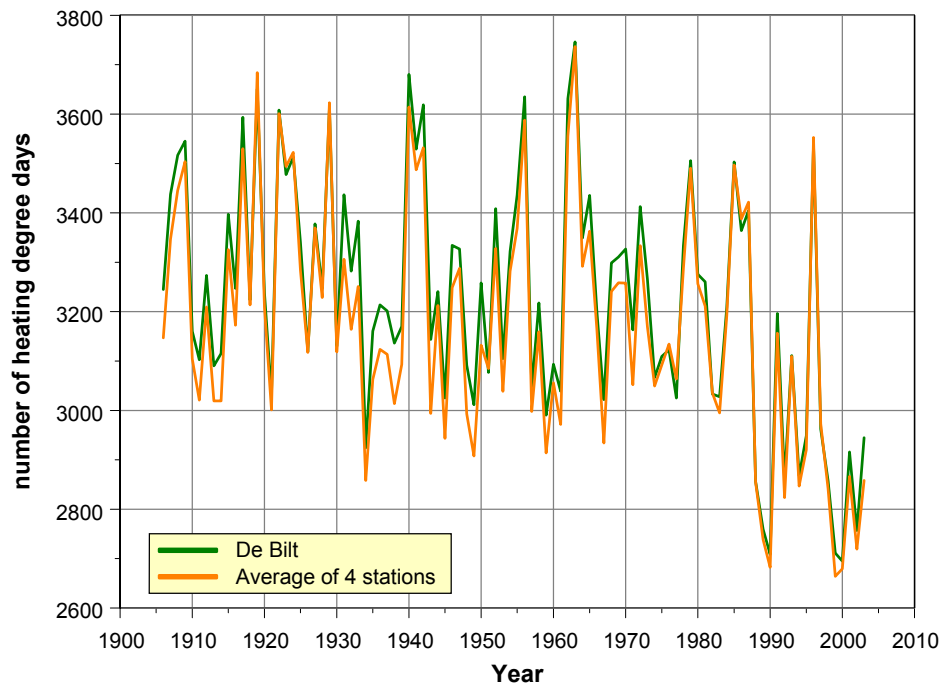


Figure A.7 Time series of the annual number of heating-degree days for De Bilt (green line) and annual averages for four stations, Den Helder, Groningen, De Bilt and Vlissingen (orange line). The lower panel shows the scatterplot between the two series.

The correlation coefficient is 0.99. Period is 1906 – 2003.



## Appendix B Wind

### B.1 Wind direction

Wind-direction data can be downloaded from the KNMI website [www.knmi.nl/product](http://www.knmi.nl/product) (click on [english] and choose data or meta data in the upper panel of the page). The data from April 1945 are missing. This series has **not** been corrected for known inhomogeneities due to changes in measurement height and environment. The original tower (37 m) on the KNMI building was demolished in 1916 and rebuilt half a metre higher in 1917 (see Figure 1.2). In 1961 the measurement site was moved to a 10 m tower in a meadow behind the institute, which was raised to 20 m in 1993 (Verkaik, 2001).

The importance of these inhomogeneities was tested by Oldenborgh (2003) in a comparison with geostrophic wind direction, computed from daily mean sea-level pressures at the stations of De Bilt, Groningen/Eelde and Den Helder/De Kooy. He concluded that though the wind direction series was *not proven to be homogeneous*, the series is very well-suited to analyses of climate related changes due to shifts in the frequencies of circulation types.

**Figure B.1** gives an impression of wind direction variations. The graph shows wind-direction histograms for the decades 1905-1914, 1915-1924, ..... and 1995-2003. The histograms suggest an increase in frequency of wind direction from ~15% to ~18% in the sector ‘south west’ (around 240 degrees).

For a better impression of the homogeneity of wind-direction records, scatterplots have been calculated for daily averaged wind direction for the five stations described in section 2.1 and shown in Figures 1.2 and 2.2: i.e. Den Helder / De Kooy, Groningen / Eelde, De Bilt, Vlissingen and Maastricht / Beek. To test the influence of changes in height of the measurements, changes in location and possibly changes in the environment (due to urbanization and growth of surrounding trees throughout the years), the periods 1908-2003 (**Figure B.2**) and 1968-2003 (**Figure B.3**) were compared. All scatterplots are based on *daily* data. The year 1968 was chosen in such a way that changes in location and measuring height were minimal for all stations considered.

From Figure B.2 we can see that the scatter is considerable. The black areas in the upper left and lower right corners of the scatter plots originate in the circular variability of the wind direction (e.g. 358 degrees is very close to 5 degrees). Figure B.3 shows the correspondence between stations to be improved if we select a period with minimal changes in instrument locations. The relation between De Bilt and Den Helder (upper panel of Figure B.3) has become ‘more or less’ reasonable.

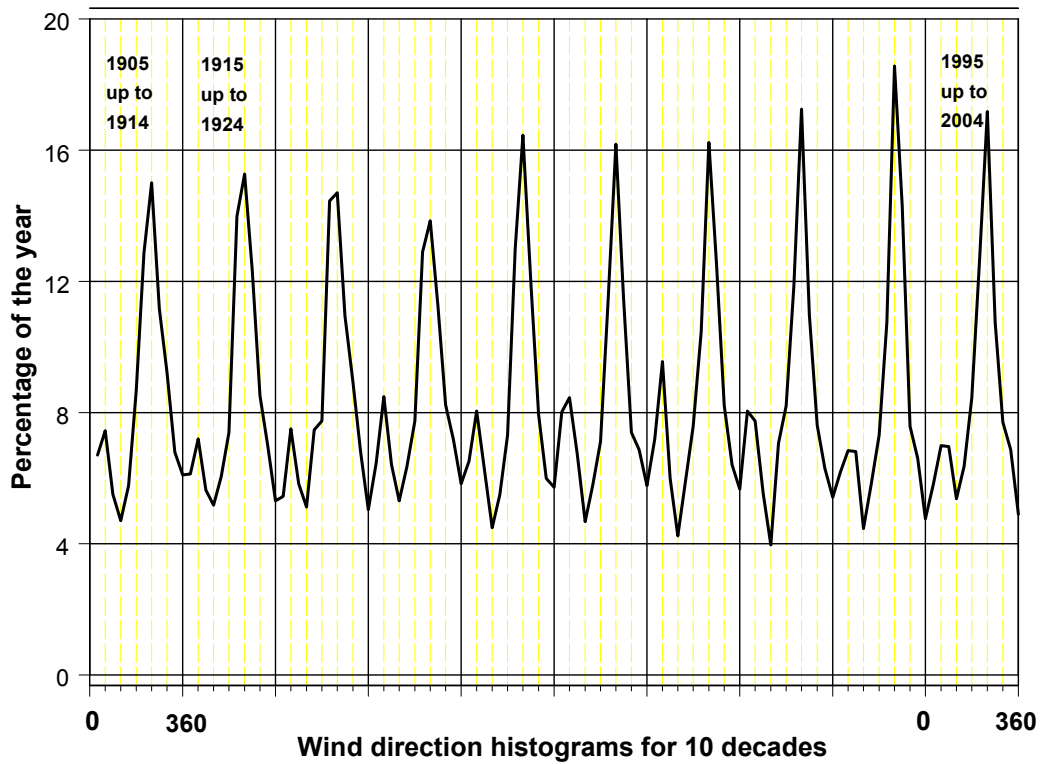


Figure B.1 Wind-direction histograms for 10 decades.

From the inferences above, the wind-direction data of De Bilt (and the other series too) can be concluded as being first homogenized, especially for apparent changes in height and location changes before 1968. Therefore, we do not treat trends in wind direction in this report.

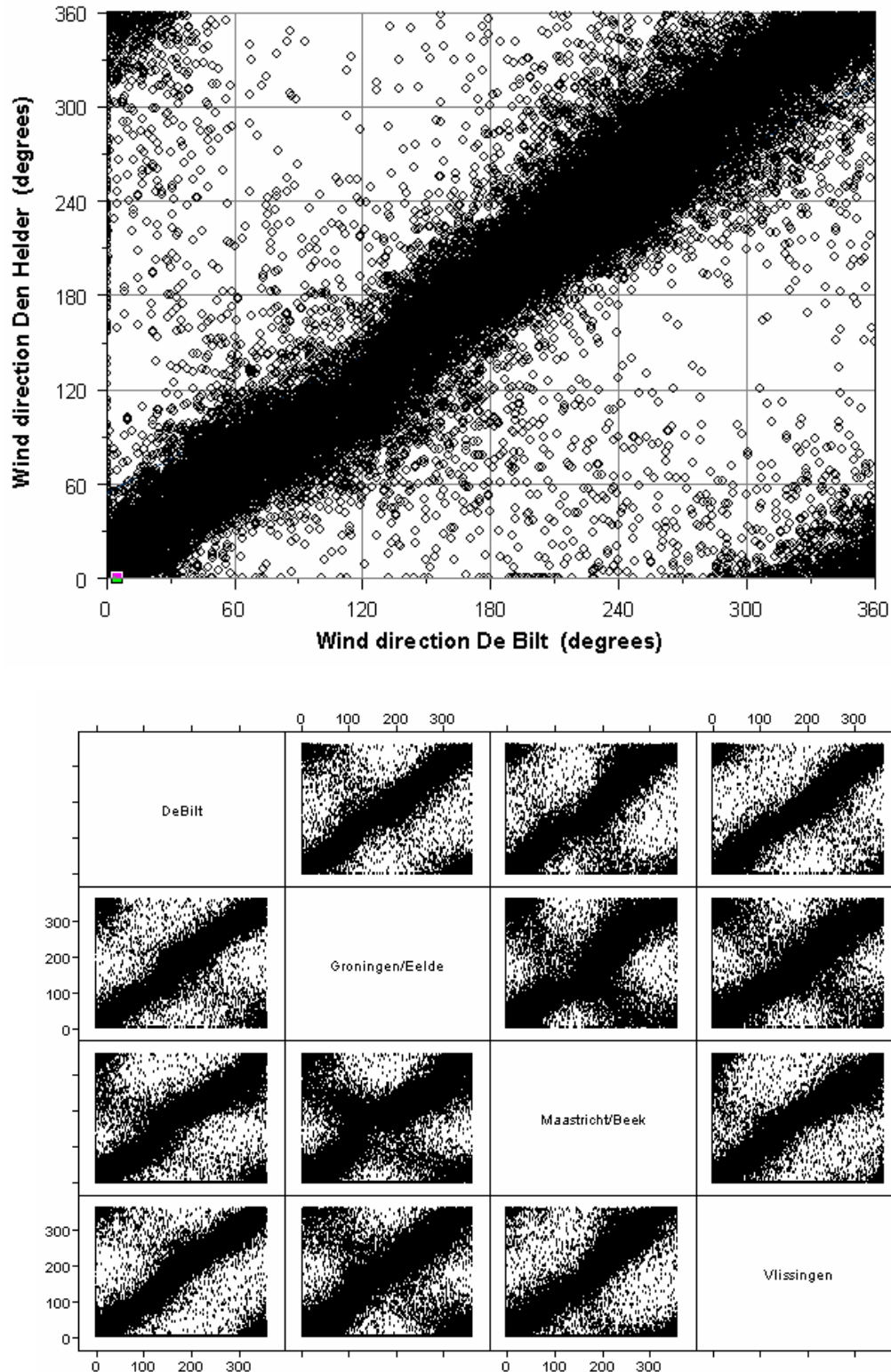


Figure B.2 *Wind direction scatterplots based on daily data over the period of 1908-2003. The upper panel shows the scatterplot between the De Bilt and Den Helder/De Kooy stations. The lower panel shows the scatterplot matrix between De Bilt, Groningen/Eelde, Maastricht/Beek and Vlissingen stations.*

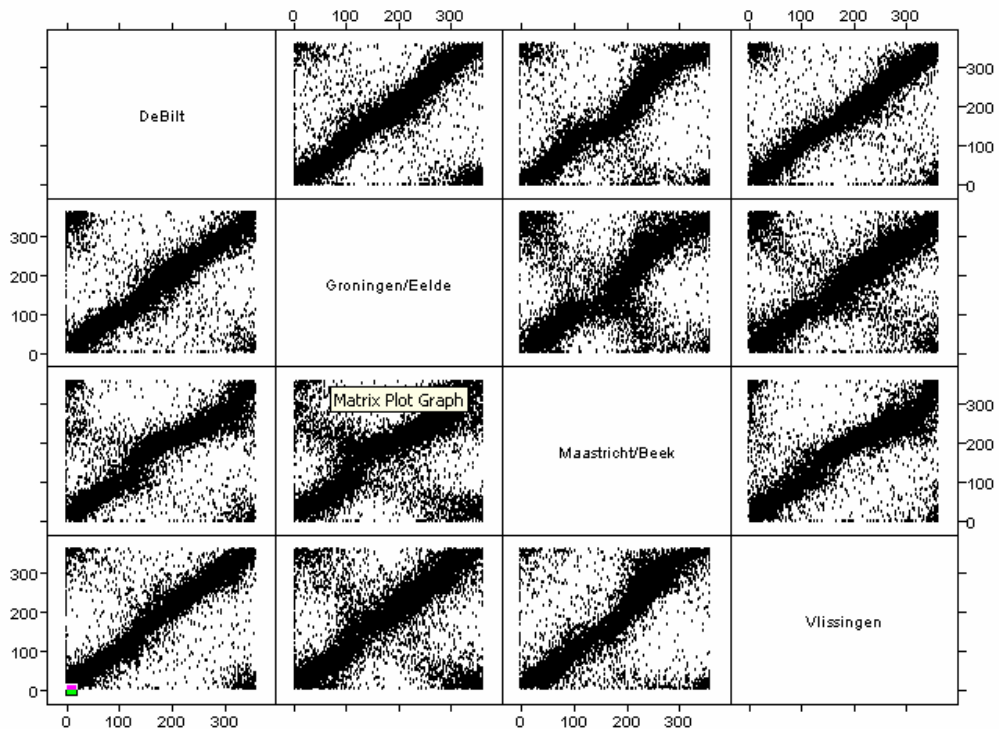
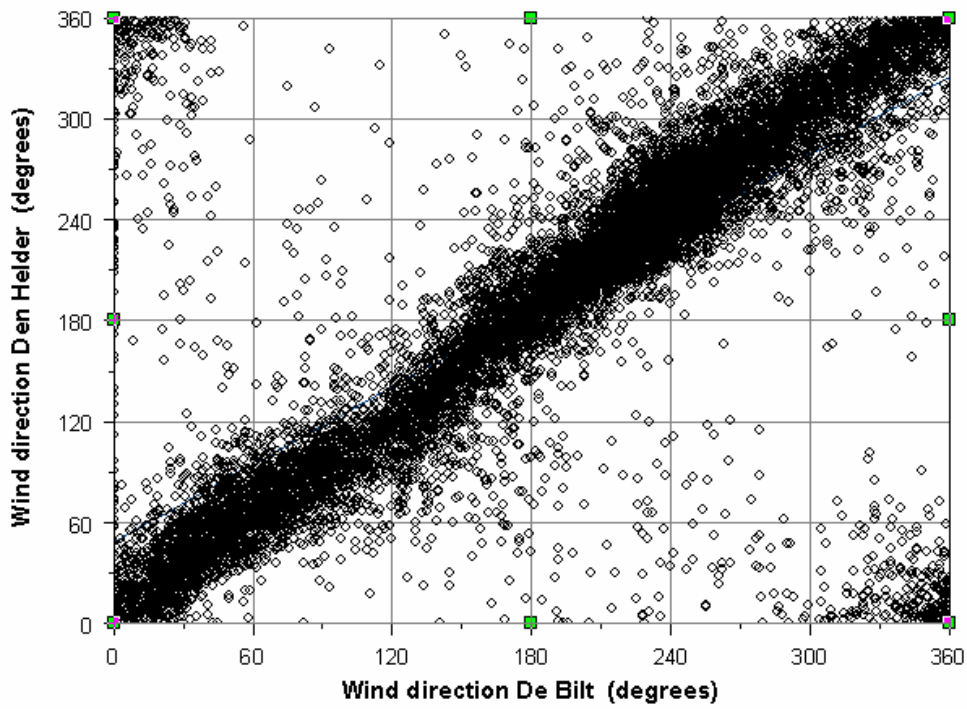


Figure B.3 Wind direction scatterplots based on daily data over the period of 1968-2003. The upper panel shows the scatterplot between the De Bilt and Den Helder/De Kooy stations. The lower panel shows the scatterplot matrix between De Bilt, Groningen/Eelde, Maastricht/Beek and Vlissingen stations.

## B.2 Wind speed

The daily mean wind speeds measured at De Bilt from 1904 onwards are available on the KNMI website ([www.knmi.nl/product](http://www.knmi.nl/product), click on [english] and choose ‘data’ or ‘meta data’ in the upper panel of the Internet page). These wind data have **not** been homogenized.

To get an impression of the influence of instrument movements to other locations or to other measuring heights, we calculated the annual averaged wind speeds the stations, Den Helder / De Kooy, Groningen / Eelde, De Bilt, Vlissingen and Maastricht / Beek. These averages are shown in **Figure B.4** for three stations. The jumps in the series coincide with station movements as given in the meta data. For example, the jump in the De Bilt record around 1960 matches, where the measuring height was lowered from 38 m to 10 m in 1961.

Another impression of the homogeneity of windspeed records is shown by scatterplots, in the same way as for wind direction. To test the influence of changes in the height of the measurements, changes in location and possibly changes in the environment (urbanization, growth of surrounding trees throughout the years), a comparison was made between the

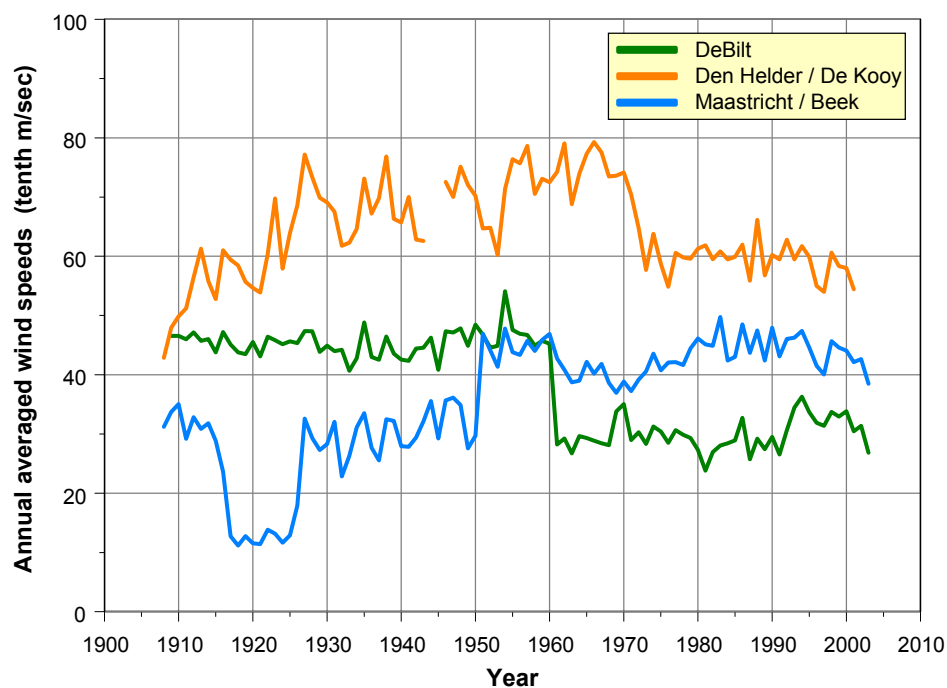


*Figure B.4 Annual averaged wind-speed records for stations at De Bilt, Den Helder/ De Kooy and Maastricht/Beek. Jumps are directly coupled to changes in height and location of the instruments.*

1908-2003 (**Figure B.5**) and the 1968-2003 periods (**Figure B.6**). All scatterplots are based on *daily* data. The year 1968 was chosen in so that changes in location and measuring height were minimal for all stations considered.

The conclusions from these scatterplots are identical to those drawn for wind direction. None of the time series can be regarded as being homogeneous. Furthermore, homogeneity improves if we analyse more recent wind speeds. Thus, these wind speed data can be concluded as not being suitable for trend analysis after 1908. Therefore, wind speed data are not further analysed in this report.

It is noted here that homogenized wind data (wind speed as well as wind direction) have been made available within the KNMI Hydra project. Within this project 54 stations were homogenized. The longest records date from 1952 (Verkaik, 2001), with the wind record for De Bilt starting in 1961. Data and information can be found on the website [www.knmi.nl/samenw/hydra](http://www.knmi.nl/samenw/hydra). However, for the trend analyses in this report these records are regarded as being too short and will not give enough information on *climate change* effects in windspeed records. For results on storm frequencies since 1961 please see KNMI (2003, p. 14) and Smits, Klein Tank and Können (2004).



*Wind speed data are non homogeneous for the pre-1960 period.  
Data from 1960 onwards have been made available by the KNMI within the HYDRA project.  
Photo: Ad Windig, HH.*

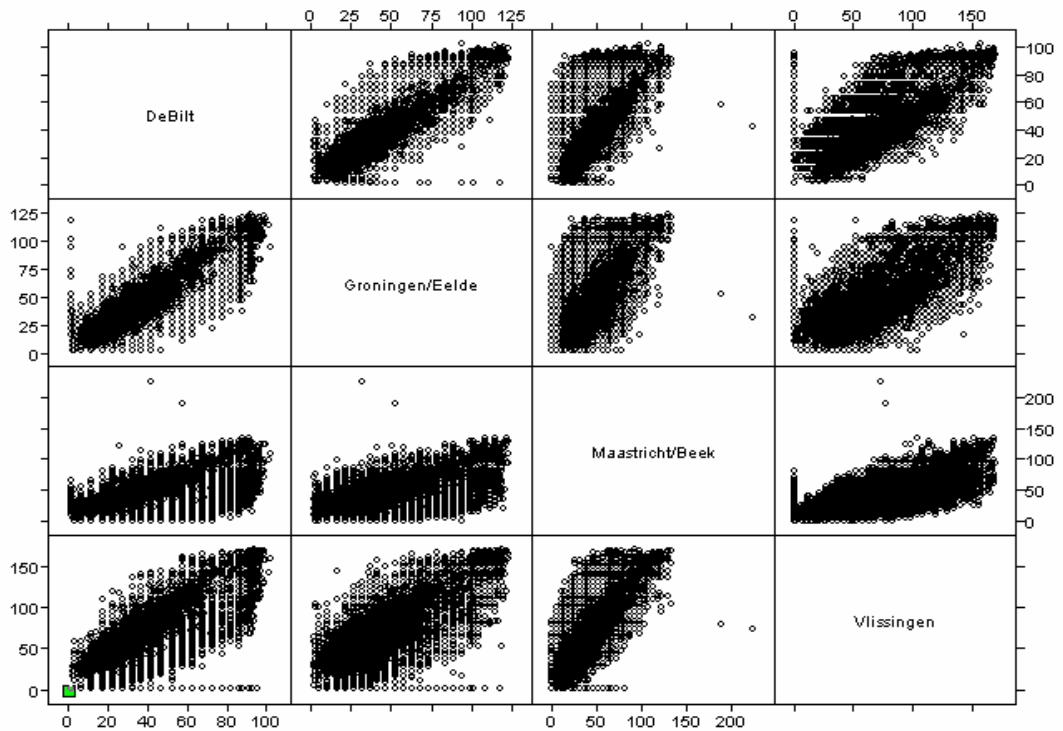
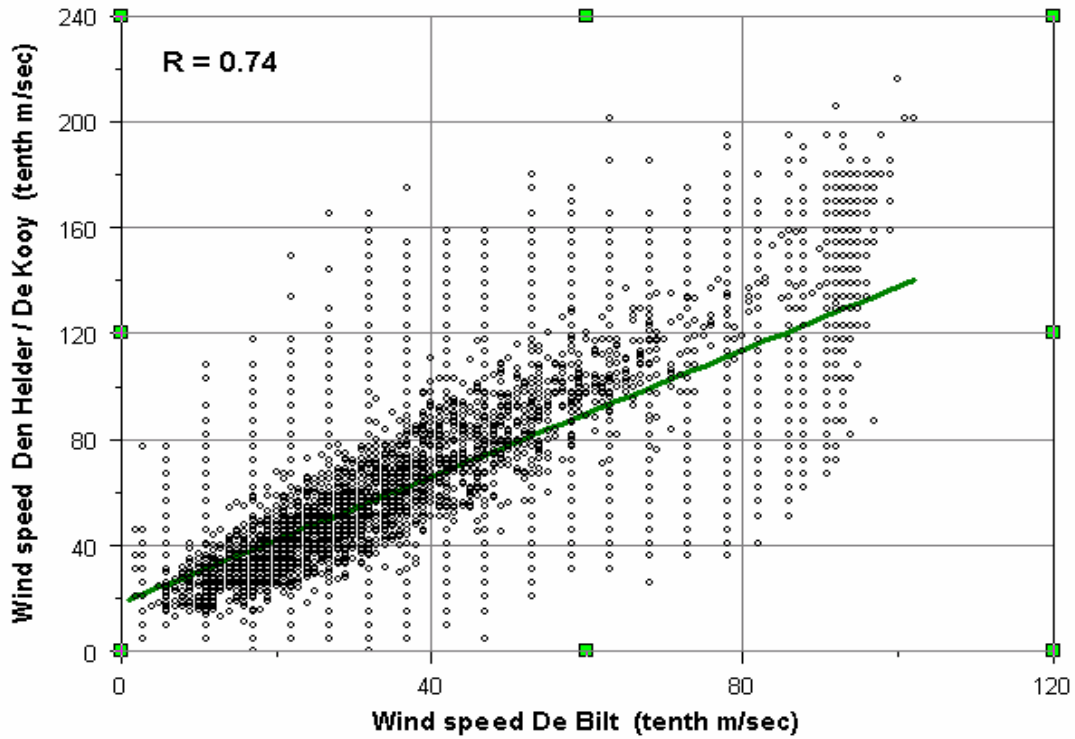


Figure B.5 *Windspeed scatterplots based on daily data over the period 1908-2003.*

The upper panel shows the scatterplot between station De Bilt and station Den Helder/De Kooy. The lower panel shows the scatterplot matrix between stations De Bilt, Groningen/Eelde, Maastricht/Beek and Vlissingen.

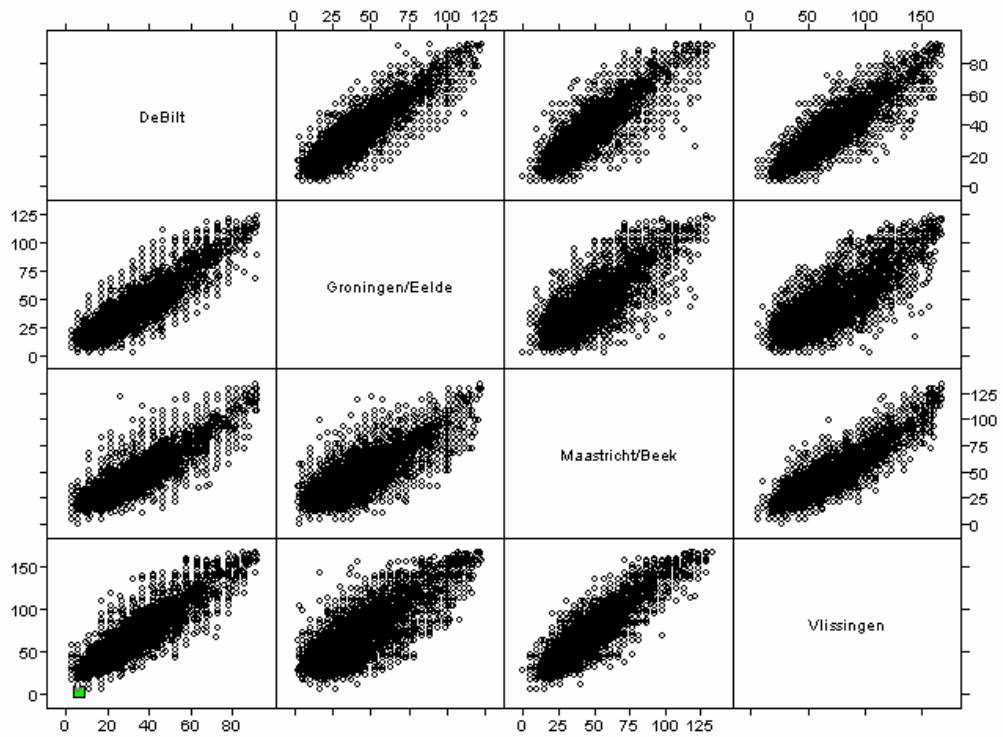
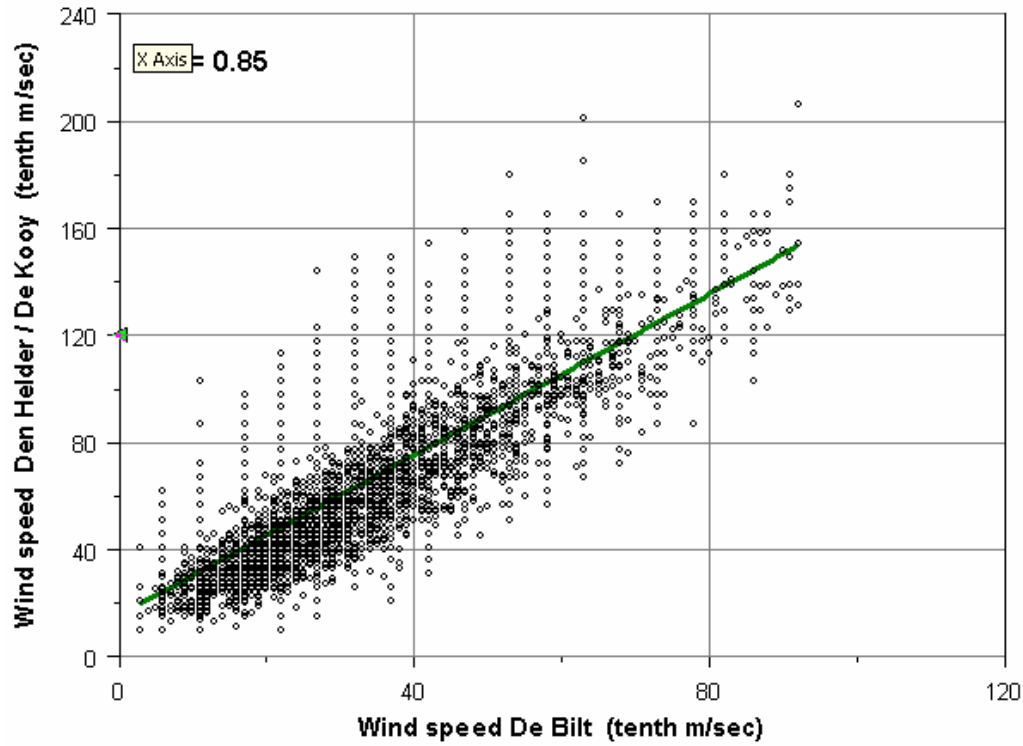


Figure B.6 *Windspeed scatterplots based on daily data over the 1968-2003 period.*  
 The upper panel shows the scatterplot between the De Bilt and the Den Helder/De Kooy stations. The lower panel shows the scatterplot matrix between the De Bilt, Groningen/Eelde, Maastricht/Beek and Vlissingen stations.

## Appendix C Global and local climates are connected

The conclusions drawn by IPCC (2001) on historical climate change will be followed here (please see summaries found in the text box in Chapter 7 and in Figure 7.1). What global temperature increases have taken place in the past, will be derived in section C.1, along with how this warming can be attributed to natural and anthropogenic sources. Then in section 7.2 the analysis of Van Oldenborgh and Van Ulden (2003) will be discussed; these two researchers showed that global and local conditions in the Netherlands are strongly connected. Finally, we will deduce in section C.3 the ratio between global and local warming. This ratio is used for the predictions used out in Chapter 7.

Changes in global *precipitation sums* have not been analysed here because (i) uncertainties are large and (ii) it is not known what changes are due to natural sources and what are due to anthropogenic sources.

### C.1 Global climate change

#### *Historical changes*

The annual global temperature series is shown in Figure 3.2. The increase since 1901 is 0.86 [0.74, 0.98] K, and the annual increase in 2003 accounts for 0.020 [0.004, 0.036] K. Not all of the warming is due to the enhanced greenhouse effect. A likely split of global warming into a natural and an anthropogenic part is given in Figure 7.1 (reproduced from IPCC, 2001). The graph shows that the warming of 0.8 K around the year 2000 can be split into two contributions: 0.2 K from natural sources and 0.6 K from anthropogenic sources. Furthermore, the natural signal is shown to vary between -0.3 and +0.5 °C, with rapid changes. The historical record shows two instances where the rate of change has varied over the full range of 0.8 K in a *decade*.

A second split considered here, is that found by the HadCM2 model, shown in Figure 12.12 of IPCC (2001). The HadCM2 model splits the global increase of 0.8 K since 1901 in an anthropogenic part of 1.0 [0.7, 1.6] K, and a natural part of -0.2 [-0.5, 0.1] K.

#### *Future changes*

What is the future of global temperatures according to Global Climate Models (GCMs)? **Figure C.1** shows the climate-change predictions for the 1990-2100 period, based on a number of emission scenarios.

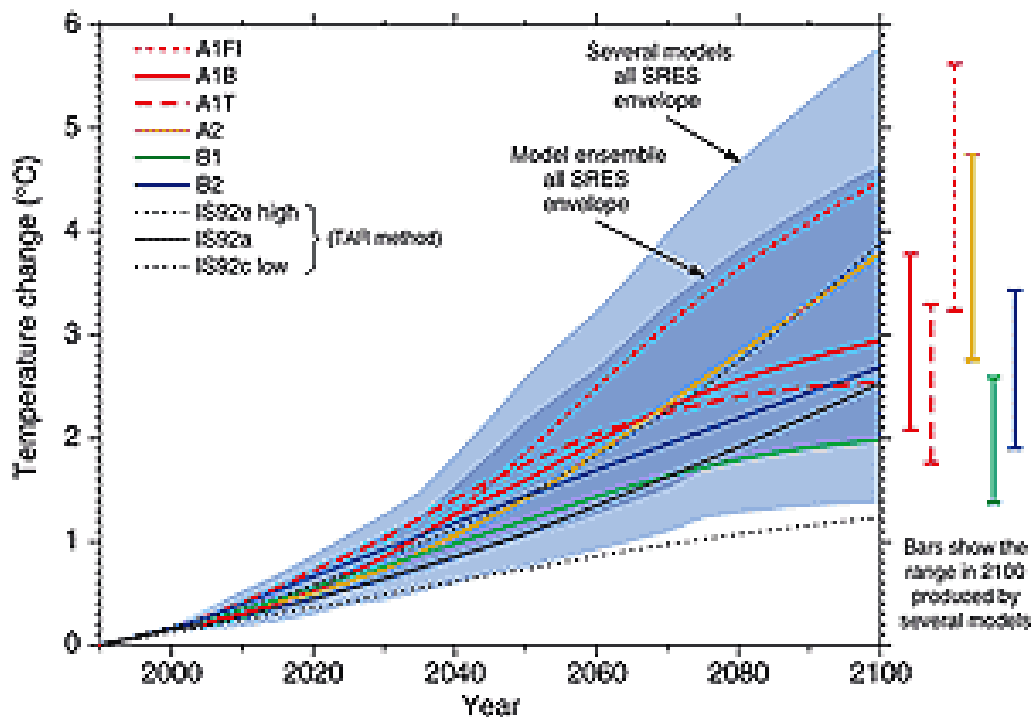


Figure C.1 Human-induced global warming over the 1990-2100 period. Source: IPCC (2001, Chapter 9, Figure 9.14).

The graph shows that:

- all predictions are predominantly linear increasing for the whole period;
- the range in warming since 1990 for the year 2100 is 1.3 – 5.8 K. For the 2000-2100 period, the warming accounts for [1.0 – 5.5] K. This implies an annual increase of [0.010 – 0.055] K/y.

Another illustration is given in **Figure C.2**. These projections are based on **one** emission scenario, calculated for **10** different climate models. Four such projections are given in IPCC (2001, Figure 9.10). Here, rates of increase range from 0.017 up to 0.045 K/y (period 2000-2100).

Eickhout *et al.* (2004) report global annual temperature ranges based on the IMAGE 2.2 model, developed at RIVM. These ranges are similar to the ones reported by IPCC (2001) and shown in Figure C.2. Their annual increases since the year 2000 covers the range [0.012, 0.048] K/y. Uncertainty limits originate from the spread in IPCC emission scenarios and two values for climate sensitivity (1.5 °C and 4.5 °C).

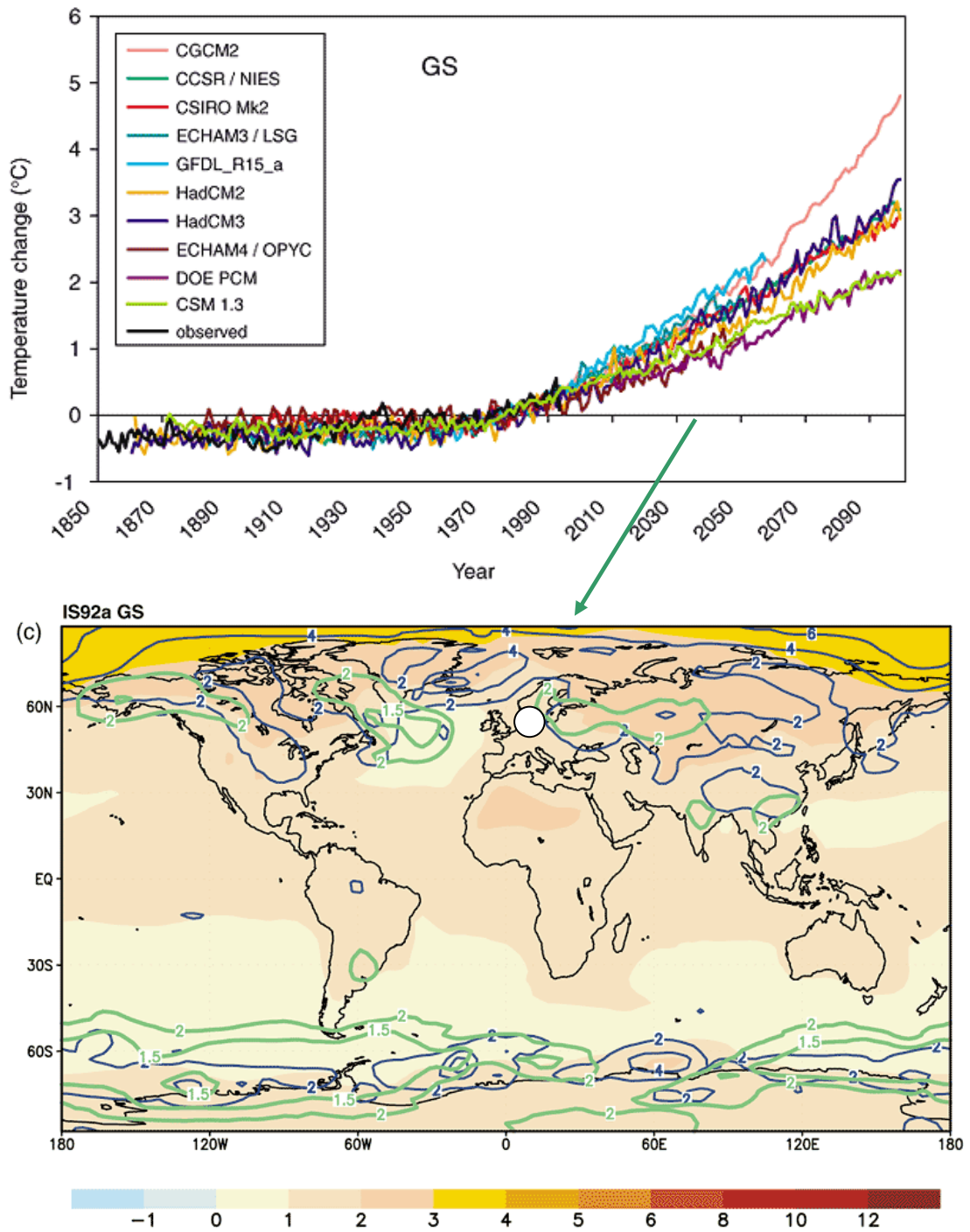


Figure C.2 *Nine global temperature projections for the 1850-2100 period (upper panel), and spatial distribution of temperature during the 2021-2050 period, relative to the 1960-1990 period (lower panel).*

The GS scenario is the same as the IPCC 1992a scenario concerning both greenhouse gases and sulphate aerosols. The thin blue lines give the temperature range in degrees Celsius and the thick green lines the multi-model ensemble divided by the multi-model standard deviation. Source: IPCC (2001, Figure 9.10c).

Visser *et al.* (2000, Figure 4) showed global warming projections based on *a wide range of uncertainty sources*: emission scenarios, gas cycle models, radiative forcing models and specific GCMs with varying climate sensitivities. They found a range of [0.1 , 1.5] K for warming by the year 2003 and a range of [0.5, 6.2] K for warming in 2100. Since all projections are approx. linear, an annual increase rate is found in the range [0.0, 0.057] K/y.

A recent example of global warming calculations has been given in the Dutch Challenge Project ([www.knmi.nl/onderzk/CKO/Challenge\\_live/](http://www.knmi.nl/onderzk/CKO/Challenge_live/)). Here, 62 simulations were run over the 1940–2080 period, using *one* climate model. The average of 62 projections appear to be linear from 2004 onwards. The increase rate over the period 2000–2080 is  $\sim 0.016$  K/y.

If we summarize all projections for the 2004-2100 period, we find human-induced acceleration rates within the range **[0.005, 0.060] K/year**, based on a wide range of uncertainty sources. As a best guess rate the value **0.025 K/year** is chosen here (this equals the acceleration rate of the IPCC A1B scenario). This leads to the following predictions for 2010 and 2020 *relative to 2003*:

$$- \Delta T_{\text{antr}, 2010} = 0.18 \text{ [0.04, 0.42] K} \quad (\text{C1a})$$

$$- \Delta T_{\text{antr}, 2020} = 0.43 \text{ [0.09, 1.02] K} \quad (\text{C1b})$$

Predictions for 2030 and 2040 *relative to 2003* are as follows :

$$- \Delta T_{\text{antr}, 2030} = 0.68 \text{ [0.14, 1.62] K} \quad (\text{C1c})$$

$$- \Delta T_{\text{antr}, 2040} = 0.93 \text{ [0.19, 2.22] K} \quad (\text{C1d})$$

The *natural* warming signal (due to sun plus volcanic forcing) varies between -0.3 and + 0.5 K, according to the study shown in Figure C.1. The best estimate of natural warming around 2000 is 0.2 K. These estimates are consistent to estimates by the HadCM3 model (see Figure 16b of IPCC (2001)). Moreover, within 16 years time the full range from -0.3 to +0.5 K may be reached, as can be seen from Figure C.1. We estimate the range for 2003-2010 to be the half range or [-0.1, 0.02].

These estimates allow us to give the natural warming in 2010, 2020, 2030 and 2040 *relative to 2003*:

$$- \Delta T_{\text{natural}, 2010} = 0.0 \text{ [-0.1, 0.2] K} \quad (\text{C2a})$$

$$- \Delta T_{\text{natural}, 2020} = -0.1 \text{ [-0.5, 0.3] K} \quad (\text{C2b})$$

$$- \Delta T_{\text{natural}, 2030} = -0.1 \text{ [-0.5, 0.3] K} \quad (\text{C2c})$$

$$- \Delta T_{\text{natural}, 2040} = -0.1 \text{ [-0.5, 0.3] K} \quad (\text{C2d})$$

However, other estimates for the natural variability exist. We name here the estimates from the HadCM2 model: a best guess value for 2000 of -0.2 K, with a range over 1900-2000 of [-0.5, 0.1] K. Using these estimates, the following values are found:

- $\Delta T_{\text{natural}, 2010}'' = 0.0$  [-0.1, 0.1] K
- $\Delta T_{\text{natural}, 2020}'' = 0.0$  [-0.3, 0.3] K

Since these values are contained in the values (C2a) and (C2b), resp., the first estimates will be used hereafter.

If we total the contributions (C1a,b) and (C2a,b), we get the following predictions for 2010, 2020, 2030 and 2040 *relative to 2003* (uncertainty ranges have a min-max character and have been added):

- $\Delta T_{\text{global}, 2010} \approx 0.18$  [-0.06, 0.52] K (C3a)
- $\Delta T_{\text{global}, 2020} \approx 0.33$  [-0.41, 1.79] K (C3b)
- $\Delta T_{\text{global}, 2030} \approx 0.58$  [-0.36, 1.92] K (C3c)
- $\Delta T_{\text{global}, 2040} \approx 0.83$  [-0.31, 2.52] K (C3d)

Clearly, the *natural-variability* component has a large impact on short-term prediction ranges.

In absolute terms we have for 2010 and 2020 (given the trend estimate of 0.47 °C in 2003):

- $T_{\text{global}, 2010} \approx 0.65$  [0.41, 0.99] °C (C4a)
- $T_{\text{global}, 2020} \approx 0.80$  [0.06, 1.79] °C (C4b)

The estimates (C4) have been applied in Chapter 7.

It should be noted that the uncertainty bands given in (C4) present minimum and maximum limits, which are very unlikely to occur. Thus, compared to the uncertainty bands in Chapters 4, 5 and 6, they have more the character of 3- $\sigma$  or 4- $\sigma$  limits.

## C.2 From global to local temperatures

Van Oldenborgh and Van Ulden (2003) analysed the De Bilt temperature and wind direction series over the 1901-2002 period, along with the global temperature record. They found the seasonally averaged temperature in De Bilt to be very well described by:

- a warming independent of wind direction and proportional to the globally averaged temperatures,
- an increase in south-westerly circulation in February–April after 1950, and
- an almost white noise signal due to other variations in wind direction and other effects.

The first term explains most (0.8 K) of the observed trend of 1.0 K over the twentieth century, while the second term contributes about 0.2 K. The random term has zero mean and a standard deviation of 0.6 K in annual temperatures. **Figure C.3** summarizes their analysis.



*Trends in global and local weather conditions appear to be connected.*

*Photo: H. Visser.*

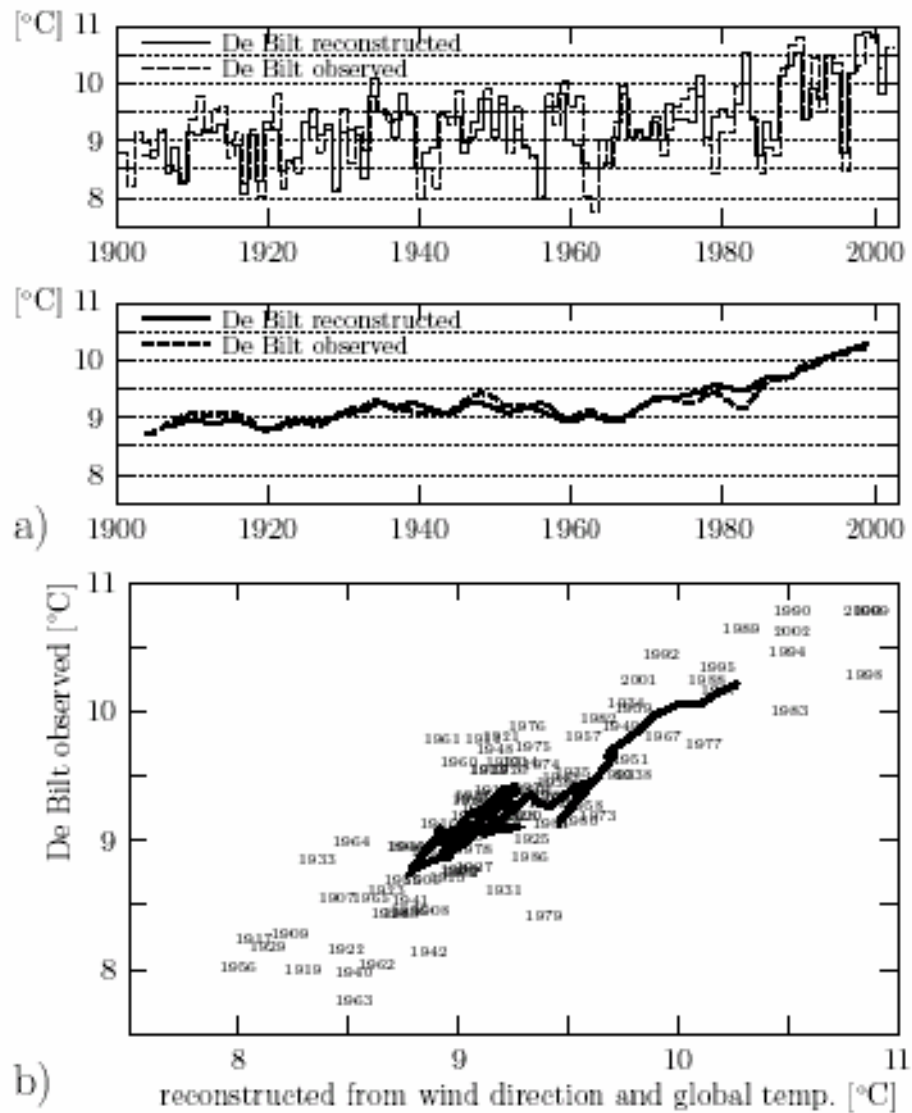


Figure C.3 Comparison of annual temperatures in De Bilt as reconstructed from monthly wind direction measurements plus global temperature (solid lines in upper two panels), and observed temperatures (dashed lines in upper two panels). The lower panel shows a scatterplot between the reconstructed and observed series. Source: Van Oldenborgh and Van Ulden (2003).

### C.3 Downscaling global annual temperatures

Because of the strong relation between global and local temperatures in the Netherlands, we can transform predictions of global warming, as derived in section C.1, to local conditions. To perform such a *downscaling*, we have to know how global and local warming are connected. In other words, we are looking for the ratio  $\Delta T_{\text{De Bilt}}/\Delta T_{\text{global}}$ .

These relations have also been derived by Van Oldenborgh and Van Ulden. They found the following ratios:

- 1901-2002:  $1.5 \pm 0.5$
- 1951-2002:  $2.2 \pm 0.9$

An example showing ratios between local and global temperature change over the period 1901-2002 is given in **Figure C.4**. The Netherlands falls in the class of  $\Delta T_{\text{local}}/\Delta T_{\text{global}} = [1.0 - 1.5]$ .

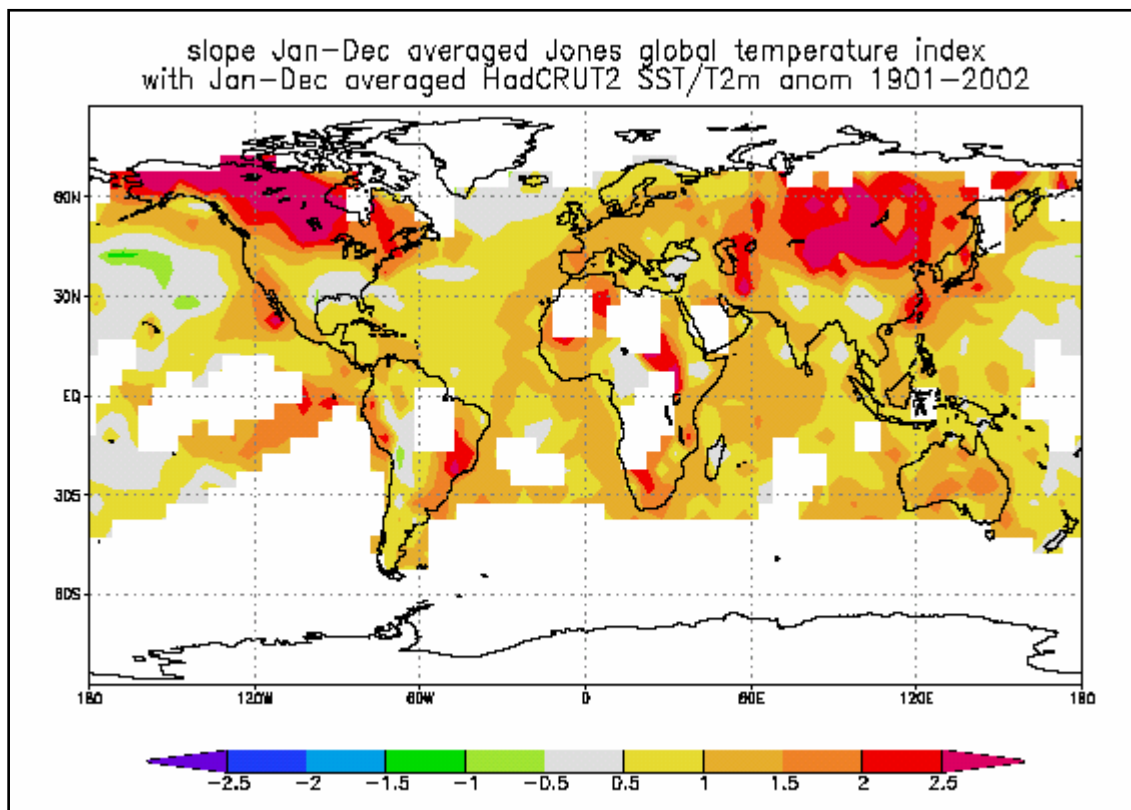


Figure C.4 Map of local acceleration rates divided by the global acceleration rate over the period 1901-2002:  $\Delta T_{\text{local}}/\Delta T_{\text{global}}$ . Source: HadCRUT data set and Van Oldenborgh and Van Ulden (2003).

Future ratios can be derived from Figure 9.10 in IPCC (2001): ratios range from 1.1 to 1.4 with a best guess of 1.25. The ratio based on local and global simulations from the Dutch Challenge Project is ~1.1.

The ratio  $\Delta T_{\text{local}}/\Delta T_{\text{global}}$  for local and global future human-induced warming respectively, can be concluded to account for **1.3 [1.1 – 1.5]**.

## Appendix D Cooling- and heating-degree days in 2040

Heating- and cooling-degree days are useful indicators for correcting future emissions of CO<sub>2</sub>-equivalents. Heating-degree days are related to the heating demand of house holds and commercial buildings, cooling-degree days to the use of (mobile) air conditionings. For various projects within RIVM predictions are needed up to the year 2040. For both indicators predictions are generated here, based on GCM-predictions, downscaled to the Netherlands. These model-based predictions are preferable to statistical extrapolations.

### D.1 Heating-degree days

The derivation of GCM-based heating-degree-day predictions follows four steps: (i) find  $\Delta T_{\text{global - GCM},t}$ , (ii) find  $\Delta T_{\text{De Bilt - GCM},t}$ , (iii) find  $T_{\text{DeBilt - GCM},t}$  and (iv) use the linear relation between temperatures in the De Bilt and heating-degree days to arrive at the GCM-based predictions.

Step 1. The following values for global warming in 2010, 2020, 2030 and 2040 have been found in (C3), relative to 2003:

- $\Delta T_{\text{global - GCM}, 2010} \approx 0.18$  [-0.06, 0.52] K
- $\Delta T_{\text{global - GCM}, 2020} \approx 0.33$  [-0.41, 1.79] K
- $\Delta T_{\text{global - GCM}, 2030} \approx 0.58$  [-0.36, 1.92] K
- $\Delta T_{\text{global - GCM}, 2040} \approx 0.83$  [-0.31, 2.52] K

Step 2. Values for  $\Delta T_{\text{De Bilt},t}$  are found according eq. (7):

- $\Delta T_{\text{DeBilt - GCM}, 2010} = 1.3 [1.1 - 1.5] * \Delta T_{\text{global - GCM}, 2010} = 0.23$  [< -0.06 , 0.78] K
- $\Delta T_{\text{DeBilt - GCM}, 2020} = 1.3 [1.1 - 1.5] * \Delta T_{\text{global - GCM}, 2020} = 0.43$  [< -0.41 , 1.98] K
- $\Delta T_{\text{DeBilt - GCM}, 2030} = 1.3 [1.1 - 1.5] * \Delta T_{\text{global - GCM}, 2030} = 0.75$  [< -0.36 , 2.88] K
- $\Delta T_{\text{DeBilt - GCM}, 2040} = 1.3 [1.1 - 1.5] * \Delta T_{\text{global - GCM}, 2040} = 1.08$  [< -0.31 , 3.78] K

Here, the notation '< -0.06' means that the lower bounds might be somewhat lower.

Step 3. Given the trend estimate of 10.4 °C for the year 2003, the following predictions for De Bilt are found:

- $T_{\text{DeBilt - GCM}, 2010} = 10.6$  [< 10.3, 11.2] °C
- $T_{\text{DeBilt - GCM}, 2020} = 10.8$  [< 10.0, 12.4] °C
- $T_{\text{DeBilt - GCM}, 2030} = 11.2$  [< 10.0, 13.3] °C
- $T_{\text{DeBilt - GCM}, 2040} = 11.5$  [< 10.1, 14.2] °C

Step 4. These values are substituted into regression equation (12)

$$I_t = 6369 - 337 * T_{De\ Bilt, t} + \varepsilon_t$$

to find the model-based predictions for heating-degree days:

- $I_{DeBilt - GCM, 2010} = 2797 [2573, 2906] \text{ } ^\circ\text{C}$
- $I_{DeBilt - GCM, 2020} = 2727 [2157, 3005] \text{ } ^\circ\text{C}$
- $I_{DeBilt - GCM, 2030} = 2595 [1853, 2990] \text{ } ^\circ\text{C}$
- $I_{DeBilt - GCM, 2040} = 2494 [1550, 2965] \text{ } ^\circ\text{C}$

Both model-based and data-based predictions (up to 2020) are summarized in **Figure D.1**.

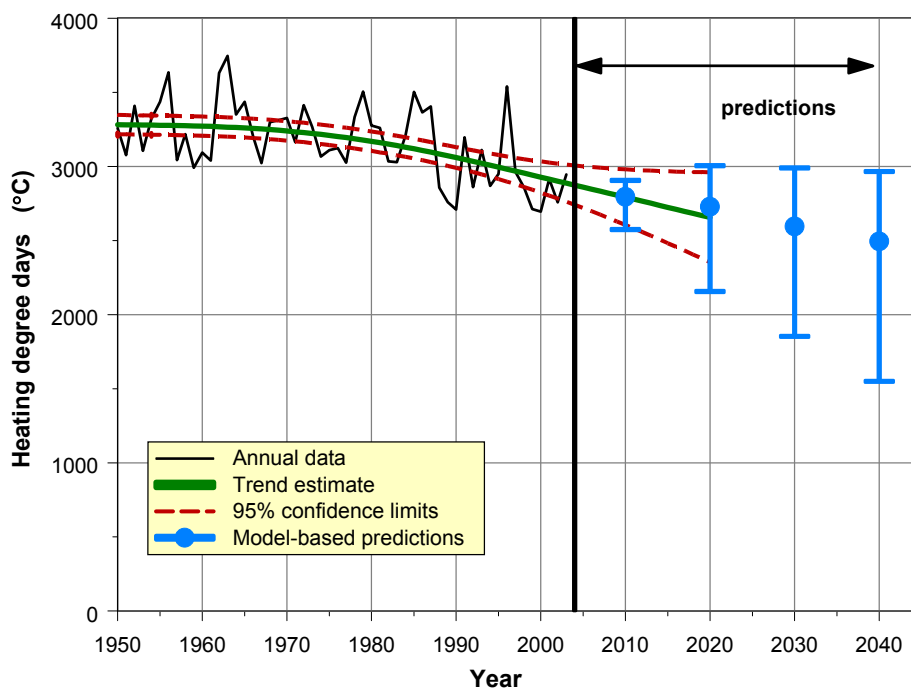
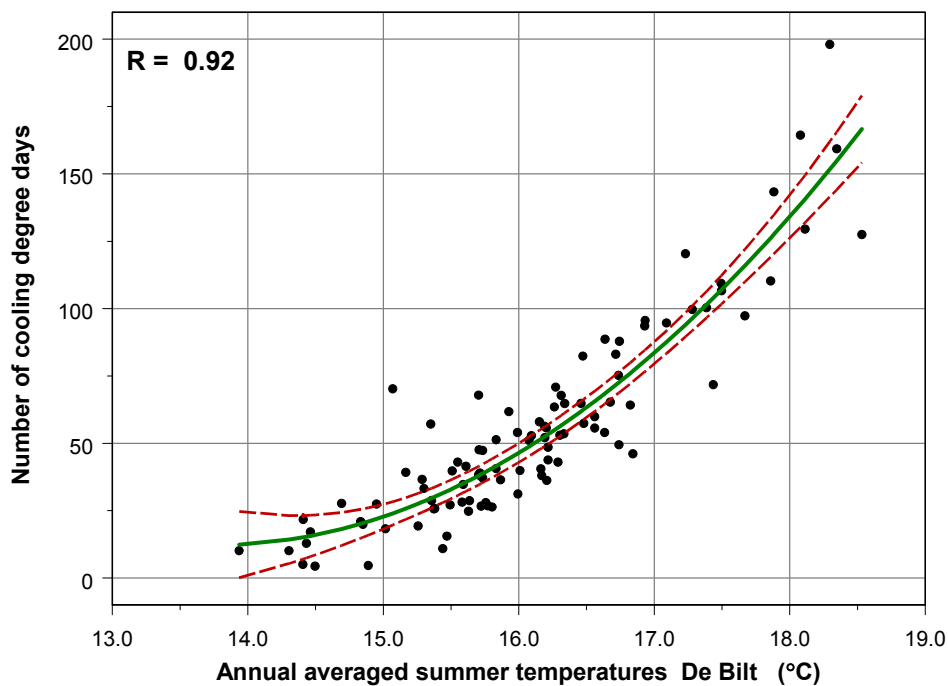


Figure D.1 Model-based predictions for heating-degree days in the Netherlands. Also the statistical derived predictions are shown up to the year 2020 (identical to estimates shown in Figure 7.6).

### D.2 Cooling-degree days

Cooling-degree days have been defined and analysed over the historic period 1901-2003 in section 6.3.2. Clearly, cooling-degree days will not be coupled to annual temperatures as is found for heating-degree days (cf. Figure 7.5). However, it appears that cooling-degree days are strongly coupled to summer temperatures ( $R = 0.92$ ). The best fit is quadratic rather than linear (as in Figure 7.5). The scatterplot between annual cooling-degree days, along with the quadratic regression line and 95% confidence limits, is shown in **Figure D.2**.



Coefficients:

	Value	Std. Error	t value	Pr(> t )
(Intercept)	1282.0706	303.1830	4.2287	0.0001
Tzomer	-184.8424	37.3435	-4.9498	0.0000
Tzomer2	6.7260	1.1476	5.8611	0.0000

Residual standard error: 14.43 on 95 degrees of freedom

Multiple R-Squared: 0.8495

Figure D.2 Scatterplot between summer mean temperatures in De Bilt and the number of cooling-degree days. The regression line (green line) is estimated by a second order polynomial. Dashed lines represent 95% confidence limits for the regression line.

Now, if summer temperatures will rise in the period 2004 – 2040 in the same way as annual averaged temperatures, we can apply the same procedure as is follows in section D.1.

Most GCMs indeed show that summer temperatures increase in a linear fashion, as annual temperatures do, and the rate of increase is the same for both summer and annual averaged temperatures. An example based on 62 simulations from the Dutch Challenge project, is shown in **Figure D.3**. The Figure shows 62 simulations for summer temperatures over the historic period 1940-2003, and future period 2004-2080. Realized summer temperatures for the Netherlands are presented by the blue dots. The black curve is the average of all 62 projections. The average annual increase is 0.015 (K/year). For annual averaged temperatures an annual increase of 0.016 (K/year) is found.

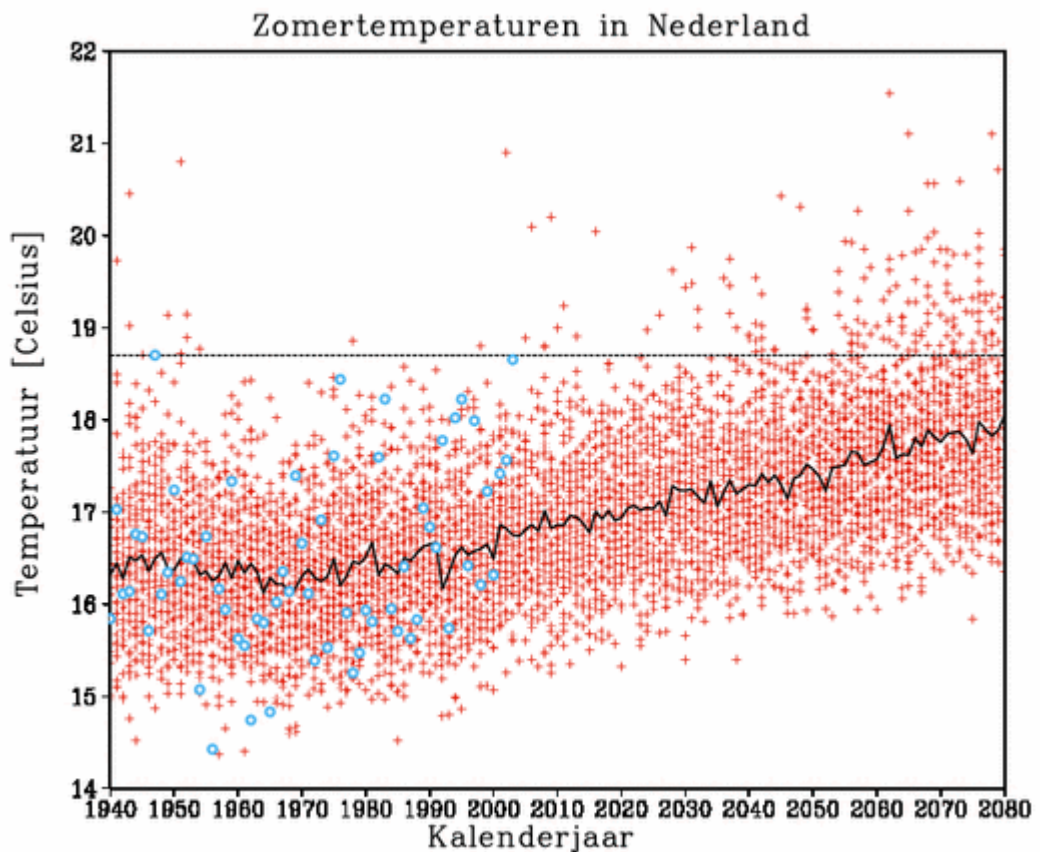


*Figure D.3* The 62 simulations of summer temperatures for grid box 'The Bilt', as found within the Dutch Challenge Project in 2004.

Simulations were calculated by the National Center for Atmospheric Research Community Climate System Model (NCAR-CCSM, version 1.4) in the Challenge ensemble experiment.

Given these results we may conclude that local summer temperatures will rise in the same way as local annual averaged temperatures. These increments  $\Delta T_{\text{De Bilt}, t}$  are identical to those given in section D.1:

- $\Delta T_{\text{DeBilt} - \text{summer} - \text{GCM}, 2010} = 0.23$  [ $< -0.06$  , 0.78] K
- $\Delta T_{\text{DeBilt} - \text{summer} - \text{GCM}, 2020} = 0.43$  [ $< -0.41$  , 1.98] K
- $\Delta T_{\text{DeBilt} - \text{summer} - \text{GCM}, 2030} = 0.75$  [ $< -0.36$  , 2.88] K
- $\Delta T_{\text{DeBilt} - \text{summer} - \text{GCM}, 2040} = 1.08$  [ $< -0.31$  , 3.78] K

Again, the notation ' $< -0.06$ ' means that the lower bounds might be somewhat lower.

Given the summer trend estimate of **17.1 °C** for the year 2003 (model not shown here), the following summer predictions for De Bilt are found:

- $T_{\text{DeBilt} - \text{summer} - \text{GCM}, 2010} = 17.3$  [ $< 17.0$ , 17.9] °C
- $T_{\text{DeBilt} - \text{summer} - \text{GCM}, 2020} = 17.5$  [ $< 16.7$ , 19.1] °C
- $T_{\text{DeBilt} - \text{summer} - \text{GCM}, 2030} = 17.9$  [ $< 16.7$ , 20.0] °C
- $T_{\text{DeBilt} - \text{summer} - \text{GCM}, 2040} = 18.2$  [ $< 16.8$ , 20.9] °C

Now, we substitute these values into regression equation (cf. Figure D.2):

$$I_t = 1282 - 184.8 * T_{\text{Zomer De Bilt}, t} + 6.73 * T_{\text{Zomer De Bilt}, t}^2 + \varepsilon_t$$

to find the model-based predictions for cooling-degree days  $I_t$ :

- $I_{\text{DeBilt} - \text{GCM}, 2010} = 99$  [**81, 135**] °C
- $I_{\text{DeBilt} - \text{GCM}, 2020} = 109$  [**69, 218**] °C
- $I_{\text{DeBilt} - \text{GCM}, 2030} = 130$  [**69, 293**] °C
- $I_{\text{DeBilt} - \text{GCM}, 2040} = 148$  [**74, 380**] °C

Both model-based and data-based predictions (up to 2020) are summarized in **Figure D.4**. Remarkable here is that statistical extrapolations fall higher than GCM-based predictions. Also confidence limits are wider for the first approach.

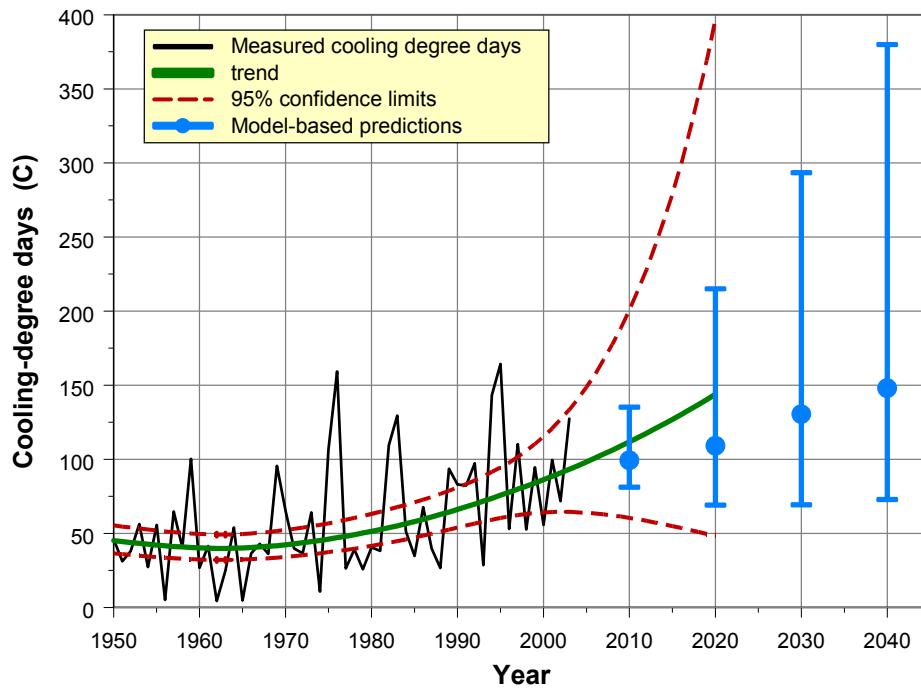


Figure D.4 Model-based predictions for cooling-degree days in the Netherlands. Also the statistical derived predictions are shown up to the year 2020.